SEARCHES OF FRACTIONALLY CHARGED PARTICLES IN MATTER WITH THE MAGNETIC LEVITATION TECHNIQUE

M. MARINELLI and G. MORPURGO

Istituto di Fisica dell'Università di Genova and Istituto Nazionale di Fisica Nucleare, Sezione di Genova, Italy

NORTH-HOLLAND PUBLISHING COMPANY - AMSTERDAM

PHYSICS REPORTS (Review Section of Physics Letters) 85, No. 4 (1982) 161–258. North-Holland Publishing Company

SEARCHES OF FRACTIONALLY CHARGED PARTICLES IN MATTER WITH THE MAGNETIC LEVITATION TECHNIQUE

M. MARINELLI and G. MORPURGO

Istituto di Fisica dell'Università di Genova and Istituto Nazionale di Fisica Nucleare, Sezione di Genova, Italy

Received 31 October 1981

Contents:

Single orders for this issue

PHYSICS REPORTS (Review Section of Physics Letters) 85, No. 4 (1982) 161–258.

Copies of this issue may be obtained at the price given below. All orders should be sent directly to the Publisher. Orders must be accompanied by check.

Single issue price Dfl. 51.00, postage included.

0370-1573/82/0000–0000/$24.50

Abstract:

A survey is given of the experiments performed with the magnetic levitation electrometer to search for stable fractional charges in matter. After a general introduction, illustrating the principle of the method, an analysis is presented of the electric forces acting on the levitating object (whose knowledge is essential to determine the residual charge). This is followed by a short account of the historical evolution of the subject, after which we proceed to a detailed description of the ferromagnetic levitation electrometer used in our laboratory and of the results obtained. The main differences with the Stanford diamagnetic (superconducting) instrument are also illustrated. The final section contains a concise summary of the other experiments of search of quarks in matter, in particular of the Millikan automated ones.

1. Introduction

This report describes several experiments to search quarks in matter performed with a new instrument, the magnetic levitation electrometer. Our personal motivation, in starting these experiments in 1965, was a series of theoretical papers by one of us (G.M.) [1, 2, 3] – written soon after the introduction of the quarks [4] – and containing the basis and the first successful results of what is now called the "naive" or "non relativistic" quark model. The results obtained looked so impressive that ref. [1] ended as follows: "Finally, if the present ideas are valid, the quarks should exist; they should not be only mathematical entities .... So one should finally discover the quarks. The most appropriate conditions for this should be investigated. I hope to come back to this point in the future."

We certainly kept the promise [5], during the past 16 years, although in this long search we did not, so far, meet the free quark.

Following our [5a, b] proposal and results, other laboratories used the same type of instrument [6]. At the time of writing, the most extensive and continuing searches along this line are those of our group and of a group at the University of Stanford [7].

This paper will present the idea of the magnetic levitation electrometer, give a description of the various experiments that have been performed and briefly discuss the possible developments.

To make this survey useful for the non-specialized reader we try to separate the presentation into sections providing the general ideas, and sections containing the more technical aspects.

The search of quarks in matter is based on three assumptions: (1) that quarks are fractionally charged, (2) that at least one of them is stable, (3) that isolated free quarks exist with some abundance in the matter around us. Some comments are appropriate:

(1) *Fractional charge.* This is a necessary consequence of the original assumption of Gell-Mann and Zweig [4], proposing three types of quarks with the properties listed in the first three lines of table 1.1. With these quarks the quantum numbers and multiplicities of the hadrons known in 1964 could be explained and, in fact, some missing hadrons (the case of the Ω^- is now classic, but also the η meson should be recalled) could be predicted.

More recently the need for other types (or flavours, as they are called) of quarks emerged to explain the famous resonances of the J/ψ and Υ families, and the related zoology of particles. No evidence

exists so far for the t quark listed in the last line of table 1.1; it should however be there according to the prevailing theoretical ideas.

The need for fractional charges is due to the fact that (in the Gell-Mann–Zweig description) the baryons consist of three quarks (not of two quarks and an antiquark as in the Sakata scheme that could not, however, account for the observed multiplicities). The proton, for instance, has a ppn structure and the neutron a nnp structure; therefore the charges of the p and n quarks, q_p and q_n, must satisfy the following equations (taking the |electron charge| as unit):

$$\begin{aligned} 2q_p + q_n &= 1 \\ 2q_n + q_p &= 0\,. \end{aligned} \tag{1.1}$$

From (1.1) one gets $q_p = +2/3$ and $q_n = -1/3$ as indicated in table 1 1.

Table 1 1

The various types of quarks with their specifications (in the first column the symbol – or symbols – currently used are indicated, the second column (flavour) gives the name, the symbol and the value of the flavour quantum number; column 3 gives the electric charge – in units of $|e|$ –, column 4 gives (in GeV/c^2) the approximate (and to some extent conventional) mass of the *bound* quark) The spin of all quarks is assumed to be 1/2 Antiquarks have values of q and the flavour quantum number with opposite sign According to the present standard picture (fig 1 1) – see text – each quark (and antiquark) exists in three varieties (colours) (Note the t quark is only a guess, there is no evidence for it so far.)

1	2	3	4
quark symbol	flavour	charge (in units of $\|e\|$)	effective mass (GeV/c^2)
u (or p)		+2/3	0.35
d (or n)		−1/3	0 35
s (or λ)	strangeness ($s = -1$)	−1/3	0 55
c (or p')	charm $c = 1$	+2/3	1 55
b	beauty or bottom number $b = 1$	−1/3	5
t(?)	top number	+2/3	?

(2) *Stability of at least one type of quarks.* Once the quarks are assumed to be fractionally charged, this is, obviously, a consequence of charge conservation. Indeed if the charge is *strictly* conserved a fractionally charged particle cannot decay into products having all integer charge. Thus, if the quarks have fractional charge, at least one stable particle must exist with fractional charge. It is that particle – quark, lepton or whatever it is – that our experiments should reveal.

(3) *Isolated free quarks with some abundance in the matter around us.* Although strong theoretical prejudices exist on the question of isolated free quarks it is our persistent opinion that this question should first be approached experimentally. It is instructive to go back to the time when these experiments started. Then – around 1965 – the prevailing idea among theorists was that (in spite of the

successes of the non-relativistic quark model in which quarks are treated in a very realistic way, like nucleons in a nucleus) isolated free quarks should not exist: quarks had to be thought of as unspecified "mathematical objects". For a long while no justification of this attitude was attempted. The justification then proceeded through several steps. It was first assumed that each quark had an internal degree of freedom, let us say an index of its wave function, with three possible values 1, 2, 3; or more pictorially, blue, red and white. As a matter of fact the original introduction [8] of this "colour" was based on the (implied) assumption that the space part of the wave function of the three quarks inside a hadron should be compulsorily symmetrical in character. Though likely, this is not a necessity: if the forces between quarks in a hadron are of the exchange Majorana type – attractive between space antisymmetrical pairs and repulsive between symmetrical pairs – the lowest bound state of three quarks in a hadron is described by a space antisymmetrical wave function.

Historically the stronger arguments (compare fig. 1.1) for colour turned out perhaps to be the following: (a) the lifetime of the π^0, that in a model without colour is predicted nine times longer than observed; (b) the ratio $R_{e^+e^-}$ between hadron production and μ^+, μ^- production in e^+e^- collisions that, in a parton description, depends heavily on the existence or non-existence of the colour degree of freedom.

Once colour is introduced it is possible to impose the following postulate: only colour singlet states (antisymmetrical under colour permutations) do exist in nature. This amounts to say that only those bound states of hadrons having space symmetrical wave functions of their three quarks exist. At this stage isolated quarks are forbidden by decree.

This postulate can be tentatively dignified into a theory if it is assumed that the field theory describing the quarks is the so called Quantum Chromodynamics (Q.C.D.), a non-Abelian gauge theory of coloured quarks and gluons; the latter are assumed to be the quanta of the coloured field transmitting the forces among quarks (as photons in quantum electrodynamics carry the forces among charged particles). If the gluons produce in Q.C.D. forces between quarks that – at variance with Q.E.D. – become more attractive with increasing distance, then quarks would be permanently confined and free isolated quarks could never be found. At the moment of writing the above "if" underlies a real uncertainty: no proof exists of such confinement. As a consequence, to decide if free isolated quarks do exist or not continues to be, to our mind, an experimental problem; in all these years our attitude has been – and continues to be – that in this question one should try not to be biassed by theoretical prejudices; a search of quarks is an important investigation and should be continued until possible, that is until technically feasible. In this respect the experiments to be described here have considerably improved – by a factor 10^6 or 10^7 – the sensitivity in the quark detection with respect to the previous situation. We are now able to establish (without any further assumption) the presence or absence of a quark inside a piece of matter weighing 10^{-4} g, whereas the Millikan droplets did weigh 10^{-11} to 10^{-10} g. It is possible that with this technique, or different ones, one may still go further.

A final comment is appropriate comparing the search of quarks produced in high energy collisions in accelerators with the search of quarks in matter. We consider these two approaches as complementary. The accelerator search is limited by the mass of the free quark: if quarks are too massive one will never be able to produce them (cosmic rays are, in principle, a possible exception). On the other hand the search in matter is independent of the mass but is limited by the quark abundance. On this no information exists at present although many ideas have been ventured.

In this respect one can ask the following general question. Suppose that the presence of quarks in terrestrial matter were due *only* to their production by the cosmic rays during the course of the years. Because we know [10] an upper limit to the quark production from cosmic rays, can we deduce from it a

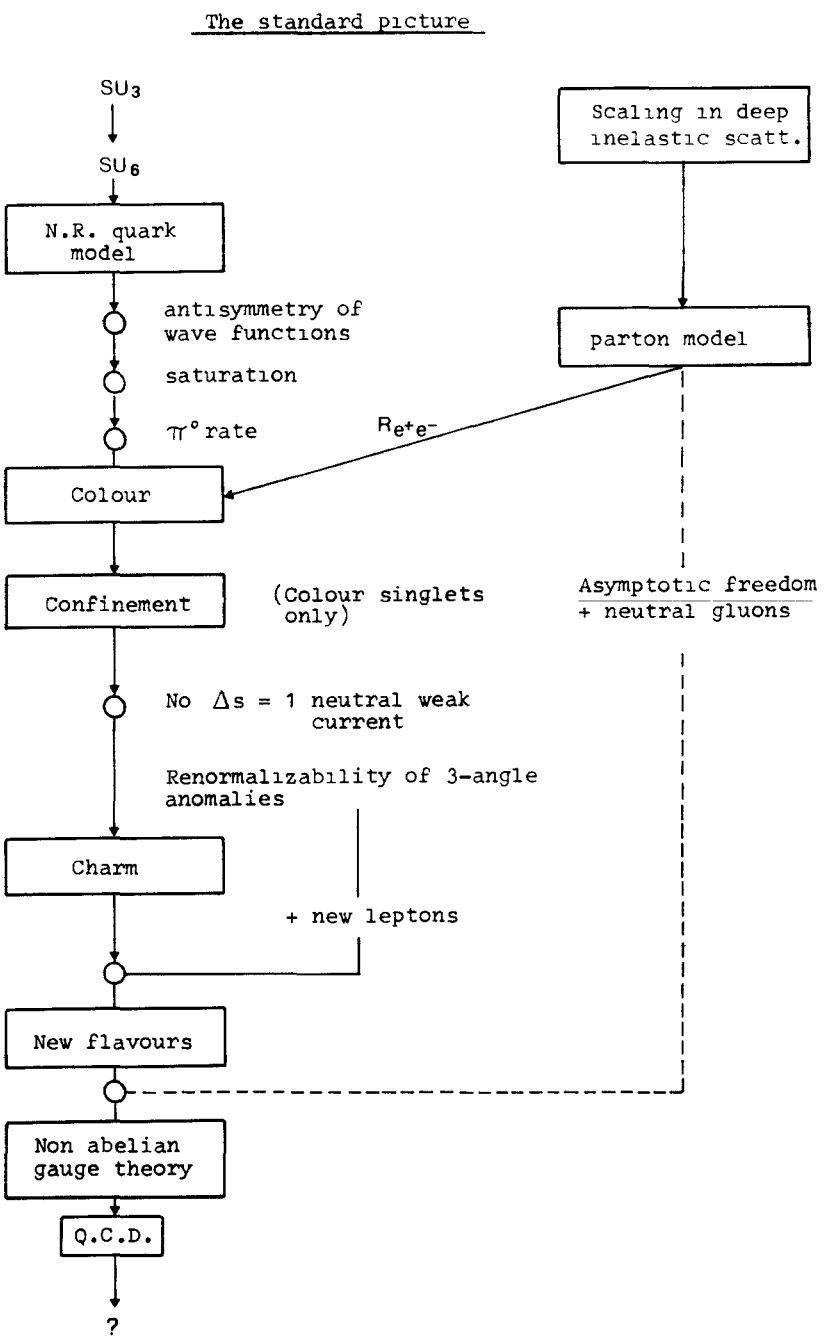

Fig 1 1 The standard picture: a short summary of the evolution of the quark model

corresponding upper limit to the expected quark concentration in terrestrial matter? The answer is yes, but only if we make several (in part doubtful) assumptions. Assume that: (a) since the formation of the Earth ($\sim 3 \times 10^9$ years ago) the flux of the cosmic rays has always remained the same as it is now; (b) that the quarks produced during this long period are all to be found in a layer having a depth of ~ 3 km; we assume in other words that, on the average, the turbulence of the Earth's crust during the life of the Earth has affected a layer of ~ 3 km. Then the upper limit to the number of quarks N created in a column of height 3 km and cross section 1 cm^2 by the cosmic rays during the life of the Earth is:

$$N < \pi \cdot 10^{17} \cdot 10^{-11} \cong 3 \times 10^6$$

where the first factor π comes from the integration over half-solid angle, the second factor 10^{17} gives the number of seconds in 3×10^9 years and the last factor 10^{-11} is the upper limit to the quark flux from the cosmic rays (compare ref. [10]). We thus obtain (dividing N by 3×10^5 cm) for the upper limit to the concentration c:

$c < 10$ quarks per cubic cm.

This is a rather small *upper limit*; so that quark hunters must hope that either, for some reason, quarks have concentrated in preferential sites during the years; or that some *relics* from the *primordial quarks* have remained with us more abundantly; or both.

Several review papers dealing with various aspects of the problem of search of quarks have been written [9, 10, 11, 12, 13] containing also a detailed list of references. In this respect we confine to the technique specified by the title, except for a few points in the last section.

2. The idea of the experiment

2.1. Introductory remark

A grain of matter containing a fractionally charged quark can never be brought to charge zero by addition or removal of electrons. If the quarks have charges $\pm e/3$ or $\pm 2e/3$ the residual electric charge of the grain Q_R (R stands for residual) defined as the value of the charge nearest to zero, is necessarily:

$$Q_R = \pm e/3 .$$

Therefore a measurement of the residual charge of the grain reveals if it does or does not contain a quark.

2.2. The Millikan experiment

In principle a Millikan experiment [14, 15] can be performed to measure Q_R (although the original Millikan experiment did not have this specific purpose). The Millikan experiment had in fact two aims: (a) to investigate the discreteness of the charge, (b) to determine the numerical value of the electron charge. Leaving aside the latter problem (there are now better ways to determine e) the Millikan experiment works as follows, as far as the question of the discreteness of charge is concerned.

A potential difference is applied between the horizontal parallel plates of a capacitor. A charged oil

droplet, injected between the plates, is observed (fig. 2.1) with a telescope while it goes up from some height z_1 to a higher height z_2 under the action of the electric field in the capacitor. The speed of the droplet is constant, due to the viscosity of the air and, therefore, the time for going from z_1 to z_2 is inversely proportional to the charge Q_i of the droplet,

$$t_i = k/Q_i .$$

Here k is a constant of proportionality depending on the mass of the droplet and on the value of the applied electric field. On changing the charge Q_i of a droplet by photo-ionization, one can measure, for the same droplet, the different t_i corresponding to different values of the charge Q_i. If the Q_i's are multiples of an elementary charge e:

$$Q_i = n_i e , \tag{2.1}$$

the sequence of t_i's that one finds has the expression:

$$t_i = \frac{k}{e}\frac{1}{n_i} = \frac{\text{const.}}{n_i} . \tag{2.2}$$

If, on the other hand, the oil droplet contains a quark, the charge Q_i is:

$$Q_i = (n_i \pm \tfrac{1}{3})e \tag{2.3}$$

and, instead of (2.2), one should find:

$$t_i = \frac{\text{const.}}{n_i \pm \frac{1}{3}} . \tag{2.4}$$

If the droplet has only a few charges it is clearly possible to recognize, measuring the sequence of the t_i's, if (2.2) or (2.4) holds and establish the presence or absence of a quark inside the droplet. However (aside from the circumstance that a neutral object cannot be kept floating for a long time because it falls under the gravity) the main inconvenience of the Millikan experiment in the search of quarks is that the size of the droplets to be used is very small and the chance to find a quark inside is correspondingly tiny.

The reason for the small size of the droplets is that in the Millikan electrometer the electric field plays two roles at the same time: it counteracts the gravity and measures the charge of the droplet. If the droplets are too heavy a huge electric field is needed in the capacitor; this produces fast ionization of the suspended droplet. The standard oil droplets used originally by Millikan had a mass of $\sim 10^{-11}$ g

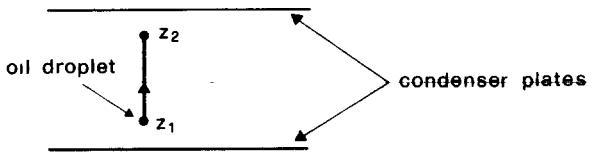

Fig. 2.1 The idea of the Millikan experiment.

(and a radius of 1 μ). Subsequent experiments were performed with somewhat heavier droplets up to 4×10^{-9} g (radius 7 μ). Indeed a search of quarks by Rank [16] has been performed by the Millikan method with droplets of that mass; but the results were disappointing: a broad distribution of residual charges from $-0.25e$ to $+0.3e$ was obtained showing – presumably – that the error in the determination of Q_R was, in these conditions, much too large for the method to be used. To employ usefully the Millikan technique in the search of quarks one has to continue using small droplets and move in the direction of fast authomatized measurements (see section 10.3 where other Millikan type experiments [17, 18, 19, 20] will be mentioned).

2.3. The basis of the magnetic levitation electrometer

The basis of the magnetic levitation electrometer is that a measurement of charge of heavy objects can be appropriately performed suspending the object by a force different from the electric force employed in measuring its charge. In other words one must be able to "levitate" an object possibly in vacuum (so that its charge does not change frequently due to the presence of ions) and, once the object is levitated, proceed to measure its charge. The more appropriate technique of levitation is the magnetic one; in the next subsection we digress briefly to illustrate some variants of such a technique.

2.4. Methods of magnetic levitation

In this type of experiments two methods of magnetic levitation have been used: (a) diamagnetic levitation, (b) ferromagnetic levitation with feedback. We shall discuss them below. Microwave induction levitation, used industrially for non-contact melting will not be considered here. Optical levitation [21] will also not be discussed.

2.4.1. Diamagnetic levitation

A sample of a diamagnetic substance tends to expel from its interior any externally applied magnetic field. A consequence of this is that if the sample is left free it moves from regions of high to regions of low magnetic field (diamagnetic bodies tend to be repelled by the gradients of the magnetic field).

Consider one of the two magnetic configurations shown in fig. 2.2. In fig. 2.2a the diamagnetic object O is shown on the axis of a horizontal coil C; in fig. 2.2b it is shown in the mid plane between the iron pole caps N, S, at some height z above the upper edge of the pole caps. In both cases the magnetic field increases when the object, moving down, approaches the plane $z = 0$; therefore the object experiences a force directed upwards. If at some z this force is sufficient to counteract the gravity, the object levitates. Stability with respect to lateral displacements is achieved by the use of a subsidiary coil D (as shown in fig. 2.2a) or by appropriately shaping the upper edges of the pole caps in the case of fig. 2.2b.

Two types of electrometers have been operated to search quarks exploiting the diamagnetic levitation: (1) Instruments at room temperature [5b, 22], making use of the small susceptivity of graphite at room temperature. Due to the smallness of this diamagnetism the magnetic configuration of these instruments is of the type of fig. 2.2b with large magnetic fields and gradients ($\sim 14 \times 10^3$ gauss, $\sim 12 \times 10^3$ gauss/cm). (2) Instruments at the temperature of liquid He [23], exploiting the huge, almost perfect diamagnetism of superconducting substances. Here a magnetic configuration of the type of fig. 2.2a is used. The magnetic field at the position of the object is ~1000 gauss and its gradient ~70 gauss/cm. Instruments using this type of levitation must be kept of course inside a cryostat.

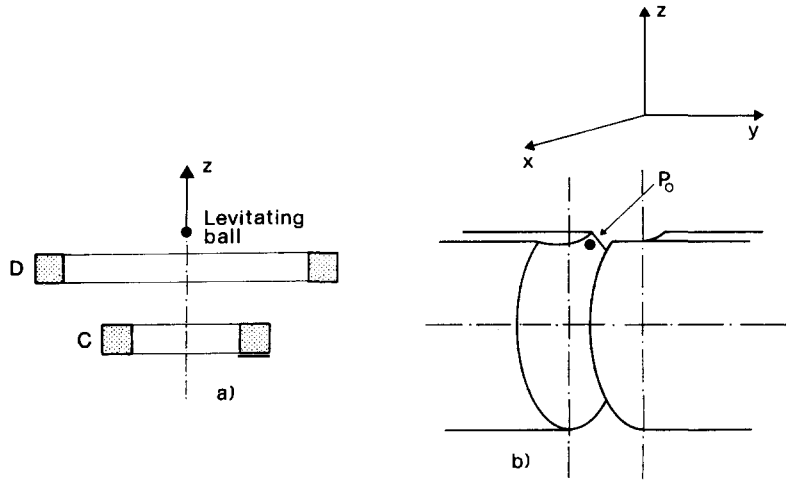

Fig. 2.2. Magnetic configurations appropriate to levitate a diamagnetic object: (a) is appropriate for strongly diamagnetic (superconducting) objects [23], whereas (b) applies to weakly diamagnetic objects [5b].

2.4.2. Ferromagnetic levitation with feedback

Ferromagnetic substances cannot have, different from diamagnetic ones, a stable equilibrium position in a static magnetic field. They can only have positions of unstable equilibrium (Earnshaw theorem [24]). Think of a piece of iron attracted upwards by a coil above it and pushed down by its weight; when displaced only slightly from its (unstable) equilibrium position it either goes up, to stick to the magnet, or falls down. To levitate it permanently a feedback mechanism has to be used: when the object tends to go up, the feedback decreases "instantaneously" the current in the coil, whereas the current is increased when the object tends to fall. In practice this feedback mechanism is produced – as shown in fig. 2.3 – by a lamp creating a shadow of the object on a photodetector. When the object falls (or raises) the shadow covers a smaller (or larger) fraction of the sensitive surface of the photodetectors and – via an appropriate amplifier – the current in the coil is increased (or decreased). The feedback system is equivalent, as far as the control of the vertical displacement is concerned, to a strong spring with strong damping, keeping the object in the preselected unstable equilibrium position. As to the lateral displacements their stability can be ensured by a proper shape of the magnetic field.

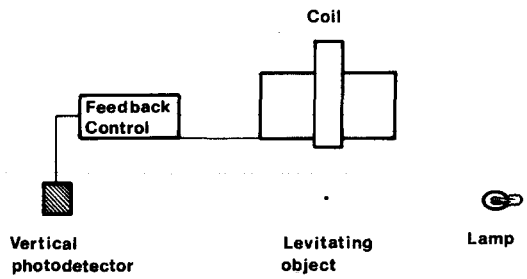

Fig. 2.3. Principle of the feedback levitation of ferromagnetic objects: the lamp produces a shadow of the object on the photodetector. This governs the current in the coil.

2.5. The measurement of the residual charge

Once the object levitates we are dealing with a harmonic oscillator having its equilibrium position at the position of levitation 0. Displacing the object by a small amount the restoring force is proportional to the displacement. The geometry of the magnetic field determines the directions x, y, z, corresponding to the proper frequencies of oscillation ν_x, ν_y, ν_z. Consider, to exemplify, the displacement along one of the above directions, say the x axis, which is taken to be the direction of the electric field (this means that the plates creating the electric field are placed as shown in fig. 2.4). We also assume, here, that the plates are wide and parallel so that the electric field between them is uniform. (Of course the assumption of a perfectly uniform electric field is never exact; the deviations from it will be discussed later.)

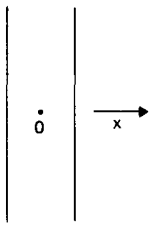

Fig. 2.4. The plates and the levitating object O. The x axis is chosen to be normal to the plates.

The force that the electric field exerts on the object is thus:

$$F_x = Q_i E_x \,. \tag{2.5}$$

Under the force (2.5) the object with charge Q_i and mass M undergoes a displacement Δ_i:

$$\Delta_i = \frac{F_x}{M\omega_x^2} = \frac{Q_i E_x}{M\omega_x^2} \tag{2.6}$$

where $\omega = 2\pi\nu_x$.

For a given electric field and a given mass we can rewrite (2.6) as:

$$\Delta_i = kQ_i \tag{2.7}$$

with $k = E_x/M\omega_x^2$. Inserting in (2.7) the expressions (2.1), (2.3) for the charge Q_i, for the two cases that a quark is not or is contained in the object, we obtain:

$$\Delta_i = n_i\delta \tag{2.8}$$

or

$$\Delta_i = (n_i \pm \tfrac{1}{3})\delta \tag{2.9}$$

where we have introduced the "step" δ:

$$\delta = ke\,. \tag{2.10}$$

The equations (2.8), (2.9) contain the principle of the method: a levitating object is prepared with an excess charge of a few electrons; ejecting these one by one, e.g. by photoionization, we record a sequence Δ_i of displacements. If the object does not contain a fractional charge, this sequence passes through the value $\Delta = 0$ (for instance, just to give an example, a sequence might be, in arbitrary units: 24, 12, 0, −12, −24...); if, instead, the object contains a quark of charge 1/3, the minimum cannot vanish; it equals 1/3 of the displacement corresponding to one electron charge, that is $\delta/3$ (the above sequence would then be: 28, 16, 4, −8, −20...., asymmetrical with respect to zero). We call Δ_R the residual displacement and Q_R the corresponding residual charge. If, for some object, a non-zero Q_R is found, one should of course be sure that this non-zero value is due to a fractional charge and not to some spurious effect produced by forces additional to QE_x (compare section 3).

Rather than operating with a static electric field it is convenient, for more than one reason, to use an alternating (square wave) field:

$$E_x(t) = E_x\,\eta(t) \tag{2.11}$$

where $\eta(t) = +1$ in the first half of each period, and $\eta(t) = -1$ in the second half.

In the field (2.11) the object oscillates with an amplitude A_i, proportional to its charge Q_i. It is:

$$A_i = f\Delta_i \tag{2.12}$$

where Δ_i is the static displacement (see eq. (2.7)); f is a frequency-dependent Lorentzian factor depending on how near the frequency of the electric field is to the mechanical frequency of the levitating harmonic oscillator. At resonance, for a square wave, it is:

$$f = \frac{4N_{1/2}}{\ln 2} \tag{2.13}$$

where $N_{1/2}$ characterizes the damping of the oscillator; $N_{1/2}$ is the number of free oscillations in the absence of the driving force after which the amplitude has decayed to a half.

All that we said in the previous section on the principle of the experiment in terms of the displacement Δ_i can be simply restated in terms of the oscillation amplitude A_i. A non-vanishing residual amplitude means – after elimination of the spurious charge effects – the presence, inside the object, of a fractional charge. The aim of the experiment is to measure the residual amplitude.

To give a feeling for the orders of magnitude we insert numbers in the formula

$$A = f\Delta = f\frac{QE_x}{4\pi^2\nu_x^2 M}\,. \tag{2.14}$$

In a typical case taking Q = one electron charge, $M = 10^{-4}$ g, $\nu_x = 1$ Hz, $N_{1/2} = 20$, $E_x = 2$ kV/cm we get $A \approx 1\ \mu$ (of course the really important number is the signal to noise ratio).

3. The electric forces on the levitating object

3.1. Introduction

Up to now we assumed, for simplicity, that the electric force on the levitating object is $Q\boldsymbol{E}^{(a)}$ where Q is the electric charge and $\boldsymbol{E}^{(a)}$ the applied electric field (the suffix a stands for applied).

This assumption is of course not true: as we shall see the force linear in $\boldsymbol{E}^{(a)}$ is not simply proportional to the electric charge Q; it has, in fact, the form (Q + "something else") $\boldsymbol{E}^{(a)}$. This "something else" implies that an object may appear possessing a non-zero residual charge also if its electric charge is zero. It is therefore essential to know precisely the expression of the force linear in the applied electric field: the "something else" in the force must either be shown to be negligible, or, if present, must be measured.

To make these remarks more concrete we anticipate here *one* piece of the electric force, to be described later in this section, the "patch" or Volta† force $\boldsymbol{F}^{V}$. It is (if $\boldsymbol{E}^{(a)}$ is directed – as we assume from now on – along the x axis):

$$F_x^{(V)} = 4\pi\varepsilon_0 r^3 \frac{\partial E_x^{(V)}}{\partial x} E_x^{(a)} . \tag{3.1}$$

In (3.1) r is the radius of the levitating object – assumed to be a conducting sphere –; $E_x^{(V)}$ is the x component of a tiny electric field (at the position of the object) due to dirt deposited on the plates or to local irregularities in the Fermi level of the metal of the plates (patches); $E_x^{(a)}$ is the x component of the applied electric field; and ε_0 is the dielectric constant of the vacuum = 8.59×10^{-12} (MKS units). Clearly $F_x^{(V)}$ adds to the force $QE_x^{(a)}$ acting on the true electric charge Q, producing a total force F_x:

$$F_x = \left(Q + 4\pi\varepsilon_0 r^3 \frac{\partial E_x^{(V)}}{\partial x}\right) E_x^{(a)} . \tag{3.2}$$

The second term in (3.2) simulates a spurious charge (we call it $Q^{(V)}$) given by:

$$Q^{(V)} = 4\pi\varepsilon_0 r^3 \, \partial E_x^{(V)}/\partial x . \tag{3.3}$$

Thus the object behaves as if it had a charge $Q + Q^{(V)}$. Unless we know $Q^{(V)}$ or eliminate it, we will not be able to determine the true electric charge Q of the object.

The equation (3.2) is only an example. Analyzing the force on the object we are going to find other "spurious terms" in addition to the "patch effect" term just described. The purpose of this section and of the ensuing one will be to identify and discuss these terms. We start with the purely electric forces, linear in the applied electric field and independent of the magnetic field. In section 3.6 we shall consider also the magneto-electric forces, again linear in the applied electric field but due to the simultaneous presence of the magnetic field.

In discussing the purely electric forces there is little to specify about the geometry or other details of

† When in ref. [22] we recognized the importance of eq. (3.1), we were led to think of the simple case of the contact potential between different metals, discovered by A. Volta (1795); hence the name "Volta force".

the instrument. We shall continue to call x the direction normal to the electric plates, assumed to be parallel, and consider the component F_x of the force, along the direction of motion of the object. The purely electric forces are: (1) The polarization force, (2) The Volta or patch force, (3) The unbalance force, (4) The force due to the permanent electric dipole moment of the levitating object (and those due to higher multipole moments). We proceed to consider the above forces in the order listed.

3.2. The polarization force

Any object in a non-uniform electric field experiences a polarization force $F_x^{(\mathrm{pol})}$: the electric field induces in the object an induced electric dipole moment and, in a non-uniform field, this moment experiences a force. For a conducting sphere the x component of this force, $F_x^{(\mathrm{pol})}$ is:

$$F_x^{(\mathrm{pol})} = \alpha \boldsymbol{E} \cdot \frac{\partial \boldsymbol{E}}{\partial x} \tag{3.4}$$

where the polarizability α is:

$$\alpha = 4\pi\varepsilon_0 r^3 \tag{3.5}$$

and r is the radius of the sphere. Inserting for $\boldsymbol{E}$ in (3.4) the applied electric field $\boldsymbol{E}^{(\mathrm{a})}$ and calling $F_x^{(\mathrm{a\text{-}pol})}$ the expression (3.4) with $\boldsymbol{E}$ replaced by $\boldsymbol{E}^{(\mathrm{a})}$, it is easy to see that no spurious charge effect arises from $F_x^{(\mathrm{a\text{-}pol})}$. The reason is that $F_x^{(\mathrm{a\text{-}pol})}$ is quadratic in $\boldsymbol{E}^{(\mathrm{a})}$ and produces a motion at frequency $2\nu_r$, twice the frequency of $\boldsymbol{E}^{(\mathrm{a})}$. If the detection system reveals selectively only the motion at the resonance frequency ν_r either because only this motion is resonance enhanced, or because frequencies different from ν_r are filtered away, or both, then $\boldsymbol{F}^{(\mathrm{a\text{-}pol})}$ is irrelevant. Note also that: (1) If $E^{(\mathrm{a})}(t)$ is a perfect square wave, $(E^{(\mathrm{a})}(t))^2$ is a constant and the signal at $2\nu_r$ is absent. (2) The above arguments showing the vanishing of $\boldsymbol{F}^{(\mathrm{a\text{-}pol})}$ are true even if $\partial \boldsymbol{E}^{(\mathrm{a})}/\partial x$ is non-zero; but in fact, in our set-up, the gradients are very small due to the parallelism of the plates and, therefore, $\boldsymbol{F}^{(\mathrm{a\text{-}pol})}$ is absent also for this reason.

3.3. The Volta force or patch effect

Though the polarization force due to $\boldsymbol{E}^{(\mathrm{a})}$ vanishes, a very important term still arises from (3.4); it was already written in section 3.1 and we now derive it [22]. It originates as follows: in (3.4) we should not insert only – as we did in section 3.2 – the applied electric field $\boldsymbol{E}^{(\mathrm{a})}$ but the total electric field $\boldsymbol{E}$ acting on the object. This total field is the sum of $\boldsymbol{E}^{(\mathrm{a})}$ plus the possible static field $\boldsymbol{E}^{(\mathrm{V})}$ due to the reasons already mentioned in section 3.1. Thus we must write:

$$\boldsymbol{E} = \boldsymbol{E}^{(\mathrm{a})} + \boldsymbol{E}^{(\mathrm{V})} . \tag{3.6}$$

The potential differences corresponding to the Volta fields have typical values of some tens millivolts and these fields are therefore exceedingly small with respect to $\boldsymbol{E}^{(\mathrm{a})}$. But, as we now see, they are important. Indeed inserting (3.6) into (3.4) we get – in addition to the unimportant term $\boldsymbol{F}^{(\mathrm{a\text{-}pol})}$ quadratic in $\boldsymbol{E}^{(\mathrm{a})}$ discussed in the previous section and to an irrelevant term quadratic in $\boldsymbol{E}^{(\mathrm{V})}$ – a cross term between $\boldsymbol{E}^{(\mathrm{a})}$ and $\boldsymbol{E}^{(\mathrm{V})}$. We call this $\boldsymbol{F}^{(\mathrm{V})}$:

$$F_x^{(V)} = \alpha\left(E^{(V)}\frac{\partial E^{(a)}}{\partial x} + E^{(a)}\frac{\partial E^{(V)}}{\partial x}\right). \tag{3.7}$$

The first addendum on the right-hand side of (3.7) is generally negligible in comparison to the second and can be omitted. Therefore:

$$F_x^{(V)} \cong \alpha E^{(a)} \cdot \frac{\partial E^{(V)}}{\partial x}. \tag{3.8}$$

It has already been noted in section 3.1 that the effects of this term simulate those of a residual charge (compare eq. (3.2)).

The procedure used in our experiment to separate $Q^{(V)}$ from the true charge Q will be sketched here – and illustrated in *much* detail later (section 8.8). Assuming that the other spurious charge effects to be considered in the rest of this section have been subtracted or eliminated, the separation of $Q^{(V)}$ from Q takes place as follows: (a) Balls with the same radius are measured in succession in conditions where the patches do not change: if a ball does contain a quark, and the subsequent one does not, the difference in their residual charge must be $\pm\frac{1}{3}e$. (b) Runs of the above type (in which different balls of diameter 0.2 mm are compared) are intermixed with runs or measurements on balls of diameter 0.3 mm. Because $Q^{(V)}$ depends on r^3 (see eq. (3.5)) this information confirms the normalization of the patch spurious charge.

3.4. The "unbalance force"

Another descendant of the polarization force is the so-called "unbalance force". We clarify its origin here.

In the square wave applied to the plates the average potential difference (over many periods) of *each plate* with respect to the walls of the levitation chamber should vanish to a good precision. Of course it vanishes exactly, by definition, for a perfect square wave, but, in the real situation, asymmetries can be present; they may be due, for instance, to a difference in the switching times of the reed relays producing the inversion of the signal of the two plates. If a non-zero average occurs, this is equivalent to a time independent potential above zero applied to the plate in question and this produces – due to edge effects – a gradient at the position of levitation (see the next section). Calling this gradient $\partial E_x^{(unb)}/\partial x$, where the suffix (unb) stands for "unbalance", we thus have an unbalance force:

$$F_x^{(unb)} = \alpha E_x^{(a)} \partial E_x^{(unb)}/\partial x. \tag{3.9}$$

As it will be seen in section 4.2 the above gradient is negligible if the plates have a large diameter and a small separation. For instance for plates with diameter 11.2 cm at 2 cm separation (as in our case) an unbalance by 0.5 V on one plate produces an effect corresponding to $\sim 10^{-2}$ electron charges on a ball with diameter 0.3 mm (and an effect $(1.5)^3$ times smaller on a ball with diameter 0.2 mm).

3.5. The permanent electric dipole force

This force due to the permanent electric dipole moment $\boldsymbol{d}$ of the ball

$$F_x^{(\text{dipole})} = \boldsymbol{d} \cdot \frac{\partial \boldsymbol{E}^{(a)}}{\partial x} \tag{3.10}$$

only exists in the presence of a non-uniform field $\boldsymbol{E}^{(a)}$ (whereas it is important to note that the Volta force (3.1) is there also if $\boldsymbol{E}^{(a)}$ is perfectly uniform). Again this dipole force is linear in $\boldsymbol{E}^{(a)}$ and simulates therefore a residual charge. To estimate (3.10) one has to know the permanent electric dipole moment of the levitating ball. This is done creating a known gradient of the applied electric field at the position of the ball and measuring the corresponding change of the force acting on the ball. Even for the largest electric dipole moment found in our experiment (~ one electron × meter) the parallelism and flatness of the plates ensure that in the normal working conditions the force (3.10) is unimportant. The same conclusion is true for the force due to the higher electric multipole moments (e.g. quadrupole).

3.6. The magneto-electric force

We now turn to those forces on the levitating object – again linear in the applied electric field – that are due to the simultaneous presence of the electric field and the magnetic field (used for the levitation). What happens can be roughly stated as follows (compare fig. 4.2): the levitating object has a permanent electric dipole moment $\boldsymbol{d}$. The alternating electric field $\boldsymbol{E}^{(a)}$ produces a torque on it – given by $\boldsymbol{d} \times \boldsymbol{E}^{(a)}$ – and therefore a tilting of the object. This tilting implies a tilting of the permanent magnetic moment of the ball $\boldsymbol{\mu}$. This, in turn, entails a variation of the force on the object because the object moves in a region of non-uniform magnetic field (a tilting magnetic moment in a non-uniform magnetic field experiences an oscillating force). The details of this magneto-electric force $\boldsymbol{F}^{(\text{m e})}$ depend on a number of circumstances and, in particular, on whether the magnetic field used to levitate is parallel or orthogonal to the applied electric field; we shall discuss all this in section 4.4.

In the Genoa experiment where the electric field is normal to the magnetic field and the ball spins rapidly around the z axis the magneto-electric force is present. As we shall see (section 4.4) it is:

$$F_x^{(\text{m.e})} = \beta E_x^{(a)} \partial H_x / \partial x \tag{3.11}$$

where β is a coefficient typical of each sphere. In (3.11) $\partial H_x/\partial x \equiv H_{xx}$ is the x gradient of the x component of the magnetic field at the position of levitation. The method we use to measure $F_x^{(\text{m e.})}$ is to change H_{xx} (keeping the ball being measured in levitation) and measure the corresponding change of the force acting on the ball. From this change we can determine β and, therefore, also the quantity of interest, namely the apparent charge due to the magneto-electric force:

$$Q^{(\text{m e})} = \beta H_{xx} . \tag{3.12}$$

This can then be subtracted. The details of the procedure will appear in section 8.

3.7. Summary

In conclusion the total electric force, linear in the applied electric field, acting on the object can be written:

$$F_x = \left[Q + \alpha \frac{\partial E_x^{(V)}}{\partial x} + \alpha \frac{\partial E_x^{(\text{unb})}}{\partial x} + \beta \frac{\partial H_x}{\partial x} \right] E_x^{(a)} + \boldsymbol{d} \cdot \frac{\partial \boldsymbol{E}^{(a)}}{\partial x} + F_x^{(\text{higher multipoles})} \tag{3.13}$$

The first term is the force on the electric charge, the second that due to the patch effect, the third the unbalance force, the fourth the magneto-electric force, the fifth that on the electric permanent dipole moment and the last that on higher multipoles. Note that the simple expression given in (3.11) and (3.13) of this magneto-electric force is only valid if the object does spin (as in our case) around the z axis, the main magnetic field is directed along the z axis and the electric field along the x axis.

As it has been stated in this section the only terms of importance in (3.13) are, in fact:

$$F_x = \left(Q + \alpha \frac{\partial E_x^{(V)}}{\partial x} + \beta \frac{\partial H_x}{\partial x}\right) E_x^{(a)} = (Q + \alpha E_{xx}^{(V)} + \beta H_{xx}) E_x^{(a)} . \tag{3.14}$$

We shall discuss this expression at length in section 8.

We underline, in concluding this section, that we have not considered the effect of the image fields (due to the presence of the plates) from the charge of the object or from its static or induced electric dipole moments. In our set up – due to spinning – no appreciable effect of this type is present, and therefore in the next section, dealing with the calculation of the electric fields at the position of the object, such image fields will not be discussed. They will be mentioned again in section 9 (see paragraph 9.3.1) in connection with the Stanford experiment, where, due to the lack of spinning and the reduced distance between the plates, they must be considered.

4. Additional remarks on the forces producing spurious effects

4.1. The electric field of a patch

We now calculate the electric field at the position of the object in several situations of interest for an estimate of the patch force. The notation is clarified in fig. 4.1; cylindrical coordinates around the x axis are used. We start with the following problems:

(a) Calculate the field at the position of the object with the boundary conditions: potentials $+V_0$, $+V_0$ on the two plates at $x = \pm a$, $\rho < R$; potential zero for $x = \pm a$, $\rho > R$.

(b) Same as above, but with potentials $-V_0$, $+V_0$ instead of $+V_0$, $+V_0$.

The case (a) will be called (+, +); the case (b), (−, +). It goes without saying that the requirement of

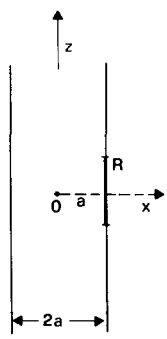

Fig. 4.1. The notation used for the calculations of patch effects. The circular plates 1, 2 (an xz section is shown) are normal to the x axis. On plate 1 a circular patch of radius R appears – at the center of the plate in front of object O; the distance between the plates is $2a$. Cylindrical coordinates x, ρ around the x axis are used.

vanishing potential for $x = \pm a$, $\rho > R$ can only be a rough simplification of the correct boundary conditions. It will appear, however, that this simplification is acceptable in our case.

Because the object is near to the origin, we are interested in the derivative of E_x with respect to x for $\rho = 0$, $x = 0$; we confine to display this quantity. In the case $(+, +)$ we produce both the exact result and approximate expressions for $R \gg a$ and $R \lesssim 2a$; in the case $(-, +)$ only the approximate expression will be given.

(1) *Case* $(+, +)$.

At $\rho = 0$, $x = 0$ we have:

$$\frac{\partial E_x}{\partial x} = \frac{6V_0R^2}{a^4} \sum_{k=0}^{\infty} (-1)^k \frac{2k+1}{[(R/a)^2 + (2k+1)^2]^{5/2}} \qquad \text{(exact)} \tag{4.1}$$

$$\frac{\partial E_x}{\partial x} = \frac{6V_0R^2}{a^4} \frac{1}{[(R/a)^2 + 1]^{5/2}} \qquad (R \lesssim 2a) \tag{4.2}$$

$$\frac{\partial E_x}{\partial x} = \frac{V_0\pi^2}{2a^2} \left(\frac{R}{a}\right)^{1/2} \exp\left(-\frac{\pi R}{2a}\right) \qquad (R \gg a)\,. \tag{4.3}$$

(2) *Case* $(-, +)$.

We have, at $\rho = 0$:

$$\frac{\partial E_x}{\partial x} = V_0 \frac{\pi^2}{a^2} \left(\frac{2R}{a}\right)^{1/2} \exp\left(-\frac{\pi R}{a}\right) \sin\frac{\pi x}{a} \qquad (R \gg a, \text{ any } x) \tag{4.4}$$

$$\frac{\partial E_x}{\partial x} = \frac{6V_0R^2}{a^4} \frac{x}{a} \left[\frac{1 - R^2/4a^2}{[1 + R^2/a^2]^{7/2}} + O(10^{-2})\right] \qquad R \lesssim 2a,\ x \ll a\,. \tag{4.5}$$

Here the second expression, eq. (4.5), holds only for $x \ll a$.

We first apply the above formulas to discuss the presence of a patch on one of the plates. The symbol V_0 in the above formulas then stands for the potential of the patch (above that of the plate); we assume a circular patch of radius R_p having its center at the center of one plate†. In calculating the spurious charge $Q^{(V)}$ (eq. (3.3)) we use the expressions of $\partial E_x/\partial x$ (putting $R = R_p$) given in equations (4.1) to (4.5). To be precise assume that a circular patch (of radius R_p and potential V_0) is present on plate 1. Its effect can be calculated decomposing $V_0^{(1)}$ as $V_0^{(1)} = \frac{1}{2}\{V_0^{(1)} + V_0^{(2)}\} + \frac{1}{2}\{V_0^{(1)} - V_0^{(2)}\}$; it is, therefore, equivalent to that produced by a superposition of the $(+, +)$ case (with potentials $+\frac{1}{2}V_0$, $+\frac{1}{2}V_0$) and of the $(-, +)$ case (with potentials $-\frac{1}{2}V_0$, $+\frac{1}{2}V_0$).

Now a straightforward consequence of the equations (4.1) to (4.5) is that $\partial E_x/\partial x|^{(-,+)} \ll \partial E_x/\partial x|^{(+,+)}$ both for $R_p \gg a$ and for $R_p \lesssim 2a$ (if $x/a \ll 1$); that is, in practice, $\partial E_x/\partial x|^{(-,+)}$ is negligible with respect to $\partial E_x/\partial x|^{(+,+)}$. It follows that in establishing the effect of a patch we can only consider the case $(+, +)$.

Assume first that $R_p \lesssim a$ (so that eq. (4.2) applies) and ask which is, for a given value of a, the radius of the most "malefic" patch. The maximum value of the right-hand side of (4.2) is obtained for:

$$R_p/a = \sqrt{\tfrac{2}{3}} \tag{4.6}$$

†We confine here to study the "worst" patches; an ensemble of "micropatches" produces smaller effects and will not be considered.

and we get:

$$\text{Max}\left.\frac{\partial E_x}{\partial x}\right|_{\rho=0,x=0}^{(+,+)} = \frac{0.56\,V_0^{(1)}}{a^2}\,. \tag{4.7}$$

We conclude that a circular patch on one plate having the most "malefic" radius and potential $V_0^{(1)}$ (the suffix $^{(1)}$ recalls that the patch is *only* on plate 1) produces a spurious charge $Q^{(V)}$ given by:

$$Q^{(V)} = 4\pi\varepsilon_0 r^3 \times 0.56\,V_0^{(1)}/a^2 \tag{4.8}$$

where r and a are expressed in meter and $V_0^{(1)}$ in volt. In our case we have for $r = 1.5\times10^{-4}$ m, $a = 1$ cm:

$$Q^{(V)} = 2.03\,V_0^{(1)} \times 10^{-18}\ \text{coulomb}\,. \tag{4.9}$$

Some knowledge of $V_0^{(1)}$ is essential at this stage. Using a Monroe electrostatic (non contact) voltmeter (Mod. 162) we could establish that the patches on plates cleaned by standard procedure and exposed to the air are usually not larger than 30 mV. Inserting this number in (4.9) we get (*for balls of* $\Phi = 0.3\ mm$)

$$Q^{(V)}_{\text{expected}} = 6\times10^{-20}\ \text{coulomb} = 0.37\ \text{electron charge}\,. \tag{4.10}$$

Obviously this is only an estimate. The 30 mV used above can reduce to 10 mV or can increase, say, to 50 mV. The radius R_p of the patch can differ from the most "malefic" one of ~0.82 cm (in our case of $a = 1$ cm). Note that for balls of 0.2 mm diameter $Q^{(V)}$ is reduced by a factor $(1.5)^3 = 3.375$ with respect to the estimate (4.10); that is *for balls of* 0.2 *mm diameter*:

$$Q^{(V)}_{\text{expected}} = 0.11\ \text{electron charges}\,. \tag{4.11}$$

We shall show in section 8.7 (see figs. 8.8 and 8.9) how these estimates compare with the experimental results.

To conclude this discussion we consider now a situation in which $R \gg a$; we assume that a patch due, for instance, to the formation of some oxide over all the surface of one plate, covers totally and uniformly a plate. In this case the equation (4.3) applies. For $R = 5.6$ cm, $a = 1$ cm, $V_0^{(1)} = 1$ volt it is, using the equation (4.3) with balls of 0.3 mm diameter, $Q^{(V)} = 2.5\times10^{-2}$ electron charges. Note that we have taken here $V_0^{(1)} = 1$ volt, a value that is certainly not justified by any measurement with the electrostatic voltmeter. We inserted this value simply to show that this case of an "extended patch" is irrelevant. The only important case is the one, described previously, of a patch having a size comparable to a (compare eq. (4.6)). *Note that, for a given* $V_0^{(1)}$, *the effect of such a patch decreases as* a^{-2}.

4.2. The unbalance effect

The equations (4.1)–(4.5) allow the calculation of the unbalance effect. A hypothetical unbalance of 1 volt on one plate produces, indeed, the same effect just calculated assuming that an oxide patch of 1 volt was covering uniformly a whole plate; namely for balls of 0.3 mm diameter:

$$Q\,(\text{unbalance with } V_0^{(1)} = 1 \text{ volt}) = 2.5 \times 10^{-2} \text{ electron charges}\,. \tag{4.12}$$

Because we control such unbalances to 0.1 volt we have, in the experimental situation, for the 0.3 balls:

$$Q(\text{unbalance}) \lesssim 0.25 \times 10^{-2} \text{ electron charges}\,. \tag{4.13}$$

For balls of diameter 0.2 mm the effect is 3.37 times smaller. The equation (4.12) can be checked experimentally creating artificially a large unbalance (say +500 V, +500 V) and measuring its effect. To 10% the result of this measurement agrees with eq. (4.12); this shows that the approximations made in calculating $\partial E_x/\partial x$ and, in particular the schematization of the boundary conditions, are good.

Larger discrepancies between the calculated and measured values do arise for the (−, +) effects, although it remains true that the measured (−, +) effects are negligible – by more than one order of magnitude – with respect to the (+, +) effects; the discrepancies just mentioned are due presumably, to the circumstance that (as it can be shown in detail) tiny asymmetries between the plates strongly influence the effects of (−, +) type, but not those of the (+, +) type.

4.3. More details on the calculations of section 4.1

For completeness we record below the main steps in the calculations leading to the equations (4.1) to (4.5). The starting equation $\Delta V = 0$ can be rewritten in cylindrical coordinates (and confining to the case of a cylindrically symmetric solution around the x axis):

$$\frac{\partial^2 V}{\partial \rho^2} + \frac{1}{\rho}\frac{\partial V}{\partial \rho} + \frac{\partial^2 V}{\partial x^2} = 0\,. \tag{4.14}$$

Particular solutions appropriate to deal with the (+, +) and respectively (−, +) boundary conditions have the form:

$$V_k(\rho|x) = C_k \cosh kx\, J_0(k\rho) \qquad (+,+)\,. \tag{4.15}$$

$$V_k(\rho|x) = C_k \sinh kx\, J_0(k\rho) \qquad (-,+)\,. \tag{4.16}$$

To satisfy the boundary conditions we form superpositions of these solutions:

$$V(\rho|x) = \int_0^\infty C(k) \cosh kx\, J_0(k\rho)\, \mathrm{d}k \qquad (+,+) \tag{4.17}$$

$$V(\rho|x) = \int_0^\infty C(k) \sinh kx\, J_0(k\rho)\, \mathrm{d}k \qquad (-,+)\,. \tag{4.18}$$

Using the Fourier Bessel transform [25], $C(k)$ can be determined in (4.17), (4.18) so as to satisfy the conditions a) or b) of the text respectively in the (+, +) and (−, +) cases. Using the equation:

$$\frac{\mathrm{d}}{\mathrm{d}y}\, y J_1(y) = y J_0(y)$$

and the Fourier Bessel transform we obtain respectively:

$$V(\rho|x) = V_0 R \int_0^\infty \frac{J_1(kR)}{\cosh ka} J_0(k\rho) \cosh kx \, dk \qquad (+,+)$$

$$V(\rho|x) = V_0 R \int_0^\infty \frac{J_1(kR)}{\sinh ka} J_0(k\rho) \sinh kx \, dk \qquad (-,+).$$

For $\rho = 0$ it is $J_0(k\rho) = 1$ and:

$$V(0|x) = V_0 R \int_0^\infty J_1(kR) \frac{\cosh kx}{\cosh ka} dk \qquad (+,+)$$

$$V(0|x) = V_0 R \int_0^\infty J_1(kR) \frac{\sinh kx}{\sinh ka} dk \qquad (-,+).$$

It is convenient to evaluate directly the expression of $\partial E_x/\partial x$ (that is $\partial^2 V/\partial x^2$), the quantity of direct interest in the evaluation of (3.3). It is:

$$\left.\frac{\partial E_x}{\partial x}\right|^{(+,+)} = V_0 R \int_0^\infty J_1(kR)\, k^2 \frac{\sinh k(a+x) + \sinh k(a-x)}{\sinh 2ka} dk \tag{4.19}$$

$$\left.\frac{\partial E_x}{\partial x}\right|^{(-,+)} = V_0 R \int_0^\infty J_1(kR)\, k^2 \frac{\sinh kx}{\sinh ka} dk . \tag{4.20}$$

In obtaining (4.19) use has been made of the identity:

$$\frac{\cosh kx}{\cosh ka} = \frac{\sinh k(a+x) + \sinh k(a-x)}{\sinh 2ka}.$$

At this point the Heine integral [26] (with $\nu = 1$) is of use:

$$\int_0^\infty \frac{\sinh \alpha y}{\sinh \pi y} J_\nu(by)\, y^{\nu+1} dy = \frac{2}{\pi} \sum_{n=1}^\infty (-1)^{n-1} \sin n\alpha \, K_\nu(nb). \tag{4.21}$$

Using eq. (4.21) we can transform (4.19) and (4.20) respectively into:

$$\left.\frac{\partial E_x}{\partial x}\right|^{(+,+)} = \frac{\pi^2}{2a^3} V_0 R \sum_{n=1}^\infty (-1)^{n-1} n^2 \sin \frac{n\pi}{2} K_1\left(\frac{n\pi R}{2a}\right) \tag{4.22}$$

$$\left.\frac{\partial E_x}{\partial x}\right|^{(-,+)} = \frac{2\pi^2}{a^3} V_0 R \sum_{n=1}^{\infty} (-1)^{n-1} n^2 \sin\frac{n\pi x}{a} K_1\left(\frac{n\pi R}{a}\right) \tag{4.23}$$

where the first expression $(+,+)$ has been written only for the case $x = 0$ (the expression (4.23) for the case $(-,+)$ vanishes of course at $x = 0$).

The equations (4.22), (4.23) can be used as they stand for large R ($R \gg a$), because then the first term in the sum on the right-hand sides dominates. Moreover for large z ($z \gg 1$) the Bessel function $K_1(z)$ is approximated by:

$$K_1(z) \approx \sqrt{\frac{\pi}{2z}}\, e^{-z}\left(1 + \frac{3}{8z} + \cdots\right) \tag{4.24}$$

so that the equations (4.3) and (4.4) are obtained.

If, instead, R is small ($R \lesssim 2a$), it is necessary to rearrange the sum on the right-hand sides of (4.22), (4.23). In doing this we confine to the case $(+,+)$; the case $(-,+)$ can be treated similarly.

We start from the identity [27]:

$$\sum_{n=1}^{\infty} (-1)^{n-1} n^2 \sin\frac{n\pi}{2} K_1(ny) = -\frac{\mathrm{d}}{\mathrm{d}y}\frac{1}{y}\left[\frac{\mathrm{d}}{\mathrm{d}t}\sum_{n=1}^{\infty} (-1)^n K_0(ny)\cos nxt\right]_{t=\pi/2y} \tag{4.25}$$

and use the following equation:

$$\sum_{n=1}^{\infty} (-1)^n K_0(ny)\cos nyt = \frac{1}{2}\ln\frac{\gamma y}{4\pi} + \frac{\pi}{2}\sum_{m=1}^{\infty}\left[\frac{1}{(x^2 + [(2m-1)\pi - ty]^2)^{1/2}} - \frac{1}{2\pi m}\right] + \frac{\pi}{2}\sum_{m=1}^{\infty}\left[\frac{1}{(x^2 + [(2m-1)\pi + ty]^2)^{1/2}} - \frac{1}{2\pi m}\right] \tag{4.26}$$

where γ is the Euler constant.

Performing the derivatives indicated in (4.25) and making some rearrangements of terms we are then led, with some algebra, to:

$$\sum_{n=1}^{\infty} (-1)^{n-1} n^2 K_1(ny)\sin\frac{n\pi}{2} = 24\pi^2 y \sum_{k=0}^{\infty} (-1)^k \frac{2k+1}{(4y^2 + (2k+1)^2\pi^2)^{5/2}}. \tag{4.27}$$

Writing in (4.27) $y = \pi R/2a$ and substituting in eq. (4.22) we obtain the exact equation (4.1). The approximate equation (4.22) is then obtained simply taking only the first term in the sum on the right-hand side of (4.22) which is acceptable if $R \lesssim 2a$.

4.4. The magneto-electric force as a "tilting" effect

We shall now expand a little on the magneto-electric force briefly described in section 3.6 and on the tilting mechanism that generates this force. It should be added, first of all, that the recognition that the tilting mechanism is responsible for the magneto-electric force is due to Buckingham and Herring [28]. When we identified the magneto-electric force [29, 30] we did, in fact, suggest [30, 31] the tilting

mechanism, but we dismissed it because we did believe, incorrectly, that the gyroscopic stability of the axis of rotation due to the spinning of the ball was strong enough to prevent the tilting. We now know, thanks to ref. [28] that, at the spinning frequency of our object, the gyroscopic stability is not sufficient to prevent the tilting and it is precisely this tilting (and not a "surface magneto-electric effect" that we had hypothetized) which is the reason of the magneto-electric force*.

Following ref. [28] we consider here the tilting in more detail because, as we shall see (compare ref. [28]) this leads to the interesting result:

$$\beta = d_z/H_z \tag{4.28}$$

an equation connecting the coefficient β in (3.11) with the z component of the permanent electric dipole moment of the sphere and the vertical magnetic field H_z at the position of levitation. This relationship can be easily checked experimentally and fits beautifully the data, as we shall show in section 8.10.

Let us recall that in our instrument – to which the discussion of this subsection refers – the ball spins at ~400 Hz around the vertical z axis so that d_x and d_y are averaged out. Only d_z does not vanish and it is d_z that appears in (4.28). To derive (4.28) assume first that the ball does not spin but that, nevertheless, $\boldsymbol{d}$ is directed along z in the absence of $\boldsymbol{E}$. Also $\boldsymbol{\mu}$ (the permanent magnetic dipole moment of the ball) will naturally be directed along z, of course, at least for a homogeneous ball (compare fig. 4.2).

On inserting E_x a torque acts on the sphere: $\boldsymbol{d}$ tends to align with E_x whereas $\boldsymbol{\mu}$ tends to stay parallel to H_z: the torque then turns $\boldsymbol{d}$ by an angle θ such that (for small θ, as it is the case in practice: the typical θ is 10^{-5} rad):

$$\mu H_z \theta = d_z E_x \,. \tag{4.29}$$

Thus:

$$\theta = \frac{d_z E_x}{\mu H_z} \,. \tag{4.30}$$

Because E_x changes sign periodically, θ does the same and μ_x can be written:

$$\mu_x = \mu\theta = \frac{d_z E_x}{H_z} \,.$$

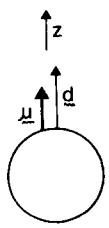

Fig. 4.2. The levitating ball with its electric permanent dipole moment $\boldsymbol{d}$ directed along the z axis and the magnetic permanent moment $\boldsymbol{\mu}$ in the same direction.

* Some statements in ref. [28] implying an inconsistency of our data have been shown to be incorrect. Compare [42]; see also section 8.11.

The force $F_x^{(\mathrm{m.e.})}$ acting on μ_x is, therefore:

$$F^{(\mathrm{m.e.})} = \mu_x \frac{\partial H_x}{\partial x} = \frac{d_z}{H_z} E_x \frac{\partial H_x}{\partial x} . \tag{4.31}$$

This is precisely eq. (3.11) with β given by (4.28).

So far we have not considered the fact that the ball spins around the z axis (we used this fact only to ignore d_x and d_y).

We now include, following ref. [28], the spin in our treatment. Calling $\boldsymbol{L}$ the angular momentum of the ball, both $\boldsymbol{\mu}$ (the permanent magnetization) and $\boldsymbol{d}$ (the permanent electric dipole moment) are directed along $\boldsymbol{L}$: the components of the above vectors orthogonal to $\boldsymbol{L}$ average out. The modulus of $\boldsymbol{L}$ stays constant in magnitude (it is equal to $I\omega$, where I is the moment of inertia and ω the spin angular velocity) and we can write:

$$\dot{\boldsymbol{L}} = \frac{\mu \boldsymbol{L}}{I\omega} \times \boldsymbol{H} + d \frac{\boldsymbol{L}}{I\omega} \times \boldsymbol{E} = \frac{\mu}{I\omega} \boldsymbol{L} \times \boldsymbol{H}_{\mathrm{eff}} \tag{4.32}$$

where, in the last expression, we have defined:

$$\boldsymbol{H}_{\mathrm{eff}} = \boldsymbol{H} + \frac{d}{\mu} \boldsymbol{E} ; \tag{4.33}$$

$\boldsymbol{H}_{\mathrm{eff}}$ is very near to $\boldsymbol{H}$, but it is precisely the difference between $\boldsymbol{H}_{\mathrm{eff}}$ and $\boldsymbol{H}$ to produce the tilting: indeed at each semiperiod the direction of $\boldsymbol{E}$ reverses so that the precession of $\boldsymbol{L}$ takes place around an axis switching its direction from that of $\boldsymbol{H} + (d/\mu)\boldsymbol{E}$ to $\boldsymbol{H} - (d/\mu)\boldsymbol{E}$. The precession angular frequency of $\boldsymbol{L}$ is $\omega_{\mathrm{p}} \cong \mu H / I\omega$ where ω is the spin angular frequency. For a μ value corresponding to a typical residual magnetization and for values of H, I and ω characteristic of our situation ($\omega = 2\pi \times 400\,\mathrm{sec}^{-1}$) it is $\nu_{\mathrm{p}} = \omega_{\mathrm{p}}/2\pi = 200$ Hz. This is much larger than the frequency of ~ 1 Hz at which the spin axis switches between the two directions mentioned above; therefore $\boldsymbol{L}$ has the time to make many turns around each of the above directions and, in practice, things go as if the static tilting described above were operating. (To cancel this tilting by what we did call the "gyroscopic stability" spinning frequencies much larger – 1000 times, say, – than that we use would be needed.) We conclude that the coefficient β in our expression of the magneto-electric force is given by (4.28) as shown by Buckingham and Herring: note the important fact that β does not depend on the residual permanent magnetic moment of the ball.

If the electric field is not uniform the expression (4.31) of the magneto-electric force has to be summed with the purely electric force acting on the permanent electric dipole moment. If we produce an inclination of the plate P_1 with respect to P_0, as we do when we measure d_z, and we create, therefore, a non-zero $\partial E_x/\partial z$ $(= \partial E_z/\partial x)$ the total force becomes:

$$F_x = \frac{d_z}{H_z} E_x \frac{\partial H_x}{\partial x} + d_z \frac{\partial E_z}{\partial x} . \tag{4.34}$$

Note that this can also be written as:

$$F_x = \beta \left(E_x \frac{\partial H_x}{\partial x} + H_z \frac{\partial E_z}{\partial x} \right) \tag{4.35}$$

as if the force in question were due to a term:

$$W = \beta(\boldsymbol{E} \cdot \boldsymbol{H}) \tag{4.36}$$

added to the energy of the object. Indeed, in our first identification of the magneto-electric force [30] we introduced precisely this assumption, that a term of the form (4.36) had to be added to the energy.

An important feature of (4.34) is that we can measure d_z exploiting the second term in the right-hand side of (4.34) (via the inclination of P_1) or we can measure it using the first term in (4.34) (via a variation of $\partial H_x/\partial x$). The two values of d_z – measured entirely independent – must turn out to be equal. Stated differently we have two independent ways to measure d_z: producing a force on d_z due to an electric gradient, or measuring the tilting force by a variation of $\partial H_x/\partial x$: d_z^{E} (determined electrically) and d_z^{M} (determined magnetically) should be equal. We have done this test on many different balls and complete agreement is obtained, as we shall illustrate in section 8. This is a gratifying check of the internal consistency of the measurements.

5. The first generation experiments

Before expanding on the two more recent and larger experiments by the Genoa and Stanford group, we digress briefly to review the first generation experiments. After the Genoa graphite electrometer (1965) [5, 22] another graphite experiment was performed by a soviet group (1968) [32] and in 1970 the Stanford group published [23] preliminary results from their low temperature niobium set up. A Syracuse experiment [33] opened the series of the ferromagnetic levitometers with feedback; this was followed by two other experiments along the same line, at the University of Virginia [34] and at Moscow [35].

5.1. The graphite experiments

The diamagnetic levitation of pyrolitic graphite at room temperature (shown to be possible in 1939 by W. Braunbeck [36]) was used in the first experiment of this type in our laboratory. The magnetic configuration adopted in the set-up consisted of two pole caps of an electromagnet having the shape sketched in fig. 5.1. Because of the small diamagnetic susceptivity of graphite (albeit much larger, per unit mass, than that of all the other diamagnetic substances at room temperature) a large product $\boldsymbol{H} \cdot \partial \boldsymbol{H}/\partial z$ is needed to sustain a graphite grain; therefore the pole caps A, B have to be placed at a comparatively small distance; with our electromagnet and pole shape, 1.8 cm was the maximum distance that we could achieve. It is possible that, with appropriate tricks, one may reach a gap of 2 or 2.2 cm but this is, probably, the maximum that one can reach with an electromagnet. We did not explore the situation with a superconducting magnet; it is possible (but we do not know) that this might allow better geometries for the experiment.

Anyway, coming back to our experiment, its geometry has a disadvantage: that the plates, or better platelets, between which the object levitates have necessarily a small size, and therefore substantial gradients of the applied electric field are present. We might have adopted another possible "longitudinal" geometry [32], with large plates and the electric field parallel to the magnetic field. We did choose the geometry of fig. 5.1 above because we wished to have the possibility of displacing the plates in the course of a measurement; this freedom turned out to be convenient for clarifying the patch effect.

Our experiment used irregular grains of graphite of mass up to 3×10^{-7} g; a total amount of graphite of

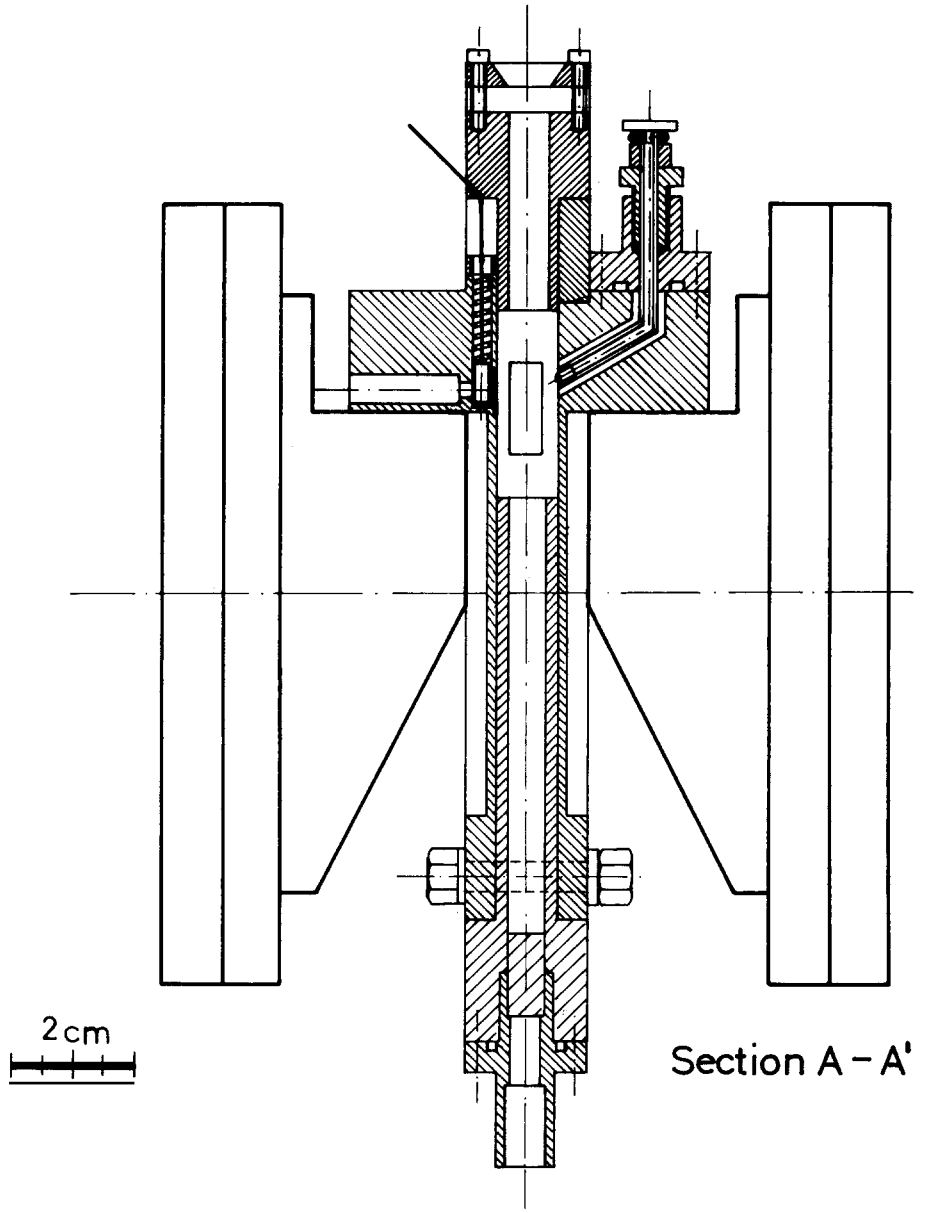

Fig. 5.1. A section of the pole caps and (in between) of the levitation chamber in our graphite experiment [5b]; a section of the platelets, of the β source and of the graphite injector are visible (for more details compare ref. [22]).

2.5×10^{-6} g was explored. No quark was found. Each grain was followed visually: the good signal to noise ratio due to small size of the object (still 10^4 times larger than the Millikan droplets), allowed to determine visually on a TV screen with a graduated scale the sequence of oscillation amplitudes after successive ionizations. The observation of a grain with a non-zero residual amplitude would have been an indication for a fractional charge; actually, when the distance between the plates was small, there were many grains with such a residual amplitude; we noted however that this residual oscillation always

disappeared when (at constant peak to peak electric field) the distance between the platelets was increased: this led us to a clarification of the importance of the patch effect. A complete description of the apparatus and its use can be found in ref. [22]; here we confine to the following points:

(a) The damping was due to the residual gas; the small size of the levitating grains produced values of $N_{1/2} \cong 100$.

(b) The ionization was obtained with an ultraviolet and β source.

(c) To reduce the effect of the permanent electric dipole moment of the grain – in spite of the comparatively large gradient of the applied electric field – the trick was to carefully place in position the grain midway between the plates, where, due to symmetry reasons, the electric gradients vanish; the electric dipole moments of the grains were never measured, however.

Altogether this experiment – besides showing for the first time that Millikan's sensitivity could be improved considerably by this technique – allowed a classification of several spurious effects, a classification performed, independently, by the Syracuse experimenters [33].

It is possible that the graphite experiment might still be improved changing the geometry into a longitudinal one, as mentioned above. We don't know; when we decided to switch to iron, we did this not only to increase the sensitivity but also to change the type of substance explored. Therefore we did not study in detail the possibility of further improvements in sensitivity of the graphite set-up.

The graphite experiment by the Soviet group [32] appears to be less elaborate than ours as far as control of the spurious effects is concerned. No quarks were found in 7×10^{-7} g of graphite.

5.2. The ferromagnetic experiments

Among the ferromagnetic levitation experiments, the Syracuse one was an interesting attempt accompanied by an extensive discussion of several spurious effects.

The balls used – only three in the course of the whole experiment – had a radius of 5×10^{-2} mm and a mass ~30 times smaller than the 0.3 mm diameter balls in use in the present generation of experiments. The distance between the plates was 3 mm and the measurements were performed at atmospheric pressure.

Although tilting effects around the easy axis of rotation were considered, the authors did not take the magneto-electric force into account. This was a posteriori one of the serious drawbacks of the experiments as far as its results are concerned.

Of the three balls examined two gave a vanishing residual charge (to $\pm 0.04e$) while the third had an erratic behaviour. The authors attributed this behaviour to strong and varying patch effects, and tried uselessly, to clean repeatedly the plates. On the basis of our present experience it is almost certain that the erratic behaviour of ball nr. 3 was due to a substantial magneto-electric force. Note, incidentally, that the original purpose of this experiment was not the search of quarks, but, rather, the measurement of a possible difference in charge between electron and proton.

The second attempt to a ferromagnetic experiment, by Garris and Ziock at the University of Virginia [34], used iron balls with a diameter of 0.2 mm. The set up is shown schematically in the fig. 5.2; the plate separation is 5 mm. The measurements took place in air at atmospheric pressure, trying to minimize the troubles due to thermal drifts. The electric field was reversed every 64 sec, the period of oscillation being 5 sec. The high frequency of spontaneous changes in charge of the levitating object was a serious drawback, due (presumably) to the very high intensity of the light illuminating the object.

Altogether 12 different balls were measured; the distribution in their residual charge is shown in fig. 5.3. To the question if the bumps in fig. 5.3 are evidence for quarks, Garris and Ziock answer:

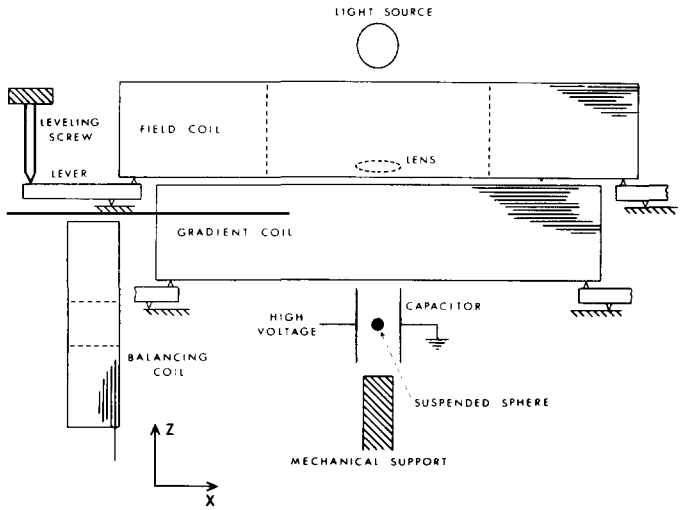

Fig. 5.2. Magnetic suspension in the Garris and Ziock experiment [34]. Instead of measuring the resonance amplitude of oscillation, the charge of the ball is obtained from the value of the current in the balancing coil (on the left in the figure) needed to keep the suspended ball at its equilibrium position when the electric field is applied.

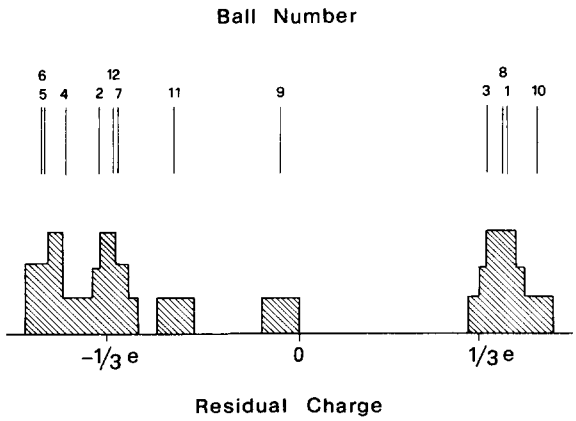

Fig. 5.3. Frequency distribution of the residual charges measured on 12 different steel balls in the Garris and Ziock experiment [34].

"Systematic errors exist that are demonstrably of the same order of magnitude and could be responsible for the observed distribution. An extended search with better statistics must be undertaken to clear up the stated discrepancies." By "the stated discrepancies" the authors mean problems of reproducibility of the patch effects, discussed (previously) in their paper. We now know that in addition to the patch effects Garris and Ziock must have had (in their geometry) the magneto-electric (or tilting effect), that they ignored. Therefore the distribution of fig. 5.3 does not really constitute evidence or hint for the existence of quarks†.

† In a report presented at a recent conference (June 1981) at the San Francisco State University Ziock did indeed confirm our result [37, 31] that an apparent continuous distribution of residual charges is obtained if the magneto-electric force is not measured and subtracted.

Finally in a short letter in 1970, Braginsky and coworkers [35] of the University of Moscow report on a ferromagnetic levitation experiment with balls of diameters ~0.2 mm. The details given are insufficient to clarify the experimental set up. Only the results are reported; on 6 balls no quark was found; the residual charges of the six balls were found to be between $0.04e$ and $0.09e$ with errors around $\pm 0.1e$. The magneto-electric force is not mentioned. No additional publication by this group appeared later – as far as we know – so that, apparently, the experiment was discontinued.

6. The Genoa ferromagnetic experiment; its evolution and a general scheme of the apparatus

6.1. A short chronology of the results

The reasons for starting the ferromagnetic experiment after the conclusion of the graphite one have been already mentioned: (a) to extend the variety of substances explored, (b) to improve the sensitivity of the instrument. The choice of the ferromagnetic levitation with feedback rather than diamagnetic levitation (possibly at low temperatures) was determined by the consideration that ferromagnetic levitation allows the use of a larger variety of substances: any ferromagnetic alloy can be used, provided that small spheres can be fabricated.

Also, in choosing the feedback way, we preferred to avoid a cryostat, necessary for the diamagnetic levitation at low temperatures, because we feared that it might reduce the flexibility of the method, the possibility of easy modifications, if necessary, during the course of the experiment.

Before going through the construction of the instrument we give a short chronology of the results: experiments of this kind undergo – along the way – some modifications and it seems appropriate that – on reading the published papers – the interested reader has an overview of how the situation evolved.

The essence of the instrument was ready in the fall of 1976 [38]. We soon got a satisfactory signal to noise ratio, but an unclear behaviour of the residual charge. Not only there appeared to be a continuous distribution of residual charges, but often the Q_R of a given object had slow variations with time; these variations – called "drifts" in what follows – were substantial in some cases, amounting, after a dozen hours, to an appreciable fraction of one electron charge.

In a few cases of particularly dirty objects, we could correlate (by looking to the levitating object on the television screen) these drifts with the onset of tiltings of the object in the x, y plane, that is around the easy z axis of rotation. We therefore decided that, first of all, we should average out these easy tiltings by spinning rapidly the object around the easy axis of rotation. We also decided to increase the magnetic rigidity – that is to make also the tiltings in the zx plane more difficult by working with cylinders instead of spheres. This is why in the first measurements we used spinning cylinders. At the beginning spinning was produced by a self-exciting mechanism giving rise to considerable noise. The first five cylinders measured after spinning was started turned out to have no appreciable drift and a residual charge consistent with zero to $\pm 0.1e$. The paper [39] was a report of these results. However, soon after these observations, the sixth cylinder did again show – as stated in [37] – a non-zero residual charge and appreciable drifts. A few months later (at the end of 1977) – after we had constructed a reliable noiseless spinning system – many spinning balls and a few cylinders revealed again non-zero residual charges and occasionally also drifts in Q_R.

The spectrum of Q_R found till the summer of 1978 [37] is shown in the fig. 6.1. Subsequent

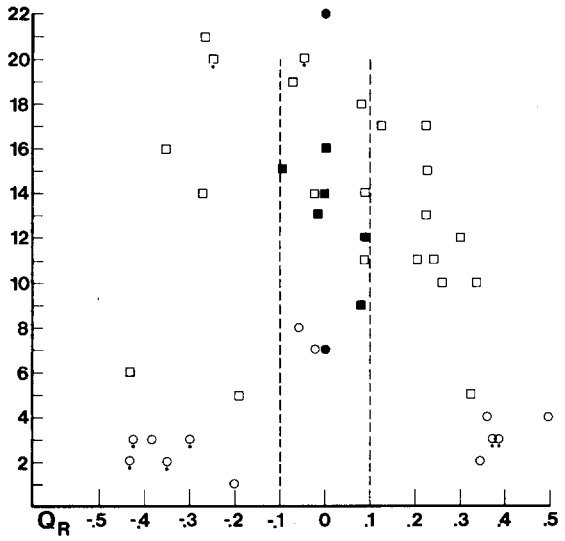

Fig. 6.1 (from ref. [37]). The spectrum of the residual charges Q_R found on 22 different 0.2 and 0.3 mm balls as it appeared before realizing the existence of the magneto-electric force and subtracting its effect. Symbols on the same horizontal line refer to different measurements of the same ball (mostly after a relevitation and cleaning); the ball number is on the ordinate. At this stage the details of this figure are irrelevant; the only important point is the continuous spectrum of the apparent residual charge, widely distributed between $-0.5e$ and $+0.5e$, and confirmed by fig. 6.2.

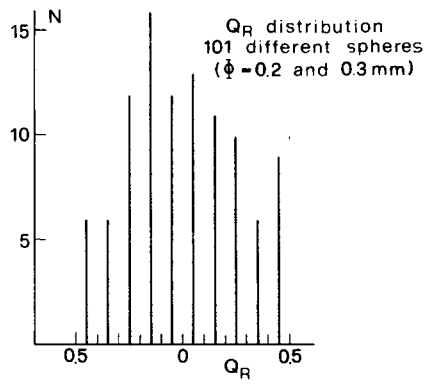

Fig. 6.2. Same distribution as in fig. 6.1 for 101 different spheres (on the abscissa Q_R, on the ordinates the number of measured balls).

observations on a total of 100 spinning balls confirmed the continuous distribution in Q_R as fig. 6.2 shows.

At this stage the question was if the continuous apparent fractional charges were produced by the patches on the plates or if they had some other unknown origin (or, less likely, were real).

To answer these questions the levitation chamber was modified to levitate in succession up to 4 different spheres and redeposit them without opening the chamber so as to be sure not to change the patches. It emerged clearly from this study that the patch effect could not account for the Q_R distribution of fig. 6.2: in fact two different spheres with exactly the same radius – levitated in succession without opening the chamber – did show frequently substantially different values of their residual charge. To be more precise let us describe below what we might have expected if only the patches were responsible for the continuous distribution of Q_R and for the "drifts" and what we did instead find.

In fig. 6.3 we plot several conceivable situations that we *might have expected* to find during a "run". (A "run" is a sequence of levitations, measurements and redepositions of at least two balls performed without opening the levitation chamber.) In detail: fig. 6.3 shows a hypothetical "expected" run performed with two spheres of equal radius measured several times in succession: (1) if there are no quarks in the two spheres and the patches do not change (fig. 6.3a); (2) if there are no quarks and the patches change with time (fig. 6.3b); (3) if one sphere contains a quark and the other does not (figs. 6.3c and d). What we did obtain in a real run is instead shown in fig. 6.4; and fig. 6.5 gives, more schematically, the results from all the runs performed. From figs. 6.4 and 6.5 it appears that: (a) often the same sphere reproduces its residual charge after a deposition and relevitation, but this reproduction is usually not exact: there is often a shift of the order $e/10$ and less frequently much larger shifts; (b)

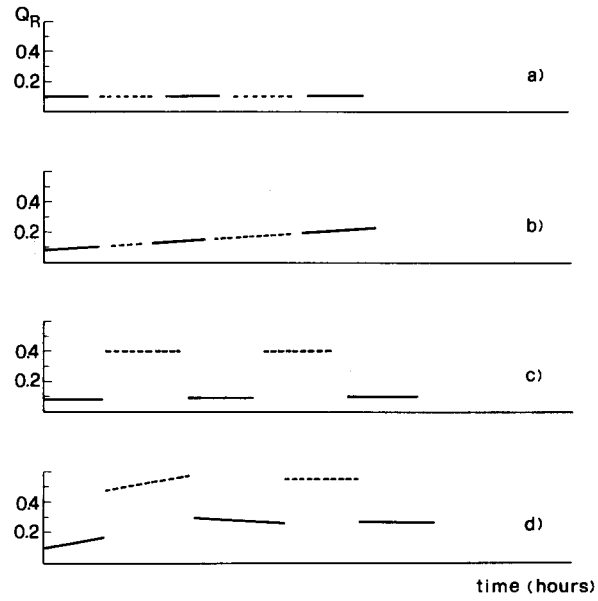

Fig. 6.3. Several conceivable situations for a run with two spheres (compare the text).

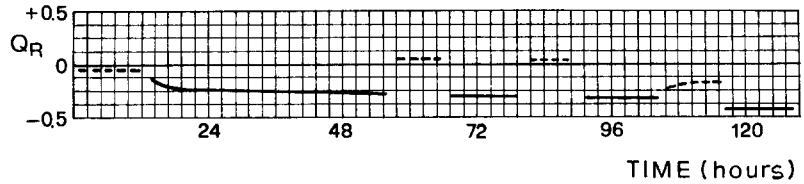

Fig. 6.4. A typical run with two balls both of diameter 0.3 mm showing drifts and shifts. On the ordinates the residual charge Q_R, on the abscissa the time; the dotted levels refer to one ball, the full levels to the other. The Q_R of the first ball was measured during 12 hours, then the ball was deposited and – without opening the chamber – the second ball was measured during 42 hours; then it was again replaced by the first ball and so on.

what is more puzzling is that we have runs (such as that of fig. 6.4) where one sphere keeps constant Q_R (or almost constant Q_R) for many levitations; whereas another sphere (the levitations of which take place between two levitations of the first) changes its Q_R gradually; so that if at the beginning the difference in Q_R between the two spheres was $e/3$, at the end it may be zero; or viceversa. Because the two spheres have exactly the same radius this shows that the shifts and drifts appearing in the various runs cannot be attributed to a variation of the patch effects. They depend on some property of the sphere, not on the plates.

The facts just described, and the additional important finding that when the oscillation of our levitating object was produced by an oscillating magnetic field (instead of the electric field), this "magnetic" oscillation had always the same amplitude to 1% (and no drifts), led us to the conclusion that another force simulating a charge should be present in addition to the patch force; and that this additional force should depend on the presence of both the electric and the magnetic fields.

We were thus led to assume a rather general expression of the energy necessary to account for this additional unknown force: $W = \beta \boldsymbol{E} \cdot \boldsymbol{H}$. This addition to the Hamiltonian – non-invariant with respect to time reversal – is the same that would arise if the electric field could induce a magnetic moment $\beta \boldsymbol{E}$

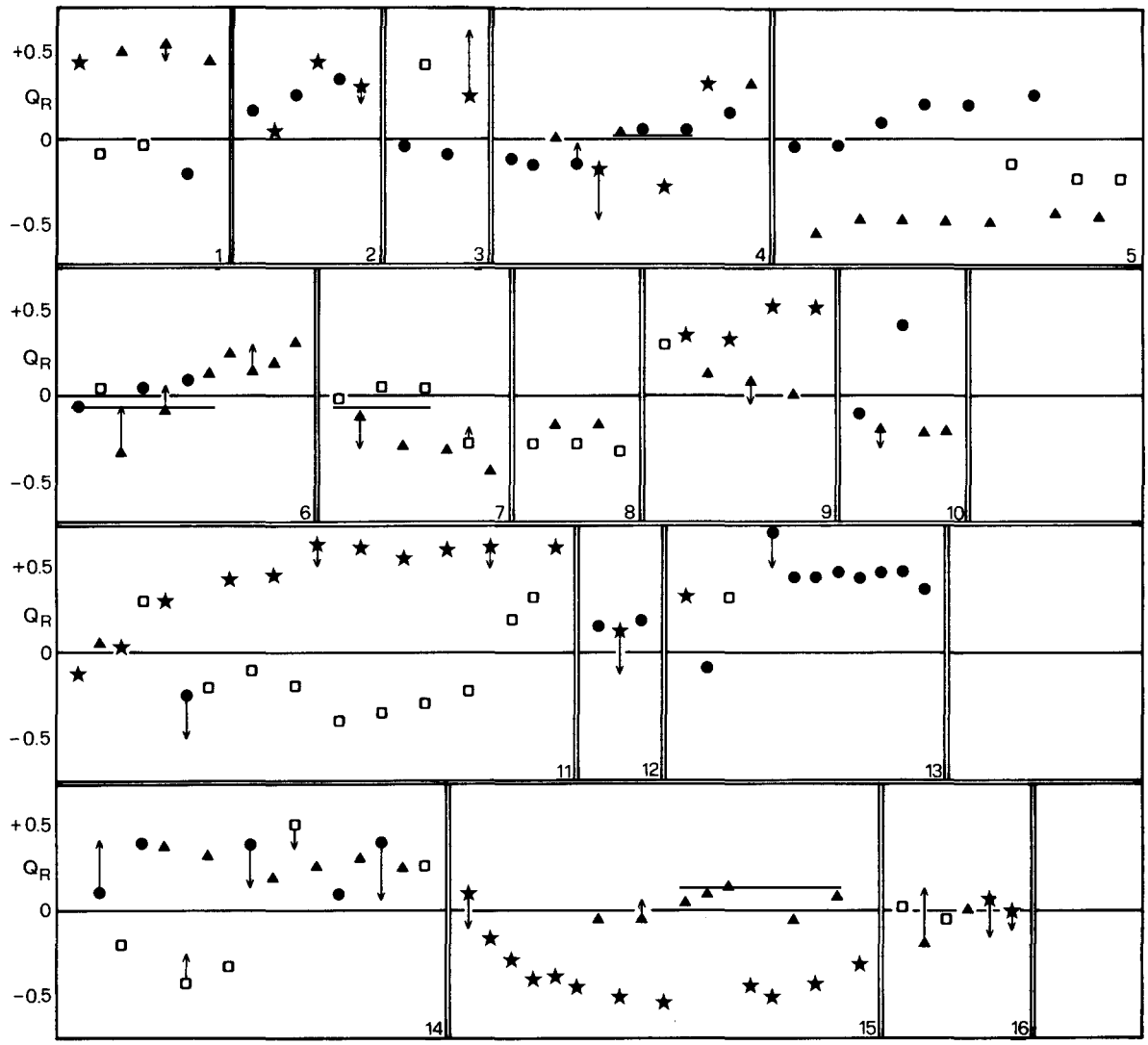

Fig. 6.5. All runs performed before realizing the existence of the magneto-electric force. The run shown in detail in fig. 6.4 is nr. 7. The following symbols are used: ● sphere 1, □ sphere 2, ▲ sphere 3, ★ sphere 4. An arrow means a drift in Q_R from the position of the symbol to the tip of the arrow. Subsequent levitations appear from left to right; for simplicity the duration of each levitation is not indicated; the duration of the various runs ranged from 2 to 10 days.

interacting with the magnetic field $\boldsymbol{H}$. As a matter of fact we found that such a force – obtained as the x derivative of the above energy – did in fact exist, although an explanation of its precise origin was still lacking (we have already discussed this force – and its interpretation – in section 4.4). We developed a method (to be discussed in detail in section 8.2) to measure the effect of this force on each object, by producing a variation of $\partial H_x/\partial x$ at the position of the object. We concluded that all the 70 different balls measured after having recognized the presence of the magneto-electric force and subtracted its effect, do not contain quarks.

It also emerged that the observed drifts are mainly due to slowly varying values of β; this quantity is related – as already stated – by the equation $\beta = d_z/H_z$ to the electric permanent dipole moment of the ball; this is not so "permanent": a slowly varying β and thus a slowly varying magneto-electric force arises if d_z changes slowly; this in turn depends on slow changes of the status of the surface of the levitating ball.

A final remark on the measurement of the patch effect is appropriate. In the initial set up – before the levitation chamber was modified to allow the levitation, in succession, of several spheres – we had movable plates. This was motivated by our experience with the graphite experiment where we could, in this way, identify the effect of the patches.

Indeed these movable plates were useful also this time: when working with them we found several times that even at a distance between the plates of 4 cm and with (spinning) balls of 0.2 mm diameter a substantial non-zero apparent residual charge was present. This value would have implied patches much stronger than expected on the basis of our results of section 4.1; this observation was the first stimulus to think in the direction that patch effects could not be responsible for all the apparent residual charge. When we modified the levitation chamber (to measure more spheres in succession without opening the chamber) we decided that the moving plates were no more strictly necessary and we preferred to have under strict control the parallelism of the plates. The distance of the plates was kept fixed at 2 cm, sufficient – according to our estimates – to make the patch effects not too dangerous. To measure the patch effect, we decided to use the comparison procedure described in section 3.3. As we shall see in section 8.8 – when the results for all the balls will be displayed in detail – the comparison procedure allows to determine for each ball the patch apparent charge (and the true residual charge), to the accuracy needed to establish or reject the presence of quarks.

6.2. *A general scheme of the apparatus*

The scheme of the apparatus shown in fig. 6.6 allows a first broad presentation, a sort of introduction to the specific illustration of the ensuing sections.

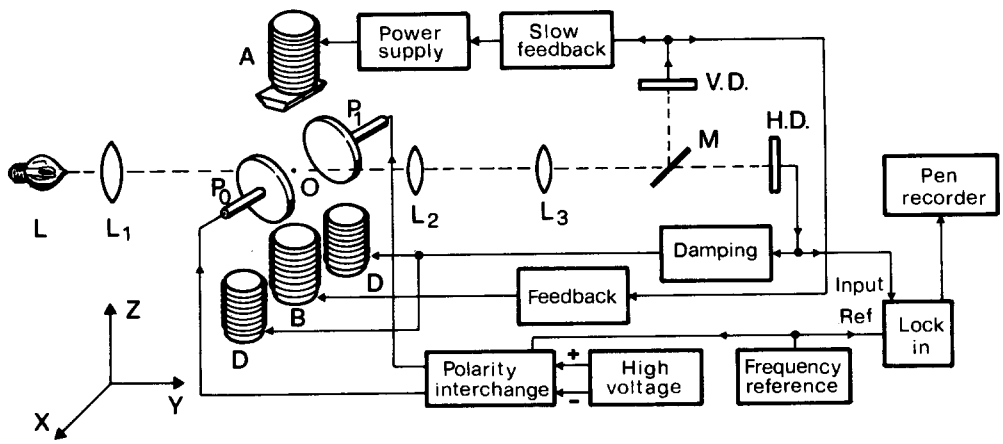

Fig. 6.6. A schematic view of the apparatus. L = lamp; L_1, L_2, L_3 = lenses; M = half transparent mirror; H.D. and V.D. = horizontal and vertical photodiode system; O = levitating object; A = main coil; B = feed-back coil; D damping and auxilary coils; P_0 and P_1 electric plates. The boxes showing the electronics are self-explanatory. We have not shown the vacuum tight box containing the plates, the ultraviolet lamp, the TV transfer system and several other minor details. The figure is not in scale. The distance between the lower part of A and the upper part of B is 15 cm. The distances between the optical components are – approximately – as follows: L_1–O = 30 cm, O–L_2 = 11 cm, L_2–L_3 = 53 cm, L_3–M = 6 cm, M–V.D. = 16 cm, M–H.D. = 20 cm (the distances from M refer to a 3/10 mm sphere and are taken from the center of M).

The coils A and B provide the feedback levitation of the object O illuminated by the lamp L. The "vertical" photodiode V.D. detecting the shadow of O (through a system of lenses and the semitransparent mirror M) controls the feedback levitation current. The "horizontal" photodetector H.D. measures the x oscillation of the object and transfers the signal to the lock-in amplifier; H.D. governs also the coils D that create the damping. Also visible in fig. 6.6 are the plates P_0 and P_1 to which the square wave high voltage is applied. The square wave is generated via the periodic interchange of the high voltage supplies (effected by high voltage reeds) piloted by a clock; the same clock governs the reference channel of the lock-in. The plates are of course inside a vacuum tight chamber (the levitation chamber), not shown in the scheme. Many other components – and in particular the four coils used for the spinning – are omitted from the figure for simplicity (they will be illustrated in the appropriate subsection).

Before giving (in the next section) a detailed presentation we list below the main problems that had to be surmounted in the construction of the apparatus.

1. To levitate a small object (0.2 or 0.3 mm diameter) at sufficient distance from all the pole caps and all the coils. Here sufficient means that the levitation chamber surrounding the object has to be large enough to allow plates with a reasonably large diameter; this requirement, in turn, is necessary to have a uniform electric field.
2. To perform the act of levitation with comparative ease so that the fraction of lost objects is small.
3. To ensure the stability of the magnetic valley where the object moves.
4. To produce a preselected damping in the equation of motion of the object.
5. To give to the levitated object a charge with predetermined sign and discharge the object to a charge value near zero in a short time.
6. To have a small rate of spontaneous changes in charge of the levitating object.
7. To spin the object.
8. To measure both the signal in phase with the applied electric field and the signal at 90° (measuring only the amplitude of oscillation is acceptable but does not ensure a complete knowledge of the force acting on the object).
9. To reject efficiently the noise.
10. To have a signal independent of the variations of the light illuminating the object (though its intensity is in practice stable to a sufficient extent).
11. To achieve a reliability in the electronics capable of guaranteeing uninterrupted operation for sufficiently long periods (a failure often implies the loss of the levitating object; the same is true for a power failure).

We now sketch how these problems were solved; the same order used above will be followed.

1. We achieved a strong feedback with the object kept at 7.5 cm from the upper pole cap and 7.5 cm above the lower coil B. This was obtained using two coils: the coil A with a large iron core is responsible for the force counteracting the gravity; the lower and smaller coil B – with a core in ferrite – produces the fast feedback.
2. In the early phase of the experiment the levitation of an object was a matter of luck. Now it is a reasonably standard operation only requiring some attention. There have been three reasons for this: (a) the construction of a horizontal feedback system, (b) an automated procedure to sweep slowly the current applied to the main coil, (c) the use of appropriate substances for the pedestal on which the spheres are deposited before levitation and of good cleaning procedures both of the spheres and of the pedestal. The horizontal feedback mentioned above is accomplished by the same coils D used to provide the damping; it must be switched on not only for the act of levitation, but

during any operation that might, accidentally, give to the object a lateral push capable of displacing the image of the object out from the sensitive area of the Vertical Detector (V.D.). Incidentally there is no need of a y feedback because oscillations along y appear to the V.D. simply as slight focussing or defocussing of the object. To conclude this point we mention that appropriate materials for the pedestal on which the ball is deposited before the levitation are, for instance, graphite, zinc, silver; diamagnetic substances appear to be preferable to paramagnetic (possibly because there is, for them, a tiny repulsion of the ball in the presence of the magnetic field). With the substances listed above the tendency to stick is considerably reduced; particularly if their surfaces are exempt from grooves.

3. By "stability of the magnetic valley" we mean that the restoring force on the object stays constant so that the natural frequency of oscillation of the object near the equilibrium position is stable. A slow feedback system acting on the current in the coil A, to be described in the next section, contributes to this stability by compensating, in part, the effect of the thermal elongations of the supports of the castle holding the coil A.
4. Damping. This is obtained sending – as fig. 6.6 shows – the signal from the horizontal photodetector to the coils D after having performed its first derivative by an appropriate RC circuit. We thus have an equation of motion of the object of the form $M\ddot{x} + \gamma\dot{x} + kx = F_x(t)$ where the value of γ depends on the selected RC. Note that in our set-up we operate at a value of $N_{1/2}$ of the order 10 to 20: the filter enhancing the signal above the noise is not the mechanical filter constituted by the oscillating object with a high Q value, but is the lock-in operated with a large integration time.

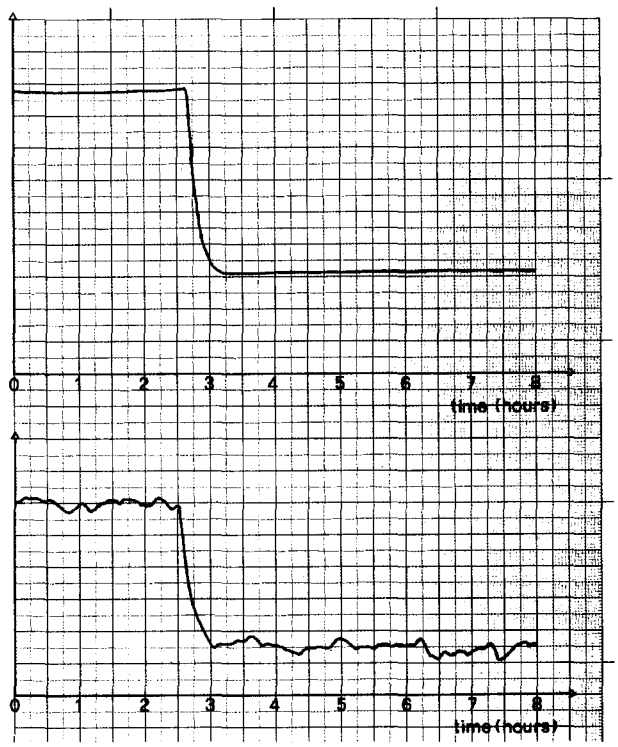

Fig. 6.7. A change of unit charge, as it appears typically in conditions of small noise (upper part referring to a measurement on a sphere of 2/10 mm diameter) and in conditions of particularly large noise (lower part – referring to a 3/10 mm sphere). On the abscissas the time (in hours); on the ordinates the output of the lock-in giving the amplitude of x oscillation (in arbitrary units).

5. A preselected amount and sign of the charge to the levitated object is obtained by an appropriate voltage (between 10 and 100 V), established, before the act of levitation, between the plates and the pedestal on which the ball is deposited. After levitation the ball is brought to a charge near to zero by a small UV lamp in about 15 minutes.
6. To have a small rate of spontaneous changes of the charge of the levitating object is a vital requirement: the charge of our object does not change for many hours. This has been obtained improving the vacuum, reducing the intensity of illumination (and filtering the light by appropriate red filters) and keeping the potential excursion of the plates between +2000 V and −2000 V.
7. Spinning is produced by four coils – external to the levitation chamber – used as the stator of an induction motor; the rotor is the levitating ball itself.
8. and 9. The use of a lock-in amplifier – having as reference signal the clock piloting the square wave electric field – solves the questions 8 and 9 at the same time. Typical plots from the pen recorder at the exit of the lock-in showing a unit change in charge of the levitating object are reproduced in fig. 6.7 in different seismic conditions.
10. With our damping procedure this requirement is guaranteed automatically, as will be explained in section 7.4.
11. For 18 months of continuous operation we could go on without failures in the electronics and with only a few power failures. Subsequently we had a bad period of three or four months with frequent failures.

7. A technical description of the instrument

We now describe the constructive data of the instrument, following closely a recent paper [40], but adding more information when needed. With reference to the scheme of fig. 6.6 and to the figures 7.1

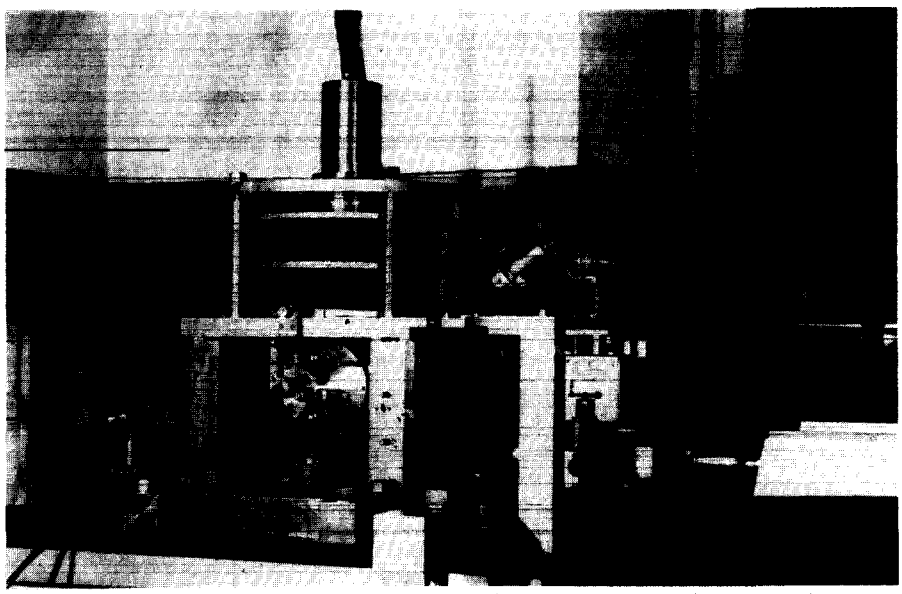

Fig. 7.1. A photograph of the castle supporting the main coil A and the levitation chamber; also the coils B and D are visible as well as part of the optical transfer system to the TV set.

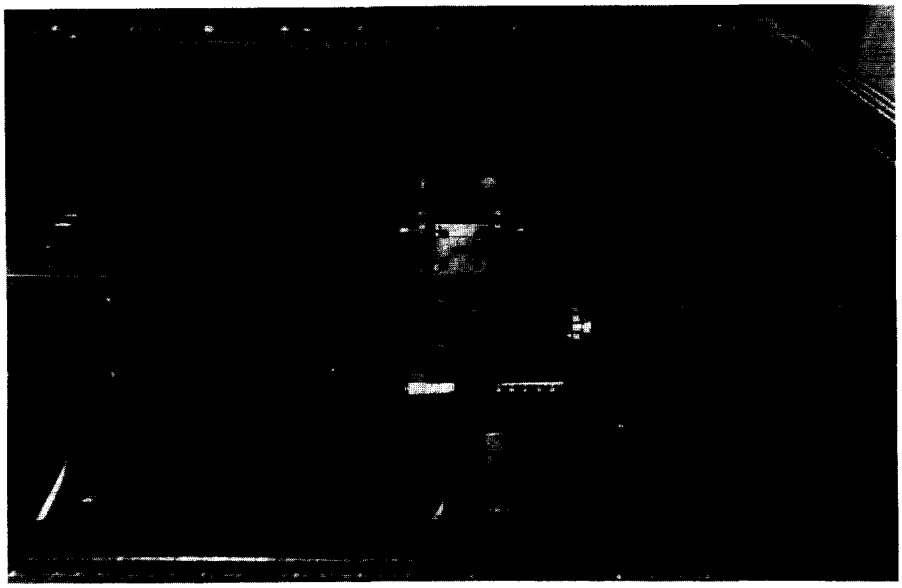

Fig. 7.2. A photograph giving some details of the optics: the lens L_3, the mirror M and the photodetectors V.D. and H.D.

and 7.2 (providing an overall view) the material is naturally subdivided as follows: (1) Vertical feedback, (2) Horizontal damping, (3) The optical system and the photodetectors, (4) The TV set, (5) The levitation chamber, (6) Spinning, (7) The vacuum system, (8) The high voltage, (9) The detection and recording of the signal, (10) The sequence of operations in a run.

7.1. The vertical feedback: (a) the magnetic configuration

A xz section of the coils positioned as indicated schematically in fig. 6.6 is presented in fig. 7.3a; fig. 7.3b gives a yz section of the iron pole cap. The characteristics of the coils appear in table 7.1. In this subsection we shall be concerned only with the coils A and B that produce the levitation and the vertical feedback. As already stated the upper coil A, with a large iron core, is responsible for the force counteracting the gravity; the lower and smaller coil B with a core in ferrite produces the fast feedback. The use of two separate coils, rather than one, was decided to have a fast and strong feedback on the object O (which has its equilibrium position 7.5 cm from the lower edge of the iron pole cap). Using one big coil only – or two coils superimposed – would have given rise to large delay times and weaker feedback, due to self-induction or mutual induction.

Let us write the vertical force due to A and B. It is, for a sphere of volume V:

$$F_z = \frac{3V}{\mu_0} \boldsymbol{B} \cdot \frac{\partial \boldsymbol{B}}{\partial z} \tag{7.1}$$

where the factor 3 is typical of a sphere, μ_0 is the permeability of the vacuum ($\mu_0 = 4\pi\ 10^{-7}$ henry/meter); the x and y components of the magnetic force are obtained from (7.1) replacing z with x or y.

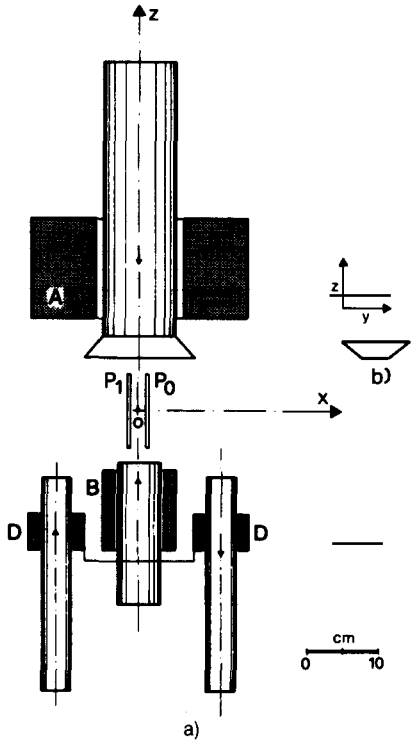

Fig. 7.3. (a) A figure (in scale) of the coils A, B, D and the xz section of the pole cap. (b) The yz section of the pole cap.

The total magnetic field $B(r)$ can be written:

$$\boldsymbol{B}(\boldsymbol{r}) = \boldsymbol{b}_{\mathrm{A}}(\boldsymbol{r})\, I_{\mathrm{A}} + \boldsymbol{b}_{\mathrm{B}}(\boldsymbol{r})\, I_{\mathrm{B}} + \cdots \tag{7.2}$$

where only the terms due to A and B have been noted: the dots in (7.2) stay for additional terms due to the coils D, C etc.; they will be considered at the appropriate place (for instance the D terms will be included on discussing the damping). In (7.2) we used the following notation: $\boldsymbol{b}_{\mathrm{A}}(\boldsymbol{r})$ is the magnetic field produced at $\boldsymbol{r}$ when a unit current passes in the coil A and no current in all the other coils; similarly for $\boldsymbol{b}_{\mathrm{B}}(\boldsymbol{r})$, etc.

Table 7.1
The constructive elements of the coils A, B, D

Coil	Nr. turns	Diameter of wire (mm)	Int. Diameter of coil (mm)	Length of coil (mm)	R (Ω)	Remarks
A	2000	3.2	120	145	5.5	Bruker B-410 C8 water cooled
B	1100	1.0	72	120	4.6	$L = 0.14$ henry
D	600	0.8	60	56	4.7	each D coil

Inserting (7.2) into (7.1) we get:

$$F_z = \frac{3V}{\mu_0}\left\{\left(\boldsymbol{b}_A \frac{\partial}{\partial z}\boldsymbol{b}_A\right)I_A^2 + \left(\boldsymbol{b}_A \frac{\partial}{\partial z}\boldsymbol{b}_B + \boldsymbol{b}_B \frac{\partial}{\partial z}\boldsymbol{b}_A\right)I_A I_B + \left(\boldsymbol{b}_B \frac{\partial}{\partial z}\boldsymbol{b}_B\right)I_B^2\right\}. \tag{7.3}$$

In our conditions of operation the average current in the coil B is zero. Therefore the last term in (7.3) is much smaller than the first two terms. The largest term is the first, counteracting the gravity; it is:

$$\frac{3V}{\mu_0}\left(\boldsymbol{b}_A \frac{\partial}{\partial z}\boldsymbol{b}_A\right)I_A^2 = mg \tag{7.4}$$

(where $m = \rho V$ is the mass of the ball); the current I_A needed to levitate the ball is $I_A = 7.2$ A and the value of the magnetic field at O and of its vertical derivatives are:

$$B_{Az} = b_{Az} I_A = -525 \text{ gauss}$$

$$\frac{\partial B_{Az}}{\partial z} = \frac{\partial b_{Az}}{\partial z} I_A = -6.1 \times 10^3 \text{ gauss/meter}. \tag{7.5}$$

The fast feedback created by the coil B exploits the second term in (7.3), the interference term proportional to $I_A I_B$.

The vertical fast feedback circuit (fig. 7.4) receives its input information from the vertical photodetector V.D.; a positive or negative I_B is produced in the coil B depending on whether the external noise tends to push the object up or down away from the predetermined position O; clearly due to the stochastic nature of the noise the average I_B is zero. In the conditions of fig. 7.3 the acceleration produced by a variation of the current I_B on the levitating ferromagnetic *sphere* at its equilibrium position O is:

$$\frac{1}{m}\frac{\partial F_z}{\partial I_B}\bigg|_O = 0.5 \frac{\text{m sec}^{-2}}{\text{A}} \tag{7.6}$$

where F_z is the vertical magnetic force and m is the mass of the sphere. The value (7.6) (as well as the subsequent equation (7.7)) are the main elements in the choice of the parameters of the vertical fast feedback circuit shown in the fig. 7.4.

In addition to the fast feedback produced by I_B, a slow feedback system (with a time constant of $\sim$140 sec) operates on the main current I_A (fig. 7.5). It compensates in part the slow thermal expansion of the supports of the coils thus contributing to ensure the stability of the oscillation frequency in the x direction. The slow feedback ensures in fact that the position of the shadow of the object on the vertical photodetector is unaffected by the thermal behaviour of the supports of the upper coil A. This requirement suffices in practice to ensure resonance stability even at values of the resonance width 4 or 5 times narrower than the ones we use.

We note the equation analogous to (7.6) for a variation of the current I_A:

$$\frac{1}{m}\frac{\partial F_z}{\partial I_A}\bigg|_O = 2.7 \frac{\text{m sec}^{-2}}{\text{A}}. \tag{7.7}$$

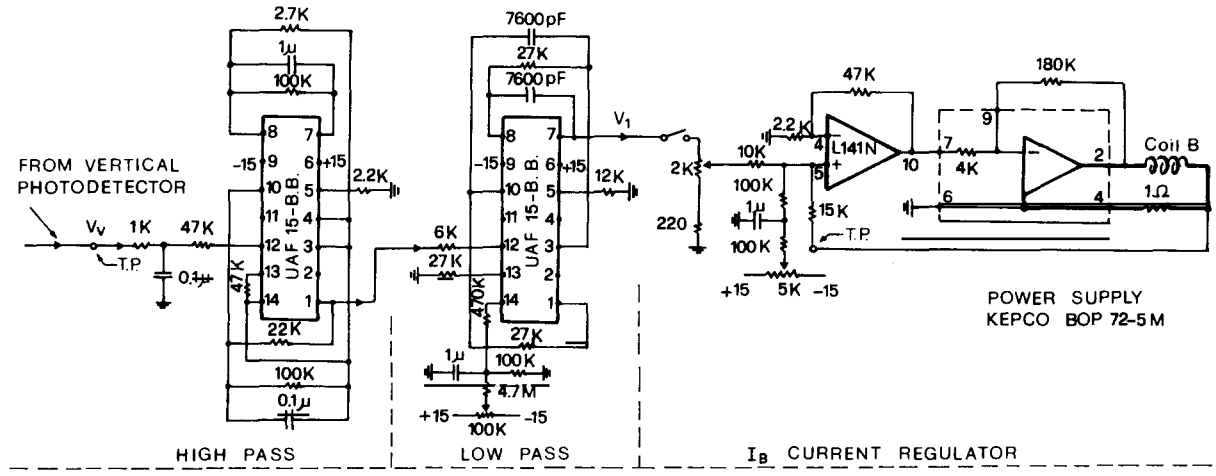

Fig. 7.4. The fast feedback circuit governing the current in the coil B.

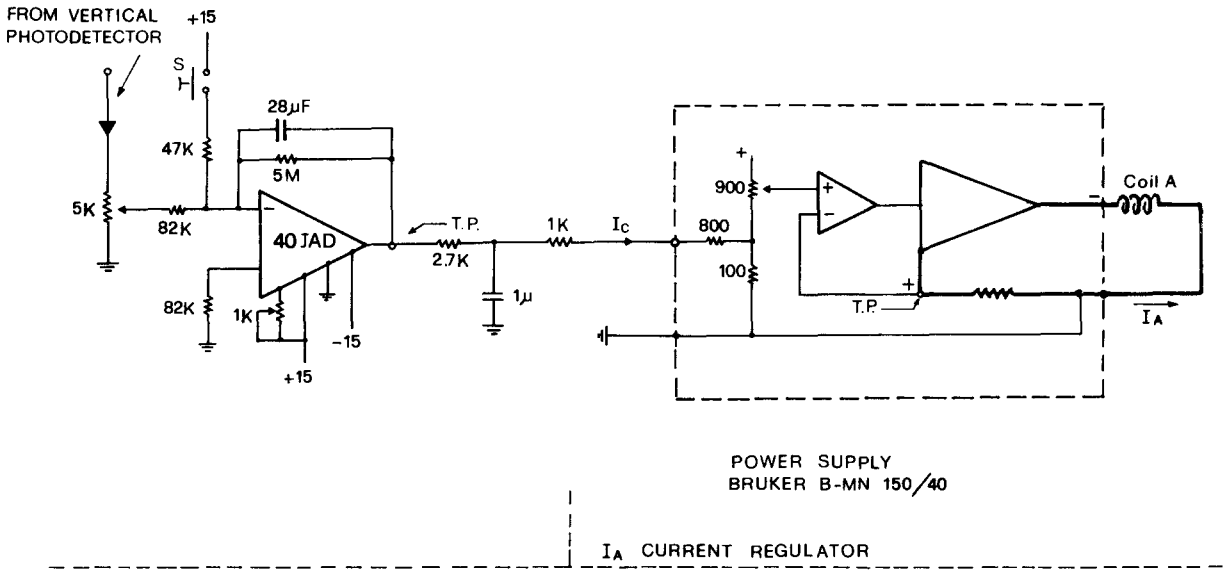

Fig. 7.5. The slow feedback circuit, operating on the coil A.

Before discussing the feedback circuitry a further remark is appropriate: the magnetic axis of the coils A and B must be collinear to a good precision. A lack of collinearity (besides amplifying the seismic noise) is an undesirable source of x damping as will be illustrated in section 7.3. Moreover the magnetic axis of A and B must intersect the optical axis of the instrument to a precision better than the diameter of the object.

7.2. The vertical feedback: (b) the circuits

We now illustrate some aspects of the circuits. Consider first the fast feedback (fig. 7.4). The input signal on the left of fig. 7.4 is the voltage V_v from the vertical photodetector, related to the vertical

displacement Δz of the levitating sphere by eq. (7.15) of section 7.4. The regulation of the current I_B in the coil B due to a variation of V_v is accomplished by a bipolar operational power supply KEPCO BOP 72-5M. The transfer function of the fast feedback circuit (in units ampere/volt) is expressed by the spectral equation:

$$\frac{I_B(\omega)}{V_v(\omega)} = -0.25 \frac{1 + 0.1\,i\omega}{(1 + 0.5\,i\omega \times 10^{-3})(1 + 0.2\,i\omega \times 10^{-3})^3}. \tag{7.8}$$

The transfer from $I_B(\omega)$ to the force on the sphere is approximately independent of the frequency up to $\omega_m = 500\,s^{-1}$; for $\omega > \omega_m$ the Foucault currents in the walls of the levitation chamber start to screen the variations in I_B. Altogether the equation of motion of the object under the vertical fast feedback is approximately that of an harmonic oscillator with $\omega_v = 50\,s^{-1}$ and damping ratio $\zeta \cong 1.5$. The slow feedback circuit (fig. 7.5) acts on the main power supply of the coil A (Bruker, mod. B-MN 150/40). The voltage-current transfer function is:

$$\frac{I_A(\omega)}{V_v(\omega)} = -\frac{5}{(1 + 140\,i\omega)(1 + 0.1\,i\omega)} \tag{7.9}$$

where, referring to fig. 7.5, the amplification $\Delta I_A/\Delta I_C$ is 1400 in our working conditions.

7.3. The horizontal damping

The coils D in the fig. 7.3 have their current I_D controlled by the output of the horizontal photodetector H.D. through the circuit of fig. 7.6; their function is double: (a) when the switch S in the circuit of fig. 7.6 is on position 1, the D coils create a feedback on the levitating object in the x direction producing a restoring force that keeps the object near to the equilibrium position; this is vital to avoid that the object falls down in the course of the operations in which it may accidentally receive large pushes in the x direction. (b) If the switch S is in the position 2 the horizontal photodetector sends in the coils D a signal proportional to ω (up to $\omega \approx 1000\,sec^{-1}$), that is proportional to the velocity of the object in the x direction; it thus creates a damping term $\gamma\dot{x}$ giving rise to a damped harmonic equation of motion of the object in the x direction. The damping constant γ can be prescribed at will by varying the potentiometer D in fig. 7.6; the stability of the damping and the possibility of selecting its value as the most appropriate to the measuring conditions are convenient features of this set up. The stability of the damping is ensured by the fact that it is produced by a simple RC circuit, as shown in fig. 7.6. In this connection the following remark is important: to ensure full stability one must be sure that the preselected damping dominates above any other conceivable contribution to the x damping. Two additional contributions are there, in principle: (a) from the residual gas: at the operation vacuum ($< 3 \times 10^{-5}$ torr – usually from 7 to 10×10^{-6} torr) this is totally negligible with respect to our usual preselected damping (corresponding, normally to $N_{1/2}$ from 15 to 20). (b) From a lack of magnetic collinearity between the coils A and B as already noted in section 7.1. Also this contribution turns out to be negligible; we wish to clarify this point here.

If the expression (7.2) of the magnetic field is completed by the addition of a term $\boldsymbol{b}_D(\boldsymbol{r})\,I_D$ from the D coils, the x component of the magnetic force – neglecting terms proportional to I_B^2, to I_D^2, or to $I_B I_D$ and omitting the terms from the current in the C coils (section 7.7) – is:

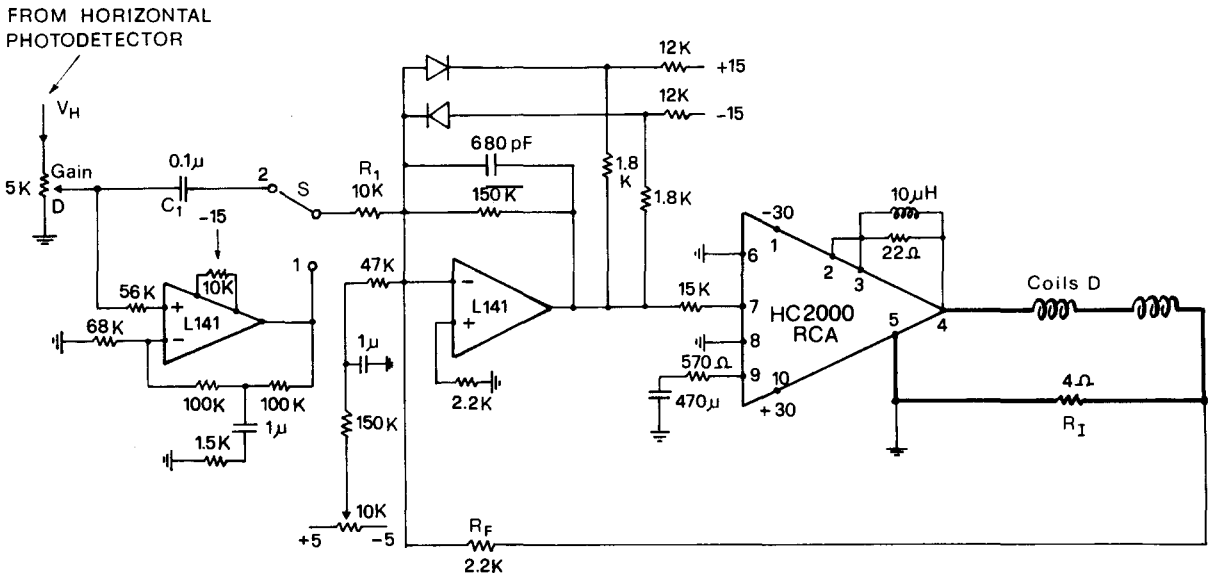

Fig. 7.6. The damping circuit.

$$F_x = \frac{3V}{\mu_0}\left\{\left(\boldsymbol{b}_A \cdot \frac{\partial}{\partial x}\boldsymbol{b}_A\right)I_A^2 + \left(\boldsymbol{b}_A \cdot \frac{\partial}{\partial x}\boldsymbol{b}_B + \boldsymbol{b}_B \cdot \frac{\partial}{\partial x}\boldsymbol{b}_A\right)I_A I_B + \left(\boldsymbol{b}_A \cdot \frac{\partial}{\partial x}\boldsymbol{b}_D + \boldsymbol{b}_D \cdot \frac{\partial}{\partial x}\boldsymbol{b}_A\right)I_A I_D\right\}. \tag{7.10}$$

If A and B are magnetically collinear both $\boldsymbol{b}_A$ and $\boldsymbol{b}_B$ are vertical at the position of equilibrium O; by definition of equilibrium position it is $F_x(0)|_{I_D=0} = 0$ and, therefore:

$$\frac{\partial}{\partial x} b_{Az}\Big|_O = \frac{\partial}{\partial x} b_{Bz}\Big|_O = 0. \tag{7.11}$$

The first two terms in (7.10) then vanish at O and the third term simplifies into:

$$F_x(0) = \frac{3V}{\mu_0}\left(b_{Az}\frac{\partial b_{Dz}}{\partial x} + b_{Dx}\frac{\partial b_{Ax}}{\partial x}\right)I_A I_D(t) \tag{7.12}$$

which is the usual term producing the damping ($I_D(t)$ is proportional to $\dot{x}(t)$). For completeness we note the value of $\partial F_x/\partial I_D|_O$ in our situation. It is:

$$\frac{1}{m}\frac{\partial F_x}{\partial I_D}\Big|_O = 0.18\frac{\text{m sec}^{-2}}{\text{A}}. \tag{7.13}$$

If A and B are not perfectly collinear magnetically, one still has, at the position of levitation $\partial b_{Az}/\partial x|_O \cong 0$ but we must now take into account the possibility that $\partial b_{Bz}/\partial x \neq 0$. The force $F_x(0)$ must therefore be written adding to (7.12) the term:

$$F_x(0) = \frac{3V}{\mu_0} b_{Az}\frac{\partial b_{Bz}}{\partial x}\Big|_O I_A I_B(t) \tag{7.14}$$

proportional to $I_A I_B(t)$. This additional term has two effects: the first is to increase the horizontal noise; in fact, although $\bar{I}_B = 0$, the instantaneous value of $I_B(t)$ depends on the vertical noise. This vertical noise is thus partially transformed into horizontal noise via the added term in (7.14); this is a minor inconvenience because when there is vertical noise there is often already horizontal noise and the new term in (7.14) only adds some amount to it.

The second effect of the added term in (7.14) is that it also contributes, slightly, to the damping: indeed if the *vertical* photodetector is not perfectly homogeneous, its response depends, slightly, on the x position of the ball. Therefore, corresponding to the x motion of the object a small periodic current $I_B(t)$ arises in the B coil. The force on the object produced by this current, via the added term in (7.14), is, in general neither in phase nor at 90° with the force producing the motion of the object. However a fraction of this force is at 90° and can contribute to the damping. In the usual conditions of magnetic alignment between the A and B coils the damping due to this force is less than 1% of our preselected damping. The only drawback of this supplementary damping is that it is not as stable as the preselected damping, depending, as it does, on a number of factors. Assuming, *pessimistically*, a long term stability of these factors of only 10%, this additional damping creates a long term instability of less than 10^{-3}, and is therefore unimportant. One reason to give these details here, has been to analyze an example of interconnected effects, that have to be controlled to ensure a proper operation of the apparatus.

Another reason to clarify the above mechanism in detail is that a similar mechanism is useful to produce a tiny ($\tau_{\text{damping}} \cong 15$ minutes) damping in the y direction (the expression of F_y is in fact similar to F_x (7.14) with the substitution of x with y and omission of the last – D coil – term). The possibility of producing this tiny damping along y depends on the non-perfect homogeneity of the light in the neighborhood of the object.

In connection with the y motion a final remark is in order: the difference by a factor ~1.7 between the natural frequencies of oscillation in the x (~1 Hz) and y directions (due to the shape of the pole cap shown in the fig. 7.3 and the presence of the iron nuclei D) and the extremely narrow frequency window created by the lock-in (section 7.10) have the important consequence that the lock-in output signal of the x motion is unaffected by the simultaneous presence of a large y oscillation; although the latter is, in fact, absent due to the above y damping.

7.4. *The optical system and the photodetectors*

With reference to fig. 6.6 the optical system is composed (from right to left) of: (1) the main lamp L (Halogen Osram 100 W, 12 V. mod. 64625 powered at 7 or 8 V rather than 12 V); the lamp is mounted in a projector (Spindler and Hoyer nr. 030123) appropriately modified to increase its mechanical stability) with a condenser lens ($f = 70$ mm and opening $\Phi = 75$ mm). (2) A set of Kodak filters (2 nr. 25 and 1 nr. 24) mounted in front of the right window of the levitation chamber. (3) A plano-convex lens L_1 ($f = 90$ mm and $\Phi = 60$ mm) on a non-metallic holder. (4) A double convex lens L_2 ($f = 50$ mm and $\Phi = 38$ mm). (5) A half-transparent mirror M. (6) The horizontal photodetector H.D., to measure the x displacements of the object. (7) The vertical photodetector V.D., to control the vertical position of the object. The optical bench and the holder of the lenses (Spindler-Hoyer nr. 023161; 023404; 023004) are in non-magnetic materials. The distances between the various components (in the normal conditions of operation) are indicated in the caption to fig. 6.6. The photodetectors (the vertical one is shown in fig. 7.7) as well as the other optical components are appropriately protected from the light of the laboratory.

Note that the power of the lamp in the conditions of operation is low (50 W); moreover the power arriving on the levitating object is considerably attenuated by the red filters. We mention this because even with the red filters (that cut off the light beyond $\lambda_{\text{min}} \cong 6000$ Å), the rate of spontaneous changes in

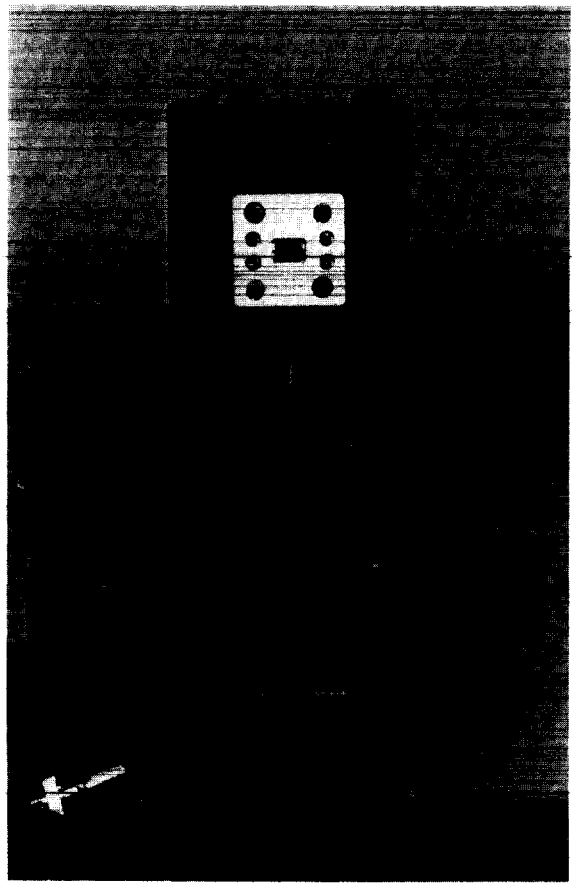

Fig. 7.7. A photograph of the vertical photodetector. The type of support used – allowing for horizontal displacements – is also visible.

charge of the levitating object increases considerably with increasing power of the lamp (some balls that change charge frequently with the lamp operated at 8 V stop to do so simply decreasing the voltage to 7 V). Operating the lamp much below its nominal power is also essential, of course, to allow a lamp to survive for the duration of an entire run (say 10 days of continuous operation). No run had to be discontinued because of the blowing of a lamp.

At the beginning of the experiment we spent some time in deciding whether to use photomultipliers or photodiodes. We decided in favour of photodiodes for a number of reasons; this decision appears now so obvious that we do not understand, a posteriori, why we could have some doubt on this matter. The photodiodes must meet to requirements: (a) a comparatively large sensitive area, (b) a low intrinsic noise.

Both for the vertical and horizontal photodetectors we used Philips BPX 42 silicon planar photodiodes, with a sensitive area of 3.7×6.7 mm; appropriately selected pieces (one in 5 or 6) do have indeed a very low noise (see below). The sensitive parts of the photodetectors are shown in scale in figs. 7.8a,b. The magnification provided by the optical system gives a shadow of the levitating sphere of $\sim$3 mm diameter on the V.D. and of $\sim$4 mm on the H.D. The reason why each photodetector is

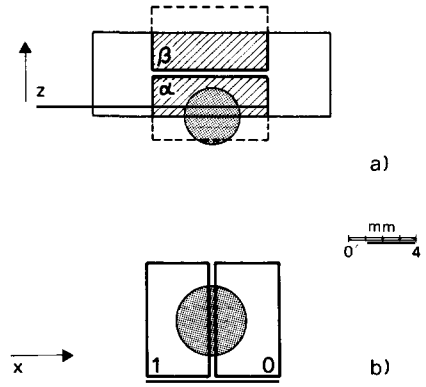

Fig. 7.8. (a) A schematic view of the shadow on the ball on the vertical photodetector V.D. The two photodiodes α and β work differentially. Only the shaded part of the photodiodes is exposed to the light. (b) A schematic view of the shadow of the ball on the horizontal photodetector H.D.

composed of two nearby photodiodes is to produce a differential input independent of the variations of the intensity of the light.

In the case of the vertical photodetector (fig. 7.8a) the area of the sensitive region covered by the shadow increases if the sphere raises, decreases if it falls. In typical conditions of illumination the sensitivity of V.D. is (for a sphere displacing vertically by Δz):

$$\Delta V_v/\Delta z = 25\,\text{mV}/\mu\,, \qquad 37\,\text{mV}/\mu \tag{7.15}$$

where ΔV_v is the variation of the output of the V.D. amplifier (shown in fig. 7.9); in eq. (7.15) the first (second) figure on the right refers to a 0.2 (0.3) mm diameter sphere. The noise figure, over a band of 10 kHz is 3 mV (with selected photodiodes) at the output of the amplifier for the vertical detector; for

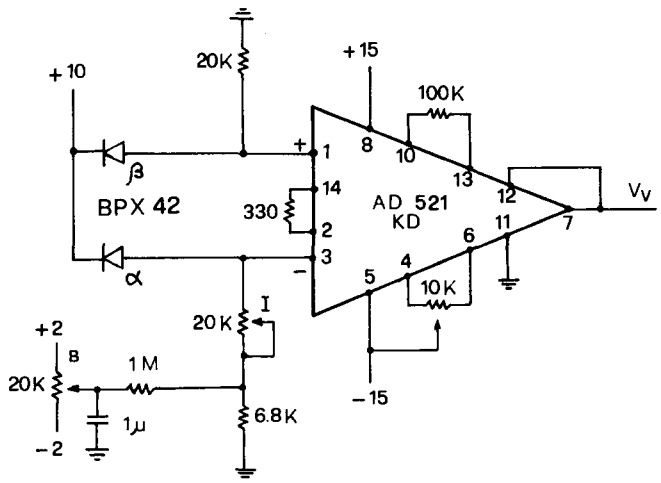

Fig. 7.9. The amplifier of the V.D. signal. The circuit of the H.D. is quite similar but has different values for some parameters.

the horizontal detector it is 0.2 mV over a band of 1 kHz (note that there is a difference in the gains of the two amplifiers). A final remark on the vertical photodetector is the following: as it appears from fig. 7.8a the levitating object, if initially at the center, can move towards the right or the left by one radius, always remaining in the sensitive region of the photodetector, and therefore without falling down. Note that the above displacements are (due to the presence of the mirror) displacements of the objects along the x axis; displacements along the y axis appear on V.D. simply as focusing or defocusing of the image.

As to the horizontal photodetector the right photodiode signal increases and the left decreases if the sphere moves to the left; viceversa for a movement to the right (fig. 7.8b). The amplifier of H.D. has an amplification smaller by a factor ~4 with respect to that of V.D., because the output from the H.D. amplifier goes to the preamplifier of the lock-in. The sensitivity at the output of the H.D. amplifier is:

$$\frac{\Delta V_{\mathrm{H}}}{\Delta x} = 12\,\mathrm{mV}/\mu\,, \qquad 18\,\mathrm{mV}/\mu \tag{7.16}$$

where, again, the first value refers to a sphere with $\Phi = 0.2$ mm and the second to a sphere with $\Phi = 0.3$ mm. We remark, finally, that the housing of V.D. and H.D. ensure the electric and magnetic shielding of the respective amplifiers and the thermal and mechanical stability of the photodiodes.

To conclude we note an important property already mentioned (section 6.2) arising from the fact that the x oscillation signal is used also to produce (via the derivative operation) the x damping. The property is this: the signal produced by a sphere oscillating in the x direction under a given external force is, at resonance, invariant with respect to changes of the intensity of the light: if, for instance, the light decreases, the amplitude of oscillation increases and, *at resonance*, the signal produced by the oscillation remains exactly unaltered. Schematically the argument goes as follows: Signal (at resonance) $\propto IA_{\mathrm{res.}}$ where I is the intensity of the light and $A_{\mathrm{res.}}$ the amplitude of oscillation at resonance. But $A_{\mathrm{res.}} \propto F/\gamma$ where F is the force producing the oscillation and γ the damping constant; the latter is proportional to I. Therefore we have: Signal (at resonance) $\propto IF/\gamma$, independent of I. This property can be useful in many circumstances; for instance when, in the course of a measurement, we wish to decrease – if needed – the rate of change of charge. Also, in view of the above property, the aging of the lamp and the related modification of the optical spectrum has no effect on the measurement.

7.5. The levitation chamber

The levitation chamber is shown (in scale) in the two sections xz and yz (figs. 7.10a,b). A photograph of the open chamber appears in fig. 7.11. Four supports (not shown) allow to fix the cylindrical main body of the chamber (in brass) – from below – to the roof of the castle (compare fig. 7.1 for a general view). The side walls of the chamber – also in brass – can be removed easily while retaining the cylindrical body in its place. In fact we remove the left side wall each time new spheres are introduced to start a new run. The use of the bar H and the elevator E to deposit a sphere and levitate another during a run goes as follows: the four spheres are first put on the top of the four small silver cylinders (1, 2, 3, 4), lodged in holes in the bar H, which is movable in the y direction; the four cylinders are shaped as shown in the insert of fig. 7.10b. The box is then closed and evacuated. To levitate a sphere, H is displaced so that the elevator E is positioned below the corresponding cylinder. Using the knob K we then raise E until the shadow of the sphere is at the position appropriate for the levitation; at this stage the usual procedure for feedback levitation, to be described in section 7.11, is adopted. The upper

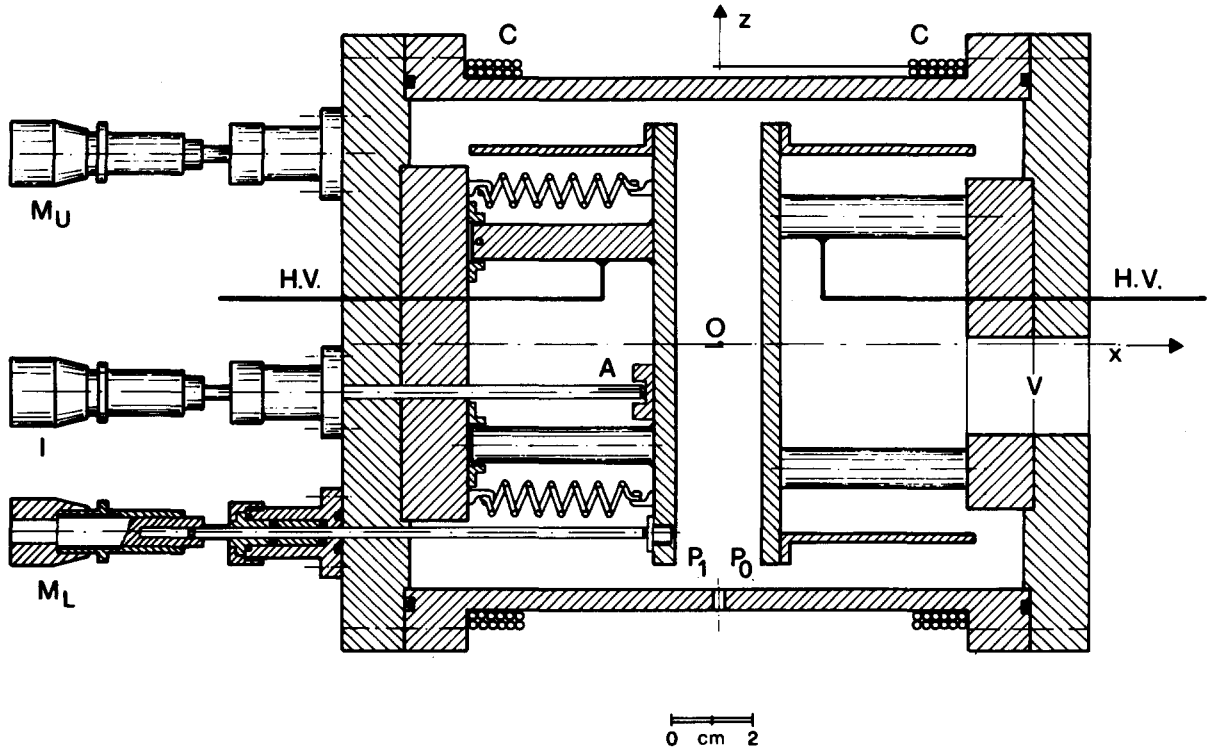

Fig. 7.10a. A mid-section in the xz plane of the levitation chamber showing the plates P_0 and P_1, the micrometers M_L and M_U, the screw I to incline the plate P_1, the exit V connecting the box to the vacuum system; also the wires H.V. connecting the plates to the high voltage system are indicated schematically as well as the coils C mentioned in text. Several details are omitted for simplicity.

part of the elevator contains, inside, a very small coil that can be energized during the act of levitation to bring the sphere precisely at the center of the cylinder so that its image appears (when everything is ready for levitation) at the center of the vertical photodetector.

After levitation the elevator E is slowly retracted down to its seat and the current in the small coil just mentioned is slowly brought back to zero. During the descent of E the cylinder (without sphere) takes again its place in its seat in the bar H; the latter is then retracted all the way to the left into its housing. The mechanical tolerances in the positioning of the bar H are better than 20 μ.

The electric plates (in brass), their supports, and the dielectric slabs providing the electrical insulation must be manufactured with precision, to guarantee the parallelism of the plates (better than 20 μ from top to bottom) and their flatness. The micrometers $M_{L(ower)}$ and $M_{U(pper)}$ allow to check, when needed, the parallelism of the plates once the box has been mounted and evacuated. (Once the parallelism has been checked the bars of the micrometers are withdrawn.)

The micrometric screw I allows to incline the plate P_1 with respect to P_0 by a prescribed amount. This is necessary to create a prescribed value of $\partial E_z/\partial x$ which is used to measure the permanent electric dipole moment $\boldsymbol{d}$ of the ball (or better its z component since the x and y components are averaged out by the spin). The springs indicated in fig. 7.10a ensure that the original position of P_1 (parallel to P_0) is restored when I is turned all the way back.

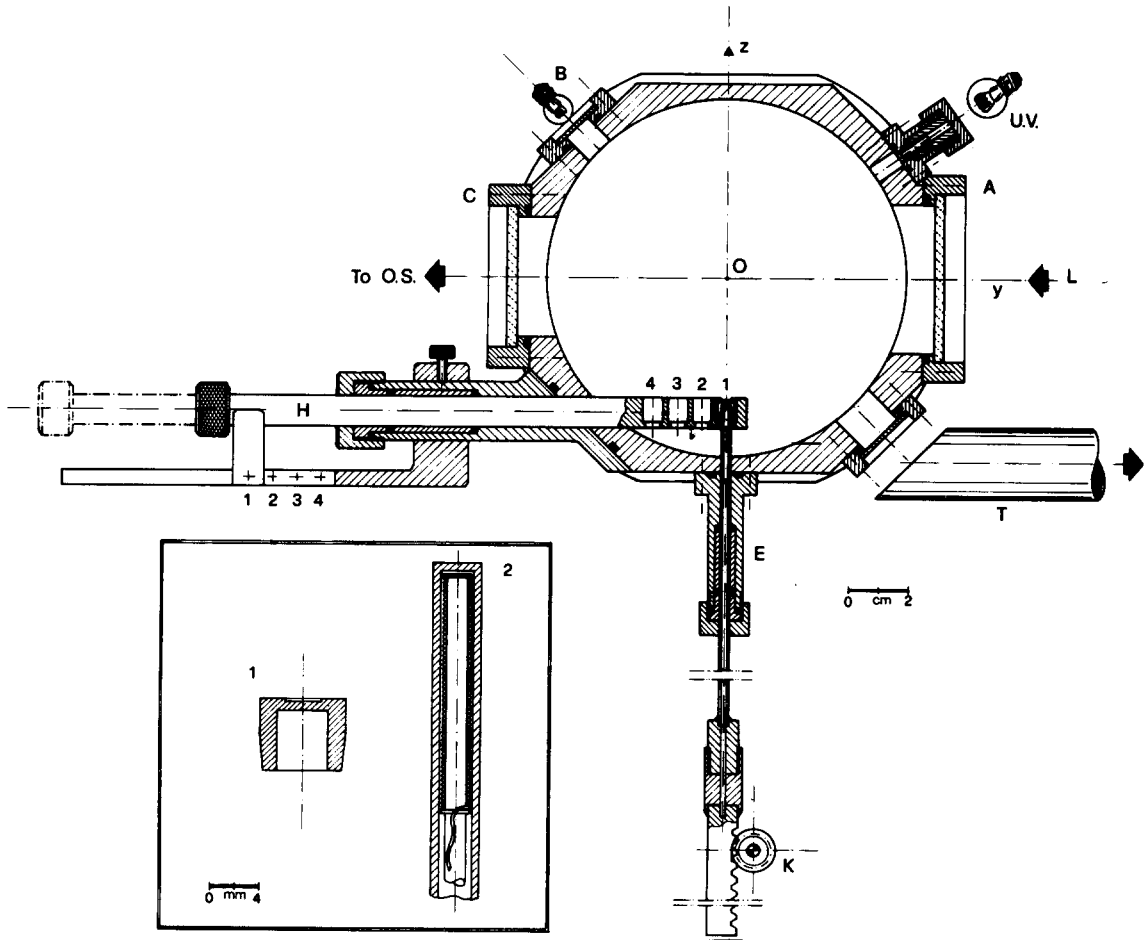

Fig. 7.10b. A mid-section in the *yz* plane of the levitation chamber showing the system to levitate several spheres in succession without opening the chamber (details of the cylinders on which the balls are deposited and of the upper part of the elevator E are given in the insert as 1 and 2). Also visible: the U.V. lamp; the main lamp L used for the illumination of the object O (the rays from O are collected by the optical system O.S. and sent to the horizontal and vertical photodetectors). The small bulb B produces – when useful – an image of the levitating object on a television screen (through the telescope T and a telecamera). Several details are omitted for simplicity.

Three additional remarks are useful: (1) Although the details of the high voltage (vacuum tight) connections through the side walls have been omitted for simplicity from fig. 7.10a it must be emphasized that any piece of metal carrying the high voltage outside the chamber must be shielded carefully to avoid that the electronics picks up radiation in phase with the reversals of the electric field. (2) The coils C are wound directly on the cylindrical body of the chamber. Their use will be illustrated later. (3) The glass windows of the chamber have been internally made conductive by application of a transparent layer of SnO_2 [41]. Some additional details of the chamber are listed in the caption to the figures 7.10a and 7.10b.

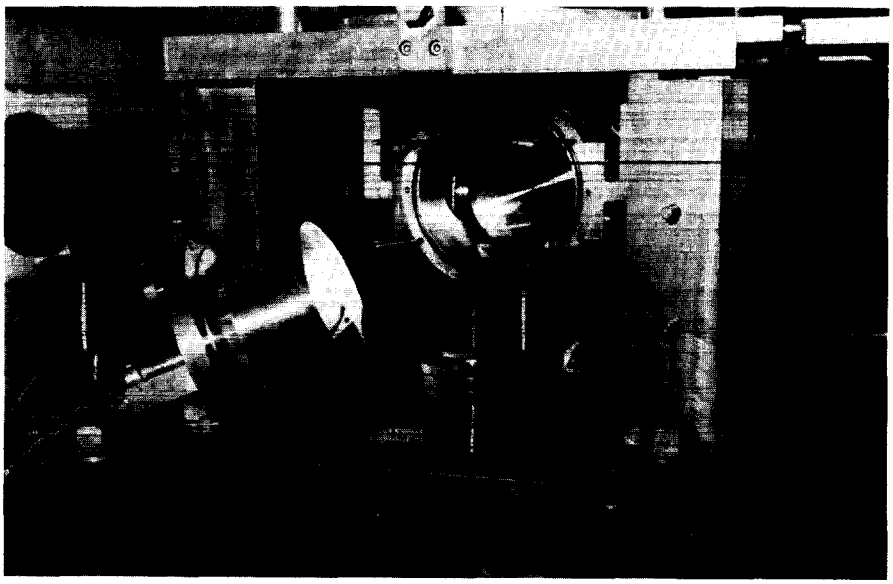

Fig. 7.11. A photograph of the open levitation chamber.

7.6. Spinning

The rotation of the sphere around the z axis is produced by a rotating magnetic field, as in the induction motors; this rotating field is created by the C and R pairs of coils, external to the levitation chamber (see fig. 7.12). The two C coils are connected in series; the same is true for the two R coils. The C coils are wound on the levitation chamber (see fig. 7.10a) while the R coils are wound on cylindrical supports in plexiglass, schematically indicated in fig. 7.12. The coils are powered (with a phase lag of 90° between C and R) by current generators with supplies KEPCO BOP 72-5M. To increase the current in the R coils (that are positioned rather far from the levitating object) a variable capacity (1 μF to 9 μF) in series with the coils is used. Its value is selected depending on the frequency. For a direct current the

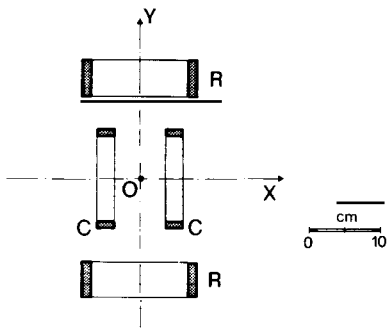

Fig. 7.12. An xy section of the coils used for the spinning. The coils C are those appearing already in fig. 7.10a. Each one of the coils C consists of 180 turns of wire $\Phi = 0.75$ mm; each coil R consists of 380 turns of wire $\Phi = 1$ mm.

field at O produced by the C coils is 19 gauss per ampere; that due to the R coils 6 gauss per ampere. Both these fields decrease, on increasing the frequency, due to the Foucault currents in the walls of the (brass) levitation chamber. In vacuum the rotation of the sphere at 400 Hz is produced with ~1 ampere in the coils C and ~1.5 ampere in the coils R. To keep the sphere rotating it is sufficient to have 300 mA in the coils only. The spinning of the ball (and the spin frequency) are seen (and measured) by looking at the signal from the horizontal photodetectors. Any tiny irregularity of the surface of the ball produces – when the ball spins – a periodic signal in the horizontal photodetector. For particularly clean balls the peak to peak amplitude of this periodic (but irregularly shaped) signal is (after amplification from the horizontal photodetector) much smaller than 1 mV.

7.7. Change of $\partial H_x/\partial x$ to measure the magneto-electric force

This operation (sections 3.6 and 8.2) is performed using the same coils C (switched to an anti-Helmotz configuration) after the ball has been set in rotation (we have just mentioned that the coils R are sufficient to keep the ball spinning). The variation of $\partial H_x/\partial x$ needed to measure the magneto-electric force is produced by letting a current of +2 ampere flow in the coils (and performing a complete set of measurements in this situation); and, repeating all the measurements with a current −2 ampere. The transition from +2A to −2A takes a few minutes; it has to be performed gradually to avoid giving sudden pushes to the levitating ball.

7.8. The vacuum system

The vacuum in the chamber is produced by a standard rotary diffusion system (Balzers PST 260 E). To avoid vibrations, the rotary pump is far away from the diffusion pump, which is in the proximity of the apparatus. Two zeolite traps are on the line from the rotary to the diffusion pump. Two vacuum pipes in parallel connect the diffusion pump to the exit V of the levitation chamber. On one of these connections a liquid nitrogen trap is inserted. On the other a Balzers gauge (mod. IMR 3) in the vicinity of the chamber measures the residual vacuum. We have mentioned this explicitely because we discovered by chance that this gauge – once its filament is switched on – can be used (in our present set-up) to change in the negative direction the charge of the levitating sphere. (Changes of charge in the positive direction are easily made by the UV light – compare fig. 7.10b – ; however changes of charge in the negative direction were difficult to produce for a long while; for instance in the previous levitation chamber – in which the plates did not have the back appendices shown in fig. 7.10a – the same operation of switching on the vacuum gauge did produce changes in charge in the positive direction.) The simplicity of performing this operation by switching on the filament of the vacuum gauge was therefore a surprise; this method is reproducible and very convenient (during this operation the oscillating electric field is set at $\sim 10^3$ V/cm instead of 2×10^3 V/cm as during the measurement).

In conclusion we add that: (a) it takes only a few hours to reach the vacuum – between 7 and 10×10^{-6} torr – at which the measurements are usually performed. This applies if the chamber has remained open only for the time necessary to deposit on the cylinders a set of clean spheres to start a new run. (b) When necessary the vacuum in the chamber can be performed through a needle valve; this allows to produce the vacuum or to put air in the chamber while keeping a sphere in levitation.

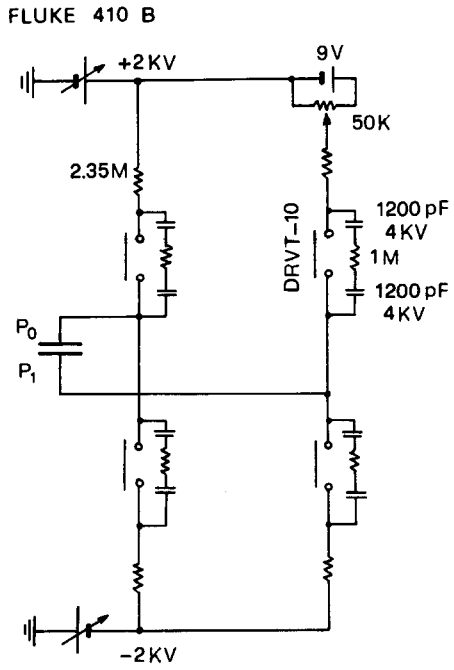

Fig. 7.13. The main elements of the high voltage circuit providing the square wave high voltage to the plates.

7.9. *The high voltage*

The square wave to the plates is provided by two high voltage (H.V.) power supplies (FLUKE, mod. 410 B). In the present conditions of operation the peak to peak excursion of each plate is from +2000 V to −2000 V. One of the high voltage supplies is at +2000 V, the other at −2000 V and a system of switches periodically interchanges the contacts between the two H.V. supplies and the two plates (see the fig. 7.13). The period between interchanges is, of course, the resonance period of the ball in the magnetic valley (as already stated of the order 1 s). We determine and fix this period by a quartz pulse generator with variable frequency; the stability of this instrument is some parts in 10^7 but we need to center the resonance only to a few parts in 10^4. The switches consist of H.V. reed relays (HAMLIN, mod. DRVT 10-selected) piloted by the quartz pulse generator. The following operations can be easily performed: (a) check of the "balancing": this means that the H.V. signal integrated to many periods must vanish (this operation has to be done separately on each plate). If a difference from zero is found it can be brought to zero (to better than 0.1 V) using the fine voltage regulation of one H.V. power supply and a small floating battery inserted in series at the output of the other H.V. supply. (b) Check of the presence of even harmonics in the electric signal to the plates. Even harmonics should not be present in an ideal square wave. Because of the opening and closing times of the reed relays (~4 milliseconds) the wave is not perfectly square, as already stated in section 3.4. In view of the fact that the amount of second order harmonics has already been very small, below the level that would create problems, we will not expand here on their measurement. A few words on the balancing system are, however, appropriate. This is shown in fig. 7.13. A byproduct of the balancing system is to check periodically the good functioning of the reeds. Although among the reeds tried the most satisfactory ones were those

quoted previously, we had to select them carefully because only a fraction satisfies our stability requirements at our voltage and switching frequency. Instabilities in switching appear as instabilities in balancing.

The reeds must be shielded and the box containing them must be kept at a few meters from the electronics and from the levitating ball to avoid both effects from the stray magnetic field of the small coils piloting the reeds (that should be disposed in a quadrupole configuration) and radiation effects; all the H.V. cables must also be shielded. A "zero" check for the absence of undesirable radiation effects and of equally undesirable effects of *any kind* (performed often during the measurements) is the following: let all the apparatus be in its working conditions, with only the plates disconnected and short circuited: the amplitude of oscillation of the levitating sphere must of course vanish.

7.10. The detection and recording of the signal

The signal from the horizontal photodetector, giving the x amplitude of oscillation, is fed to a PAR Lock-in Mod. 124 A (extended to the low frequencies from 0.2 Hz) with a preamplifier PAR Mod. 116. The reference signal in the lock-in is locked to the quartz signal generator that pilots the reed relays; in other words it is locked to the square wave electric field. The resonance frequency is determined for each sphere; it usually differs little (by less than a part in a thousand) from sphere to sphere. In the usual working conditions the output of the lock-in (giving the signal to be recorded) is integrated with an integration time $\tau = 300$ s, 12 db/octave. This amounts to say that the lock-in does create a window (equivalent noise band-width) of 0.4×10^{-3} Hz centered around the frequency of oscillation; any noise outside this window is rejected. We insert in addition, the entrance filter of the lock-in with a Q value of 20. Besides recording the signal of the horizontal photodetector in phase with the electric field we also measure and record, using an auxiliary circuit, the signal 90° out of phase.

The sensitivity scale of the lock-in is selected so that: (a) a change in charge by one electron can be measured with the requested precision, (b) the lock-in does not get full scale for a change of two charges in both directions. With these requirements the scale of the lock-in sensitivity to be used depends on the preselected value of the damping constant; also it is different depending on whether we measure spheres of diameter 0.2 or 0.3 mm. To give a number we mention that convenient sensitivity scales of the lock-in are often respectively 50 mV and 20 mV. The output from the lock-in – as well as the signal at 90° – is recorded on a pen recorder (YOKOGAWA mod. 3047). Typical records of the output of the lock-in versus time have been presented in the fig. 6.7 and others will appear in section 8.

7.11. The sequence of operations in a run

A run consists typically of the following sequence of operations:

(1) Opening of the levitation chamber, deposition of four clean spheres on their cylinders; restoring of the vacuum.

(2) Levitation of the sphere nr. 1, spinning, search of the resonance frequency, progressive discharge using U.V. light. (During this stage the resonance frequencies are determined with the two values for the gradient of H_x: $H_{xx} = H^{\circ}_{xx} \pm \Delta H_{xx}$; this information is necessary to perform, afterwards, all the measurements needed in the two conditions, to extract the magneto-electric part of the force.)

(3) When the sphere has an apparent charge of one or two electrons the measurement starts, first with $H_{xx} = H^{\circ}_{xx} + \Delta H_{xx}$, then with $H_{xx} = H^{\circ}_{xx} - \Delta H_{xx}$. By measurement we mean the determination, in each of the above two conditions, of an appropriate number of charge levels, with a sufficiently small error.

The duration of a measurement depends on the signal to noise ratio which, in turn, depends on the seismic conditions.

(4) The sphere 1 is deposited and the sphere 2 is levitated (without opening the chamber); a similar set of operations then takes place. The same applies to the spheres 3 and 4 (if no one gets lost in the act of levitation). The time usually needed to deposit one sphere and to have ready the subsequent one for starting the measurement is about one hour.

Each of the above operations consists of course of a number of sub-operations. We shall not describe them all, but to give a feeling of the experiment we insert below a sort of summary of the operation manual that should of course be skipped by the readers not interested in the details.

1. To start a run open the levitation chamber, take off the four cylinders, pick up the four balls of the previous run.

2. Clean the four spheres to be used (cleaning is made by ultra sound washing in CCl_4 or alcohol), and deposit each of them on its cylinder. Be sure that no sphere is stuck to the cylinder; this would make the act of levitation difficult or impossible.

3. Close the levitation chamber and start doing the vacuum: first – in rotary pump regime – using the needle valve so as to avoid abrupt depressions that might displace the balls from their lodgements; next in the diffusion regime.

4. Create a potential difference (from +10 V to +100 V between one plate and the sphere holder E (grounded)). This potential difference has the purpose, illustrated in section 6.2 number 5 of providing an appropriate negative charge to the levitated sphere.

5. Have the main lamp L (fig. 6.6) powered at 10 or 11 volts (after the levitation this will be reduced to 7 or 8 volts).

6. Be sure that the switch S in the x damping circuit is set on the feedback position, so that accidental pushes to the ball during the levitation procedure do not produce the falling of the ball.

7. Be sure that the power supply of the main coil A is on but that the magnetic field is at a value insufficient for levitation. Be also sure that the vertical feedback is switched on.

8. By positioning the bar H (fig. 7.10b) select the sphere to be levitated. Raise the elevator E as described in section 7.5; the upper edge of the shadow of the sphere should be ~0.5 mm below the lower edge of the sensitive area of V.D.

9. Switch on the current in the small coil inside the upper part of the elevator E. Operate the sweeping system of the current in the main coil A. During the increase of the current in A produce gentle strikes on a bar attached to the elevator. If the ball is not stuck to its cylinder it moves, during this process, towards the center of the cylinder. When the current in the main coil reaches the value appropriate for levitation the ball detaches from the cylinder, jumps up and floates.

10. Retract down E and decrease slowly the current in the small coil inside E: switch it off. Retract H all the way to the left. Measure by the appropriate instrument the force required by the horizontal feedback to keep the object at the center of the vertical photodetector. If this force is not exactly zero displace the main lens by a few microns.

11. The TV set can now be lighted on to give a look to the floating sphere. Reversing the voltage between the two plates from say +200 V to −200 V and observing the displacement of the sphere on the TV one can also check that the sign of the charge of the ball is the correct negative one.

12. If this check is satisfactory, the spinning procedure can be started. Before this look, however, to the current in the slow feedback system: if non-zero operate on the fine regulation of the main power supply.

13. To start the spinning procedure turn on the sine wave generator and the related power supplies.

Increase slowly the frequency, controlling on the oscilloscope (see the section 7.6) the rotation signal of the ball up to a rotation frequency of ~400 Hz.

14. The ball is now ready for measuring the resonance frequency of the magnetic valley. After checking again that the horizontal feedback force is zero, switch S to position 2 thus inserting the x damping. Be sure that the damping is inserted at the normal value, corresponding to the full insertion of the potentiometer in fig. 7.6. Apply a very small oscillating electric field, of the order 1 V/cm peak to peak (it has to be small because the charge of the ball is large and an excessive amplitude of oscillation of the ball would make it fall down). Keeping the lock-in on its less sensitive scale (500 mV) change slowly the frequency of the quartz pulse generator – governing the reeds – until the amplitude of oscillation is maximum; or more precisely (this is in fact what we do) the signal at 90° is zero. We stress that this determination of the resonance frequency is performed when the sphere is still *highly* charged: one can thus be sure that the force acting on the sphere is, overwhelmingly QE, and the phase of the resonance signal determined in this way is that of the above force. This is an important point; it has been with this procedure for determining the resonance frequency that we did establish that no signal proportional to $d\boldsymbol{E}/dt$ appears – for a spinning object – after the charge is reduced to a small value.

15. The search of the resonance frequency described under 14 must be repeated, in fact, at each of the two different values of $\partial H_x/\partial x$ obtained as explained in section 7.7.

16. Start the U.V. discharge of the ball keeping the current in the C coils at one of the two values just stated (say at the −2A value) and operating, of course, at the corresponding frequency. Use, initially, the U.V. lamp at full intensity. As the charge of the ball decreases, reduce progressively the intensity of the U.V. lamp and increase, at the same time, the electric field producing the oscillation of the ball. When the charge of the ball has reached low values such that the electric field can be set at its final value (+2000 V, −2000 V) the U.V. source must be controlled very accurately so as to be sure not to extract too many electrons, thus leaving the ball with a sizeable positive charge (should this happen by an overdose of U.V. light, use, to go backwards, the filament method described in section 7.8). Leave the ball with one or two electrons and turn off the U.V. lamp.

17. Insert the lock-in filter after appropriate adjustment; be sure that the sensitivity and integration times of the lock-in are positioned correctly. Switch off the TV, insert the pen recorders, check the nitrogen level in the cold trap of the vacuum line.

18. Insert an automatic switch to ensure that if, for any reason (e.g. momentary power failure) the ball falls, the power supplies are switched off to avoid a useless operation of the instrumentation (this is particularly important during the night operation). Note that all the operations performed so far from the insertion on the diffusion pump on, take – on the average – about one hour.

19. The measurement starts at this stage and consists in the determination of a set of charge "levels" (section 8 will describe in detail the analysis of a measurement).

20. Once a measurement with the minus setting of the current in the C coils is completed, reverse this current to the +2A value so as to start the measurement with $(\partial H_x/\partial x)^+$. In reversing the current the following operations must be performed: (a) set the quartz pulse generator at the frequency corresponding to the value +2A (already determined, compare 15.), (b) reset the filter of the lock-in to this frequency, (c) change slightly the balance of the H.V. power supplies (the commutation times of the reeds – and therefore the balancing – slightly depend on the switching rate). Be sure of making again at this stage (or later) the reverse transition +2A → −2A, to check that the charge of the ball has not changed accidentally during the −2A → +2A operation. (This is unlikely because this operation takes five minutes, whereas the spontaneous changes in charge occur every several hours.)

21. Once the measurement with both values of H_{xx} is performed all the data are available to

determine the residual charge and the magneto-electric part of it. One can still determine the permanent electric dipole moment of the ball in the way mentioned in sections 3.5, 7.5; the measurements on the sphere are thus completed. To continue the run the sphere should be deposited and another one levitated.

22. To deposit the sphere: (a) insert the x feedback, (b) switch off the H.V. power, (c) set the current in the C coils to zero, (d) extract the bar H to the position where the silver cylinder stays above the elevator, (e) raise the elevator until its shadow is very near to the levitating sphere, (f) exclude the automatic switch mentioned at 18., (g) decrease abruptly the current in the main coil A, (h) reset down the elevator all the way.

8. The measurements

8.1. Introductory remarks

We are now going to describe and display all measurements performed so far on a total of 70 different steel balls (34 with diameter 0.3 mm and 36 with diameter 0.2 mm). As stated in section 3.7 only two apparent spurious charges remain to be considered when the plates are parallel and after the balancing has been checked: the magneto-electric charge $Q^{(\mathrm{m.e.})}$ and the Volta patch charge $Q^{(\mathrm{V})}$. The total charge Q can thus be written:

$$Q = q + \alpha E_{xx}^{(\mathrm{V})} + \beta H_{xx} \equiv q' + \beta H_{xx} . \tag{8.1}$$

In the last passage we introduced, to simplify the notation, the abbreviation q' to indicate the sum of the true† and Volta charges:

$$q' = q + Q^{(\mathrm{V})} . \tag{8.2}$$

We now describe in the order: (1) how $Q^{(\mathrm{m.e.})}$ is measured and subtracted, (2) what is the resulting distribution of q', (3) how in each case $Q^{(\mathrm{V})}$ is subtracted and the values of q are obtained from the values of q'.

8.2. The elimination of the magneto-electric force

Start from the equation $Q = q' + \beta H_{xx}$ and call:

$$H_{xx}^{\pm} = H_{xx}^{\circ} \pm \Delta H_{xx} \tag{8.3}$$

the two values of $H_{xx}(= \partial H_x/\partial x)$ obtained reversing the current in the C coils from +2 ampere to −2 ampere; these two values are used to perform the measurements on each ball (always kept levitating). Also call $\beta^{\pm}$ the two values of $\beta = d_z/H_z$ that correspond to the above values of H_{xx}; indeed when a variation of H_{xx} is made, also H_z changes slightly. We thus introduce:

† The true electric charge will be indicated from now on by small q rather than by capital Q as in section 3 and the suffix R in Q_R will be omitted; therefore from now on Q is the total apparent charge, q the true charge and $Q^{(\mathrm{V})}$ the patch charge.

$$H_z^{\pm} = H_z(1 \pm \varepsilon) \tag{8.4}$$

and we call $\beta^{\pm}$ the two values of β corresponding to the above values of H_z:

$$\beta^{\pm} = d_z/H_z^{\pm} \cong \beta(1 \mp \varepsilon)\,. \tag{8.5}$$

The numerical values of the magnetic field and their variations will be given in section 8.9.1. Calling respectively Q^+ and Q^- the residual charges measured in the +2A and −2A conditions, we have:

$$Q^+ = q' + \beta^+(H^{\circ}_{xx} + \Delta H_{xx}) \tag{8.6}$$

$$Q^- = q' + \beta^-(H^{\circ}_{xx} - \Delta H_{xx})\,. \tag{8.7}$$

Subtracting and summing we get:

$$X = Q^- - Q^+ = 2\beta(\varepsilon H^{\circ}_{xx} - \Delta H_{xx}) \tag{8.8}$$

$$Y = \frac{Q^- + Q^+}{2} = q' + \beta(H^{\circ}_{xx} - \varepsilon\,\Delta H_{xx}) \tag{8.9}$$

where the abbreviations X and Y indicate:

$$X = Q^- - Q^+ \tag{8.10}$$

$$Y = \frac{Q^- + Q^+}{2}\,. \tag{8.11}$$

We now write:

$$k = \frac{H^{\circ}_{xx} - \varepsilon\,\Delta H_{xx}}{2(\varepsilon H^{\circ}_{xx} - \Delta H_{xx})} = k'\frac{1 + \varepsilon/2k'}{1 + 2\varepsilon k'} \tag{8.12}$$

where

$$k' = -\frac{H^{\circ}_{xx}}{2\Delta H_{xx}}\,. \tag{8.13}$$

Eliminating β from the two equations (8.8), (8.9) we get:

$$q' = Y - kX\,. \tag{8.14}$$

Each measurement consists in determining Q^+ and Q^-; from these we can obtain X and Y (equations (8.10) and (8.11)). At this stage q' is determined by eq. (8.14), adding or subtracting an appropriate integer if $|q'|$ is larger than 0.5. The parameter k is a constant of the instrument depending only on the magnetic field and its gradient at the position of levitation (compare eq. (8.12)); its determination will be illustrated later. The value of k is:

$$k = 1.69 \pm 0.015\,. \tag{8.15}$$

To clarify the meaning of eq. (8.14) note that in the hypothetical case where the Volta patch effect vanishes and the true residual charge q is also zero (no quark), the X and Y coordinates of all the balls should stay on a straight line through the origin with angular coefficient $k = 1.69$. The first data [30, 31] obtained were plotted in a X, Y plane to show how, after the identification of the magneto-electric force, this pattern indeed appeared (we reproduce below – from ref. [31] – the fig. 8.1 referring to balls with $\Phi = 0.2$ mm). In this plot q' is read as the vertical deviation of the ordinate of each point from the line $Y - kX = 0$. From now on, however, we prefer to display for each ball the value of q' with its error, rather than continuing to give the X, Y inclined plots of the type shown in fig. 8.1. Before reporting the complete data on all the balls we shall show, in a few cases, how the determination of Q^+, Q^-, X, Y and q' actually takes place from the raw data given by the pen recorder at the output of the lock-in.

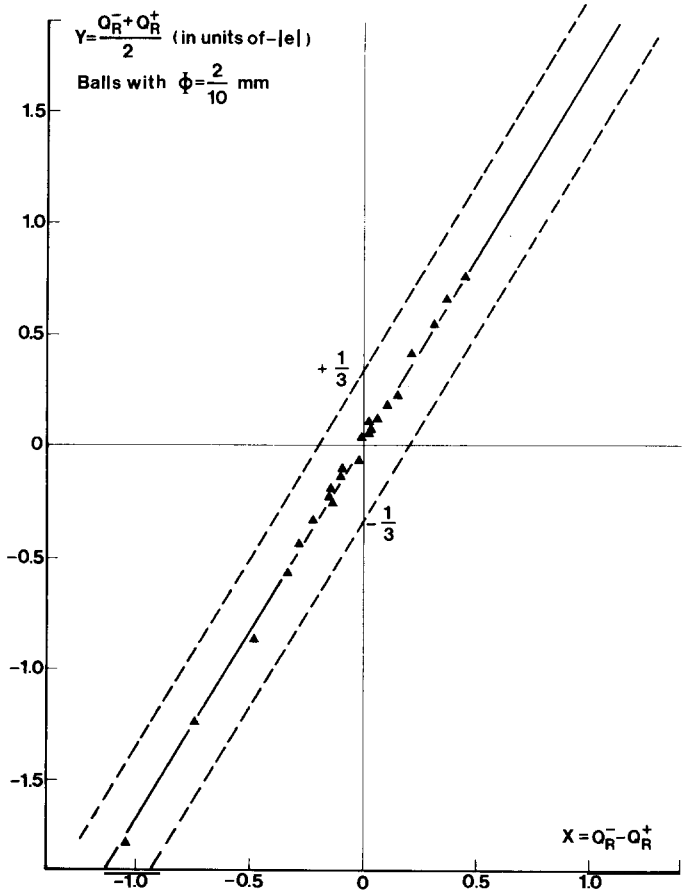

Fig. 8.1. The X, Y plot of the first 23 balls with $\Phi = 0.2$ mm, measured (see ref. [31]) after the identification of the magneto-electric force. (We take this opportunity to note that the analogous figures for the balls of diameter 0.3 mm in refs. [30, 31] contain some errors.)

8.3. The raw data

For each ball the raw data consist essentially of two "levels" of charge: the level L^+, when the current in the C coils is +2A, and the level L^- when the current is −2A.* The errors on these levels,

* Compare the figures 8.2, 8.3 and 8.4.

related to their duration and, of course, to the noise during the period of measurement, will be discussed, together with the whole problem of the errors, in section 8.6; here we note only that the integration time of the lock-in is 300 sec (12 db/octave) and, therefore, the lock-in signal loses its "memory" in approximately 25 minutes. Thus a "level" lasting 3 hours amounts to 7 independent, repeated, measurements. To obtain from L^+ and L^- the quantities Q^+ and Q^- to be used in (8.10), (8.11), we must know the "steps" P^+ and P^- respectively in the +2A and −2A situations. If these "steps" (that is the level variation for a change of charge by one unit) are known, it is:

$$Q^+ = L^+/P^+ , \qquad Q^- = L^-/P^- . \tag{8.16}$$

Note that P^- and P^+ are different; their ratio is ≈ 1.25. The reason for this difference is that the magnetic field configuration at the position of levitation depends on whether the current in the C coils is +2A or −2A. This implies that the frequency of oscillation along the x axis is different in the two cases; the −2A frequency (~0.94 Hz) is smaller than the +2A frequency; because – at resonances – the steps are, at equal damping, in the same ratio as the reciprocal frequencies, this explains the difference between P^- and P^+; in fact however also the damping depends on the current in the C coils, due to the interference term between the magnetic fields produced by the D and C coils (this term was omitted, for simplicity, in eq. (7.12)). Altogether the change in frequency and in damping produce the ratio ≈ 1.25 stated above.

The equality of the balls used in the experiment is very strict so that, keeping the damping fixed (and barring any modification of the damping circuit), all P^+ steps for the different balls are remarkably equal, and the same is true – of course – for the P^- steps. For the balls with diameter 0.3 mm the steps were found to be (in the same units used to measure L^+ and L^-; see below):

$$P^+ = 17.25 \pm 0.25 , \qquad P^- = 21.55 \pm 0.25 . \tag{8.17}$$

These values and errors were obtained considering a sample of steps measured accurately and determining the average value and the dispersion: this dispersion (the standard error) is not due to a dispersion of the mass of the balls (they are equal to better than 1/3000) but, presumably, to a lack of complete rigidity of the magnetic structure of the apparatus; a slight variation of the geometrical configuration in the act of levitation can affect the damping, and thus the "step", as it appears from eq. (7.12).

For the balls with diameter 0.2 mm the steps (and their dispersion) have been found:

$$P^+ = 22.8 \pm 0.35 , \qquad P^- = 28.65 \pm 0.45 \tag{8.18}$$

where the larger errors (with respect to the 0.3 case) are due to a smaller sample of accurately measured steps. In the following we are going to use the above values (8.17), (8.18) of the steps for those balls for which they have not been measured (or they have been measured with lower precision); we shall use the directly measured steps when these are known with better precision; or we use the error weighted value of the steps if an actual measurement exists with error comparable to that in (8.17) or (8.18) (for instance if, for a 0.3 ball we have a direct measurement giving 17.1 ± 0.2 we may average it with 17.25 ± 0.25).

Because of the replacement of a component of the damping circuit after the measurement of ball 48 the value of the steps for the balls 49 to 70 were slightly modified with respect to the values (8.17), (8.18) and were mostly measured directly.

All the numbers appearing above have been expressed in our "practical" units, that is small graduations (in the following s.g.) of the record paper. A small graduation is 2 millimeters. For the 0.2 mm balls the lock-in is operated in the 50 mV scale and a lock signal of 50 mV corresponds to 20 cm. For the 0.3 mm balls the lock-in operates in its 20 mV scale and 20 mV corresponds to a 20 cm displacement of the pen of the recorder. Thus, for instance, for a 0.3 mm ball in the −2 A situation, a displacement P^- of 21.55 s.g. corresponds to a change in signal of 4.31 mV; this is the signal (root mean square amplitude) corresponding to a unit charge in these conditions (it can of course be checked that this signal is that expected from eq. (2.14) with the value of $N_{1/2}$ at which we operate).

8.4. Drifts

To determine and subtract the magneto-electric force the value of the levels L^+ and L^- must be taken at the same time, say at the time when the transition of the current in the C coils from −2A to +2A is performed. This remark is of little importance if the levels are flat – that is if they have no drifts; it is instead to be taken into account if a drift is present: although the drifts (whose origin will be clarified in a moment) are usually comparatively slow, attention must be taken, in the case of drifts, to determine Q^+ and Q^- at the time of transition using a best fit procedure for the levels, especially in the case of noisy levels.

There are two possible origins of a drifting level: 1) a variation with time of the patch force, corresponding, say, to desorption from one of the plates; this drift (if it occurs at all) takes usually place (appreciably) only in the first 12 hours from the beginning of a run. In some cases we had indications of this type of drift but, in our conditions of operation (as we shall see our patch force has always been comparatively small) this has not been a frequent source of drifts. A more frequent source of drifts lies in the slow change of the "permanent" electric moment of the levitating ball – a change due, presumably to desorption of material from the surface of the ball. If the "permanent" electric dipole moment changes, the same occurs to the magneto-electric force (recall that $F_x^{(\mathrm{m.e.})} = (d_z H_{xx}/H_z)E_x^{(\mathrm{a})}$) and a drift of the level occurs. A check of this interpretation of the drift is found in the circumstance that the rate of drift in the −2A situation is usually larger (by a factor ~2) than that in the +2A situation. This difference in drifts is expected because the magneto-electric force is larger by a factor ~2.3 in the −2A situation than in the +2A situation ($H_{xx}(-2\mathrm{A}) = 1.7 H_{xx}(+2\mathrm{A})$); a related check is that during this drift the value of q' stays constant (within the errors).

8.5. Description of some measurements

We now proceed to a description of a few typical measurements to illustrate, in practice, the remarks of the previous subsections. We shall show, below, the recorded data of four different balls, two with $\Phi = 0.2$ mm and two with $\Phi = 0.3$ mm.

Case a (ball nr. 47, $\Phi = 0.2$ mm), fig. 8.2. The whole measurement on this ball lasts 14 hours, from 5 p.m. of 13/6/80 to 8 a.m. of 14/6/80 (each unit – in the abscissa – from 1 to 14 is one hour). The measurement starts with the current in the C coils at the +2A value. After about one hour the ball changes spontaneously its charge from a level +17.5 s.g. of the graduated record paper to −6.4 s.g. (the zero is the central line). At 8.30 p.m. we perform the transition from the +2A current to the −2A current in the C coils (in fact this operation was repeated twice: +2A → −2A → +2A → −2A, so as to be

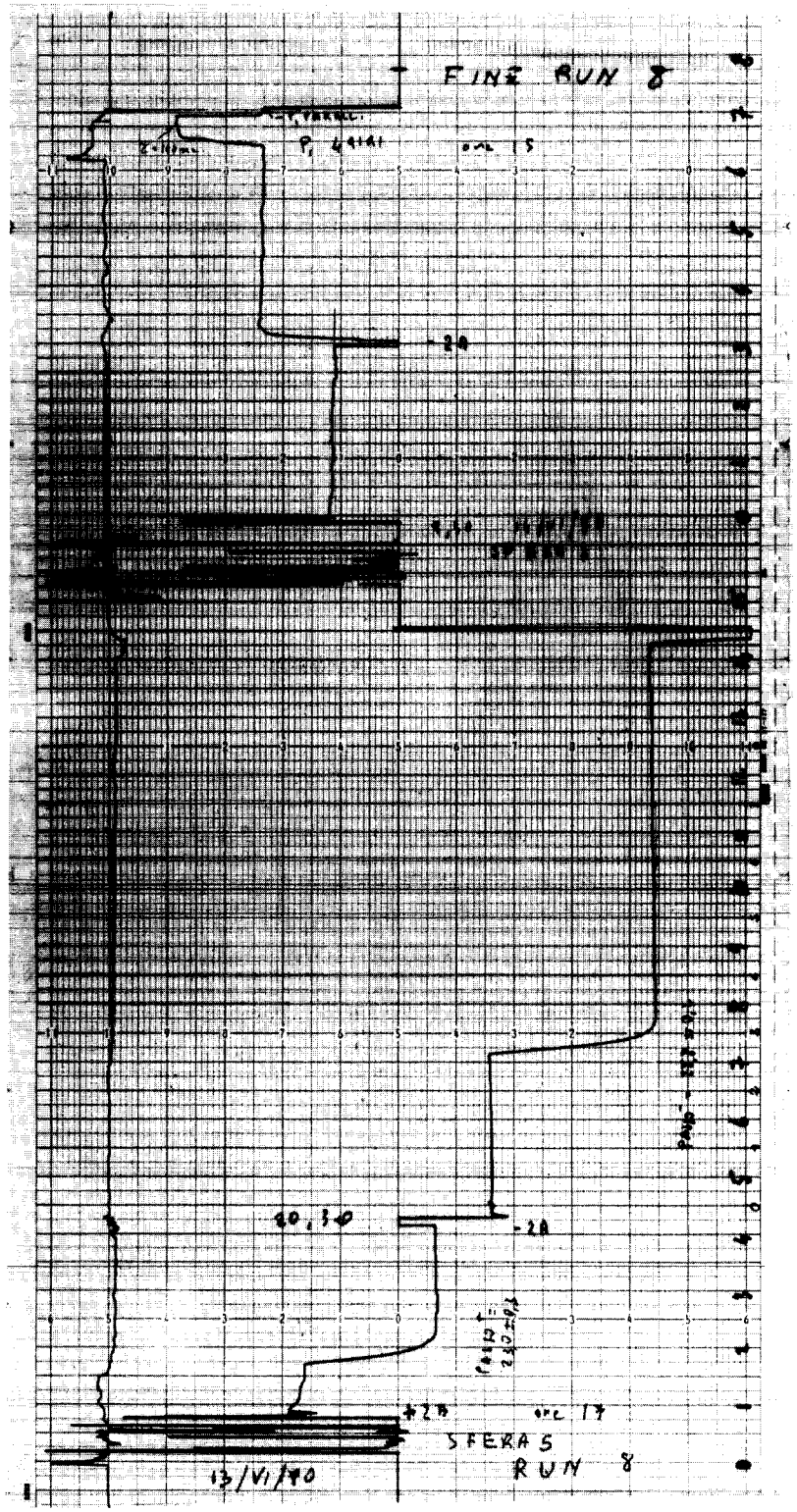

Fig. 8.2. The raw data for the balls nr. 47 and nr. 48 (both with $\Phi = 0.2$ mm). The figure is a photograph of the plot from the record plotter directly at the exit of the lock-in. It gives (in the ordinate) the amplitude of oscillation versus time (in the abscissa) for the balls stated above. Amplitude zero is at the center of the plot. (The record of ball nr. 47 goes – starting from left – from time 0 to time 15; that of ball nr. 48 from time 0 to time 8 (on the right).) The details of the charge "levels" and of their changes are explained in the text. The reason why a (instantaneous) change in charge takes almost half an hour, is the long integration time of the lock-in ($\tau = 300$ sec, 12 db/octave) used to suppress the noise.

sure that no change of charge has occurred during the transition). The change $+2A \rightarrow -2A$ produces a displacement of the charge level from -6.4 s.g. to -16.3 s.g. The level remains at this value for three hours; at about midnight the ball undergoes a spontaneous change of charge by one (negative) unit, leading to a charge level of -34.6 s.g. (Incidentally: from this transition the step P^- in the $-2A$ situation can be determined; it is $P^- = 28.8 \pm 0.25$ s.g.; we use this value instead of the "standard step" (8.18) known with much larger error. For determining P^+ we exploit the knowledge of the ratio 1.25 ± 0.015 between the two steps, measured independently (in the preparation period of the object); we thus obtain $P^+ = 23.0 \pm 0.15$.) From the above numbers we get:

$$Q^+ = \frac{-6.4 \pm 0.25}{23 \pm 0.3}, \qquad Q^- = \frac{-16.3 \pm 0.25}{28.8 \pm 0.25}$$

and, therefore

$$X = -(28.8 \pm 1.5) \times 10^{-2}, \qquad Y = -(42.2 \pm 0.8) \times 10^{-2}.$$

Hence

$$q' = Y - kX = (6.4 \pm 2.6) \times 10^{-2} \text{ electron charges}.$$

(Here and always in this paper one electron charge means -1.6×10^{-19} coulomb, with the minus sign.)

Case b (ball nr. 48, $\Phi = 0.2$ mm), fig. 8.2. This ball belongs to the same run as ball 47. (Incidentally the plot recorder was kept going – at its usual speed (two cm/hour) – during the substitution of ball 47 with ball 48; thus it can be seen that this substitution took a little more than one hour and a half, including of course all the time having ball 48 ready for starting the measurement.)

The measurement on the ball 48 is short, it only lasts 7 hours, thanks to low seismic noise. We have an initial level (with current $+2A$ in the C coils) at $+11.2$ s.g. and a $-2A$ level at $+24$ s.g., both with errors of ± 0.25. The steps are taken to be the standard ones (8.18). It is therefore:

$$Q^+ = \frac{11.2 \pm 0.25}{22.8 \pm 0.35}, \qquad Q^- = \frac{24.0 \pm 0.25}{28.65 \pm 0.45}.$$

We thus get:

$$X = (34.6 \pm 2.1) \times 10^{-2}, \qquad Y = (66.4 \pm 1.1) \times 10^{-2}$$

and obtain, finally:

$$q' = (7.9 \pm 3.5) \times 10^{-2} \text{ electron charges}.$$

The measurement on ball 48 also includes a measurement of the electric dipole moment of the object performed inclining the plate P_1 by a prescribed amount (this inclination is performed at time 6.5); the value of d_z^E is, in units $10^{-2}|\text{electron}| \times \text{meter}$, 14.2 ± 1.1 whereas the value of d_z^M – obtained via magnetic measurement – is 13.2 ± 1.0.

Case c (ball nr 22, $\Phi = 0.3$ mm), fig. 8.3. This case is instructive because it demonstrates the trivial

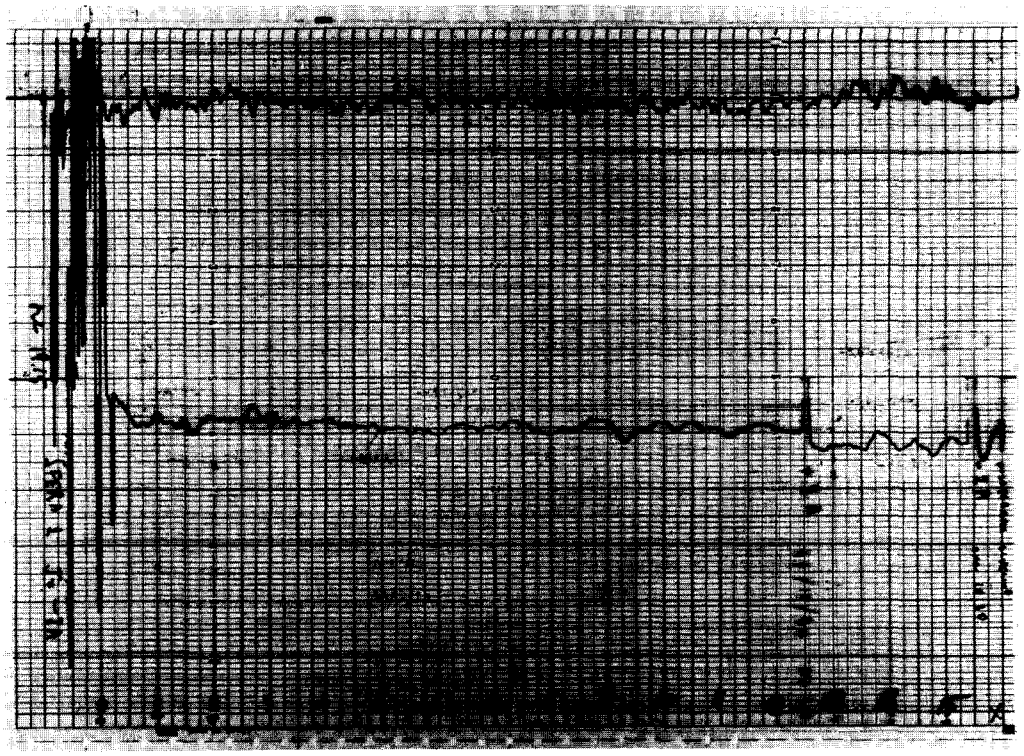

Fig. 8.3. The raw data for ball nr. 22 ($\Phi = 0.3$ mm). Same type of plot as that of fig. 8.2. In this case no spontaneous change in charge occurred during the whole period of measurement (~16 hours). The only operation performed was the reversal of the current in the C coils from −2A to +2A at time 12.5. This case is interesting as an example of noisy case with drift. Compare the text for a detailed discussion.

fact that in a noisy situation a long measurement allows to reach comparatively small errors. The steps have not been measured and, again, we use the standard steps (8.17). From the plot (fig. 8.3) one sees that at the moment of changing the current in the C coils from −2A to +2A the −2A level was -9.4 ± 0.3 s.g.; the transition to +2A leads to -12.1 ± 0.5 s.g.; a remark is appropriate on these errors, in particular on the last one: the "short" level lasting 3 hours from the insertion of the +2A current is equivalent to 6 independent measurements. The average value of this (noisy) level (−12.1 s.g.) as well as its error (±0.5 s.g.) are determined by averaging these 6 independent measurements and determining their standard width. Using the above values we obtain:

$$Q^- = \frac{-9.4 \pm 0.3}{21.55 \pm 0.25}, \qquad Q^+ = \frac{-12.1 \pm 0.5}{17.25 \pm 0.25}.$$

It is therefore $X = (26.5 \pm 3.4) \times 10^{-2}$, $Y = (-56.9 \pm 1.7) \times 10^{-2}$ and $q' = (-101.7 \pm 7.0) \times 10^{-2}$ that is, adding 1, $q' = (-1.7 \pm 7.0) \times 10^{-2}$ electron charges.

Case d (ball nr. 32, $\Phi = 0.3$ mm), fig. 8.4. This measurement lasts 23 hours. At time 4.5 we perform the transition from −2A to +2A (the level moves from 14.9 ± 0.2 s.g. to 34.0 ± 0.2 s.g.); at time 8 we incline the plate 1 producing a displacement of the level from 33.7 ± 0.3 (the decrease from 34 to 33.7 is due to a slight drift) to 57.5 ± 0.25. This transition allows to calculate the electric dipole moment d_z^E;

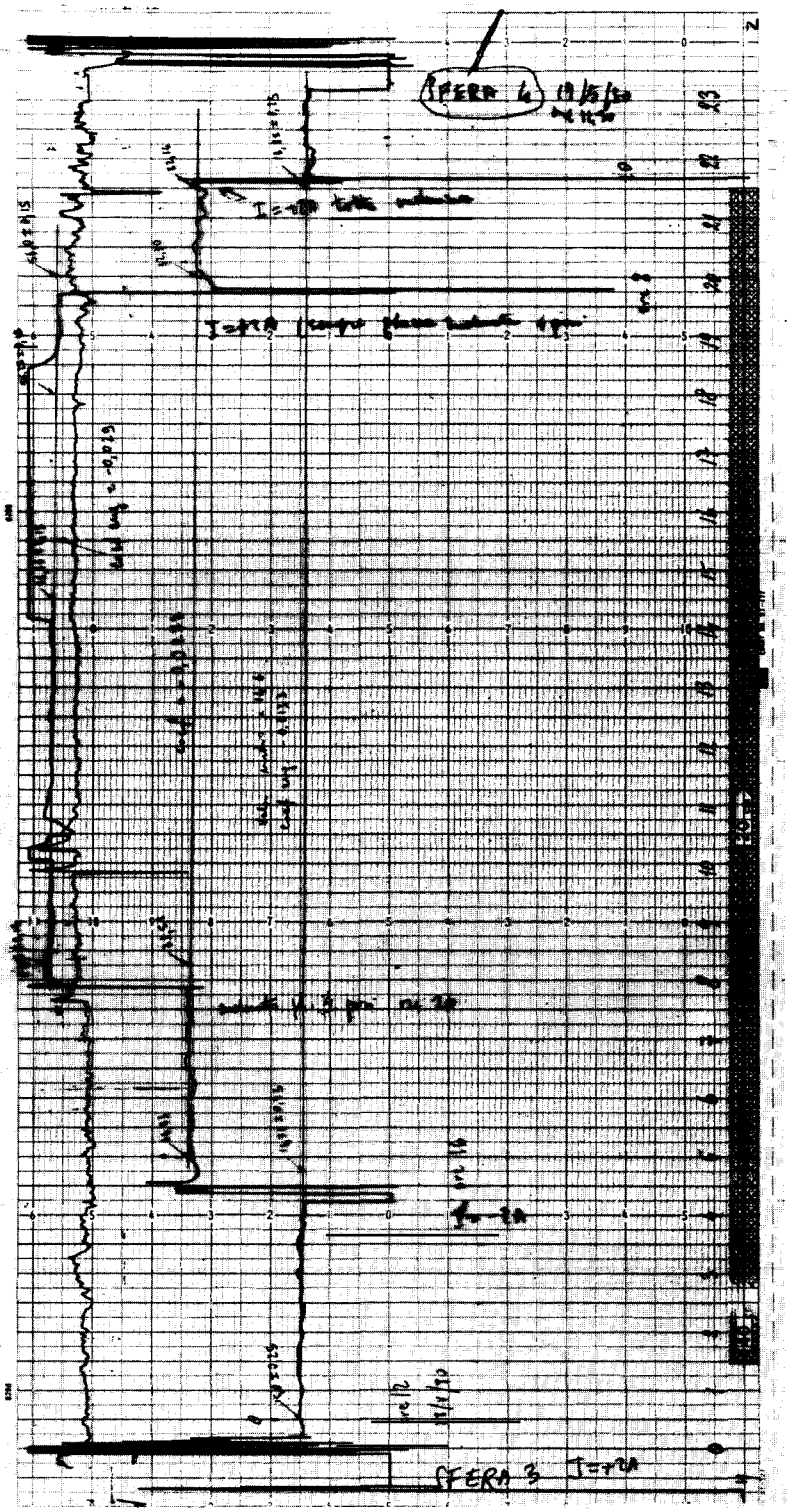

Fig. 8.4. The raw data for ball nr. 32 ($\Phi = 0.3$ mm). Same type of plot as in fig. 8.2. The discussion is presented in the text.

during the night – with the plate always inclined – a change of charge takes place (at time ~14); this change is wholly visible in another record plotter in parallel, operating on a reduced scale (incidentally because when P_1 is inclined the electric field increases, the "step" with inclined plates is larger than the step with parallel plates by a factor 1.085 – which is in agreement with the number expected from the geometrical estimate based on the inclination of the plate). At time 19 the charge changes spontaneously again in the reverse direction. At time 20 we restore the parallelism of the plates, and around time 22 we reverse again the current in the C coils from −2A to +2A. It is interesting to note that the drift in the −2A situation has been more than double that in the +2A situation (even if both are small) as expected (comp. section 8.4).

Using the standard steps and the numbers given above we obtain: $X = (71.4 \pm 2.7) \times 10^{-2}$, $Y = (122.1 \pm 1.4) \times 10^{-2}$ and $q' = (1.4 \pm 4.7) \times 10^{-2}$ electron charges. We also obtain $d_z^{\mathrm{E}} = (29.8 \pm 1.2) \times 10^{-2}$ and $d_z^{\mathrm{M}} = (27.2 \pm 1.8) \times 10^{-2} |\text{electron}| \times \text{meter}$.

The above four examples illustrate the main points of the analysis of the raw data. Only one additional remark is necessary. It may happen that on a given ball we perform several $+2\mathrm{A} \rightarrow -2\mathrm{A}$ transitions, starting from different charge levels; say a transition from some charge level L_1^+ to a level L_1^-; after a while another transition from level L_2^+ to the corresponding level L_2^-; etc. All these transitions can be used to determine q', and, if the patches did not change in the time between one measurement and the other, all must produce within the errors, the same value of q' (modulus an integer number of electron charges). This is what we find, in fact (we have stated already that, except at the beginning of a run, a clear change of patch never emerged). Of course in those cases where several determinations of q' are performed on the same ball, the statistical errors are reduced, as we shall discuss in section 8.6.

A final remark in connection with the extraction of the magneto-electric force is the following: in comparing a level with +2A with the corresponding level with −2A (to determine $\beta = d_z/H_z$ and subtract the magneto-electric force) it is necessary that we do not produce a change of d_z between the measurement of L^+ and the corresponding L^-. We have noted that sometimes (not always) a bombardment of the levitating ball with electrons or negative ions (performed by the filament (section 7.8) in order to change the charge of the ball in the positive sense) can change, by some per cent, its electric dipole moment d_z. Sometimes (but again not always) the previous value of d_z is slowly reached again in a few hours from the bombardment (due to this the $-2\mathrm{A} \rightarrow +2\mathrm{A}$ transitions had to obey the requirement that no bombardment took place in between).

8.6. The analysis of the errors

We now discuss the errors in the measurement of q'.

Often (e.g. in most of the examples of the previous subsection) the determination of q' is based only on one pair of charge levels L^+, L^-. In the general case, however, the measurements produce, for a given ball, a set of several pairs of charge levels L_i^+, L_i^- ($i = 1, 2, \ldots, n$); in what follows we refer to this general case.

Using the known steps P^+ and P^- we *reduce*, first, all levels L_i^+, L_i^- to the same charge value; in performing this operation the new levels are assigned errors that result from the quadratic composition of the errors of P and those of the original, measured, levels. After this reduction we thus have – for the ball under consideration – several different determinations of the *same* pair of charge levels; we continue to use the symbols L_i^+, L_i^- to indicate these different reduced determinations (but stress that, in spite of the same notation, the reduced L_i^+, L_i^- pairs differ from the directly measured L_i^+, L_i^- pairs by the addition or subtraction of some integer number of steps).

The value of q' – call it q'_i – from the ith determination L_i^+, L_i^- is easily found from the previous formulas:

$$q'_i = Y_i - kX_i = \frac{Q_i^- + Q_i^+}{2} - k\frac{Q_i^- - Q_i^+}{2} = \left(\frac{1}{2} - k\right)\frac{L_i^-}{P^-} + \left(\frac{1}{2} + k\right)\frac{L_i^+}{P^+}. \tag{8.19}$$

We now call ΔL_i^+, ΔL_i^- the errors on L_i^+, L_i^- respectively. The statistical part of the error on q'_i is then:

$$(\Delta q'_i)_{\text{stat}} = \{[(\tfrac{1}{2} - k)\Delta L_i^-/P^-]^2 + [(\tfrac{1}{2} + k)\Delta L_i^+/P^+]^2\}^{1/2}. \tag{8.20}$$

The weighted average of q'_i – we call this simply q' – and its error $\Delta q'$, are obtained from the values of q'_i (8.19) and their errors (8.20) using the standard statistical formulas:

$$q' = \sum_{i=1}^{n} q'_i(\Delta q'_i)^{-2}_{\text{stat}} \Big/ \sum_i (\Delta q'_i)^{-2}_{\text{stat}} \tag{8.21}$$

$$\Delta q'_{\text{stat}} = \left[\sum_{i=1}^{n} (\Delta q'_i)^{-2}\right]^{-1/2}. \tag{8.22}$$

The above statistical error is not, however, the total error on q'. We must add to it (quadratically) the error arising from the uncertainty in the values of P^+, P^- and k in eq. (8.19). This additional part of the error is called "systematic" because an incorrect determination of P^+, P^- and k affects systematically all n measurements of the ball under consideration (like trying to measure repeatedly a distance with a wrong meter). The expression of $\Delta q'_{\text{systematic}}$ is:

$$\Delta q'_{\text{syst}} = \left\{\left[(X\,\Delta k)^2 + \left[\left(\frac{1}{2} - k\right)\frac{L^-}{P^-}\frac{\Delta P^-}{P^-}\right]^2 + \left[\left(\frac{1}{2} + k\right)\frac{L^+}{P^+}\frac{\Delta P^+}{P^+}\right]^2\right]\right\}^{1/2} \tag{8.23}$$

where Δk, ΔP^+ and ΔP^- are the errors on k, P^+ and P^-; and we can use in the determination of $\Delta q'_{\text{syst}}$ any one of the reduced determinations of L_i^+, L_i^- and X_i (eq. (8.10)), because this in general introduces a minor effect on (8.23). In (8.23) we have called L^+, L^-, X the values of the above quantities in the last measurement.

In conclusion, with reference to the equations (8.20), (8.22) and (8.23) the total error $\Delta q'$ is given by:

$$\Delta q' = [(\Delta q')^2_{\text{stat}} + (\Delta q')^2_{\text{syst}}]^{1/2}. \tag{8.24}$$

A final remark is in order with respect to the errors ΔL_i^+, ΔL_i^-, ΔP^-, ΔP^+, Δk introduced above; these are meant to be the "standard" errors in the conventional (68%) sense of the word. We should also mention that for the 0.2 balls we have always added quadratically in (8.24) an additional error of $\pm 0.01e$.

To clarify the contents of this subsection we display in table 8.1 the analysis of three balls (nrs. 19, 20 and 21). For ball nr. 19 only one pair of levels L^+, L^- was measured ($n = 1$); for ball 20 two pairs of levels were measured ($n = 2$); finally the measurement on ball nr. 21 consists of three independent pairs of charge levels ($n = 3$).

Table 8 1

The detailed analysis of three balls (nrs 19, 20, 21), these balls belong to the same run In the case of ball 19 only one pair of levels was measured, two pairs for ball 20 and three pairs of levels for ball 21 The columns of the table – numbered from 1 to 20 – give (1) ball number; (2) date of the beginning of the measurement, (3) hour, (4) ball diameter in mm, (5) step P^+ (expressed in small graduations – s g), (6) error on P^+ (s.g.); (7) step P^- (s g), (8) error on P^- (s.g), (9) level(s) L^+ (if more than one level is measured, the levels are reported in the table after reduction to the same charge value – see text) with current +2A (expressed in s g), (10) error on L^+, (11) (reduced) level(s) L^- with current −2A (s g), (12) error in L^- (s g.), (13) X (expressed in 10^{-2} electron charges) – (the numbers in the column, multiplied by 10^{-2}, give X in electron charges); (14) error on X (same units), (15) Y (same units), (16) error on Y (same units), (17) residual charge q' (including the patch spurious charge) (same units as described for column (13)), (18) statistical error on q' (same units), (19) systematic error on q' (see text for definition of "systematic") – same units, (20) total error on q' – same units

1 Ball	2 Date (1980)	3 hour	4 diam mm	5 P^+	6 ΔP^+	7 P^-	8 ΔP^-	9 L^+	10 ΔL^+	11 L^-	12 ΔL^-	13 X $\times 10^2$	14 ΔX $\times 10^2$	15 Y $\times 10^2$	16 ΔY $\times 10^2$	17 q' $\times 10^2$	18 Δ_{stat} $\times 10^2$	19 Δ_{syst} $\times 10^2$	20 Δ_{tot} $\times 10^2$
19	18 4	8p m.	0.3	17 2	0.25	21 55	0 25	3	0 25	−8 7	0.3	−57.8	2 1	−11 5	1 05	−13 8	3 6	1 4	3 8
20	19 4	4p.m.	0.3	17.25	0 25	21 55	0 25	0 55	1.0	4 45	0.43	17 5	6 1	11 9	3 05	−17 6	12 9		
	20 4	1p.m						0 4	0 2	3 6	0 4	14 4	2 2	9 5	1 1	−14 8	3 4		
																−15 0	3 3	0 4	3 3
21	20 4	8p.m.	0.3	17 25	0.25	21 55	0 25	3 5	0.25	−6 9	0 25	−52 3	1 9	−5.9	0 95	−17 5	3.5		
	21 4	7a.m.						3 15	0.35	−8 05	0 65	−55.6	3.7	−9.5	1.85	−15 6	5 7		
	21 4	noon						2 7	0 3	−8 6	0 3	−55 6	2.3	−12 1	1 15	−18 2	4 2		
																−17 4	2 4	1 3	2 7

8.7. The determination of k

The above discussion of the errors would be incomplete without stating how k was determined. The quantity k is a constant of the instrument, depending – compare eq. (8.12) – on the values of the magnetic field gradients at the position of levitation. Thus k can be determined through measurements of the magnetic field, but to obtain an accurate determination is much more convenient to exploit the fact that balls with the different values of β and the same q' (that is belonging to the same run) must be fitted with the same value of k. In fact the ideal case is that of a ball having a drifting value of d_z (that is of β), and our first determination of k was made using such a ball (ball nr. 3, $\Phi = 0.2$ mm), and ball nr. 2 (also $\Phi = 0.2$ mm) belonging to the same run. Figure 8.5 shows the drifting levels of ball nr. 3; and fig. 8.6 shows, with their errors, the measured values of X and Y for these balls. The best fit to the points in fig. 8.6 gives:

$$k = 1.675 \pm 0.015\,, \qquad q' = -0.53 \times 10^{-2} e \tag{8.25}$$

and the analysis of refs. [30, 31] was performed using the above value of k (we used in fact 1.67). Subsequent measurements using other balls slightly changed – within the error – the above determination of k. The new k is:

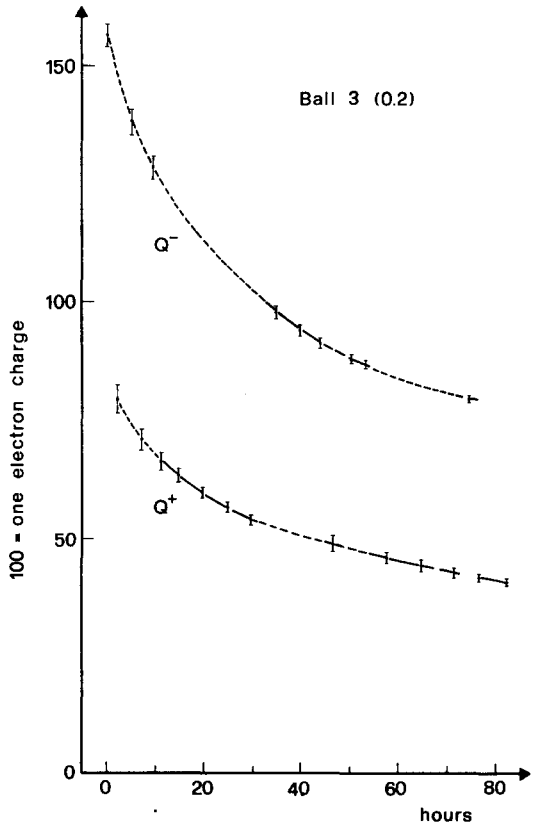

Fig. 8.5. Drifting Q values of ball nr. 3 used for the determination of k.

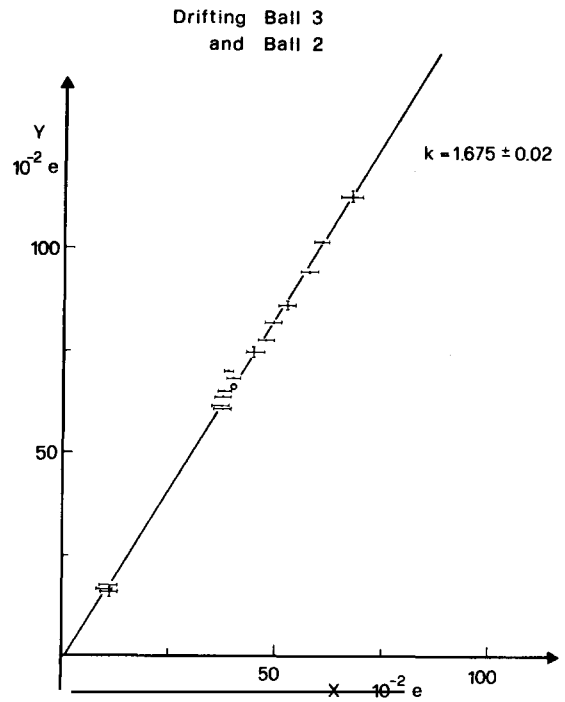

Fig. 8.6. The X, Y drifting values of ball nr. 3 (upper points) obtained from the data of fig. 8.5; and the X, Y value of ball nr. 2 (group of points near to the origin).

$$k = 1.69 \pm 0.015 \tag{8.26}$$

and in the following analysis we shall use this value (with a rounded error of 0.02). The following remarks are of interest:

(1) We could establish that no change of k took place between the beginning and the end of our measurements on the 70 balls reported here; the measurements on the first and last ball are separated by an interval of ~1 year.

(2) The above value (8.26) of k is perfectly compatible with the value of k obtained using eq. (8.12) from direct measurements on the magnetic field: the latter value has of course – as stated above – a much larger error; it is $k = 1.67 \pm 0.1$.

(3) An uncertainty in k of ± 0.01 produces an uncertainty in q' of ± 0.01 if $X = 1$. The distribution in X for all 70 measured balls is reported in fig. 8.7. Only three balls (balls nrs. 13, 28 and 29 with $\Phi = 0.3$ mm) do have $|X| > 1.4$ and receive a significant contribution to their error from the uncertainty in k (compare also fig. 8.13).

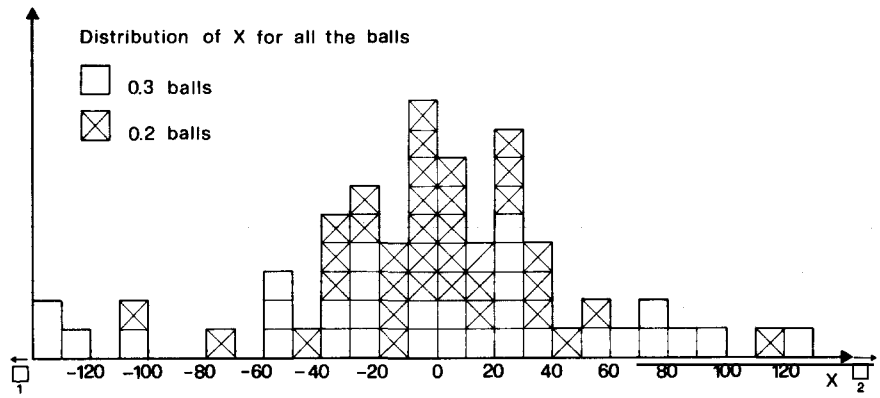

Fig. 8.7. Number of balls (each ball is represented by a square) having the value of X indicated in the abscissa (X is expressed in 10^{-2} electron charges). The figure contains all 70 measured balls but to avoid expanding the scale excessively the 3 balls with $|X| > 1.4$ are only indicated; two balls have $X > 1.4$ – ball nr. 13 (with $X = 2.9$), and ball nr. 29 (with $X = 2.5$); one has $X < -1.4$ (ball nr. 28 with $X = -2.8$).

8.8. *The distribution of q'*

We now display (table 8.2 and figures 8.8 and 8.9) the distribution of q' for all 70 balls measured. We recall again that:

$$q' = q + Q^{(V)} \tag{8.27}$$

where q is the true residual charge and $Q^{(V)}$ is the Volta or patch residual charge:

$$Q^{(V)} = 4\pi\varepsilon_0 r^3 (\partial E_x^{(V)}/\partial x)\,. \tag{8.28}$$

In (8.28) r is the radius of the ball. At equal value of $\partial E_x^{(V)}/\partial x$ (the gradient of the patch field at the position of the object) the 0.3 mm balls are affected by a $Q^{(V)}$ larger by $(1.5)^3 = 3.375$ than that of the 0.2 mm balls.

Table 8.2

The values of $q' \pm \Delta q'$ for each of the 70 balls measured; q' is the true charge plus patch charge; $\Delta q'$ is the total error. The values of q' and $\Delta q'$ reported (in columns 4 and 5) must be multiplied by 10^{-2} to have them in electron charges. We also list (column 6) the values of d_z^M, and, for those balls where d_z^E was measured, also this quantity (column 7); d_z^M and d_z^E are expressed in $10^{-2}|\text{electron}| \times$ meter. In a few cases several pairs of d_z^M and d_z^E are listed for the same ball. These measurements are reported to show that when one of these quantities drifts with time, so does the other, as expected. Finally the meaning of the first three columns in the table is the following: (1) ball number, (2) date when the measurement was started; (3) ball diameter.

1 Ball number	2 Date	3 Φ mm	4 q' $10^{-2}e$	5 $\Delta q'$ $10^{-2}e$	6 d_z^M $10^{-2}\|e\| \times$ m	7 d_z^E $10^{-2}\|e\| \times$ m
1	18/3/80	0.3	−11.2	4.0	5.5 ± 1.1	
2	24/3/80	0.2	−1.7	1.3	4.3 ± 0.4	
3	26/3/80	0.2	−1.1	2.0	20.2 ± 1.3	19.2 ± 1.6
					15.4 ± 1.1	16.2 ± 1.3
					14.5 ± 1.0	14.2 ± 0.7
4	30/3/80	0.2	+1.5	2.5	−3.8 ± 0.6	
5	31/3/80	0.2	+2.1	2.8	0.8 ± 0.7	
3	1/4/80	0.2	+1.2	2.3	20.1 ± 1.2	
6	3/4/80	0.2	−1.1	2.8	−5.4 ± 0.6	
7	3/4/80	0.2	0.0	4.2	2.7 ± 0.9	
8	5/4/80	0.2	−1.8	4.6	−40.0 ± 2.3	
9	7/4/80	0.2	−5.8	2.7	−0.4 ± 0.6	
10	7/4/80	0.3	−17.4	4.6	29.5 ± 1.9	
11	9/4/80	0.3	−18.0	4.3	2.4 ± 1.4	
12	9/4/80	0.3	−15.3	4.2	46.0 ± 2.5	
13	10/4/80	0.3	−8.3	12.9	109 ± 6.0	
14	11/4/80	0.3	−22.0	4.4	−42.4 ± 2.6	
15	14/4/80	0.3	−19.4	4.8	31.6 ± 2.6	
16	16/4/80	0.2	−5.6	2.9	−18.3 ± 1.2	
17	17/4/80	0.2	−6.4	2.4	6.4 ± 0.6	
18	17/4/80	0.2	−5.1	3.3	−4.5 ± 0.7	
19	18/4/80	0.3	−13.8	3.8	−22.0 ± 1.4	
20	19/4/80	0.3	−15.0	3.3	5.5 ± 0.9	
21	20/4/80	0.3	−17.4	2.7	−20.0 ± 1.3	
22	24/4/80	0.3	−1.7	7.0	10.1 ± 1.4	
23	24/4/80	0.3	−4.8	6.9	21.0 ± 2.0	
24	25/4/80	0.3	−9.7	4.1	−1.5 ± 1.2	
25	26/4/80	0.3	−15.9	6.7	0.8 ± 1.7	
26	27/4/80	0.3	−10.6	7.8	10.1 ± 1.5	
27	28/4/80	0.2	−2.1	2.1	−9.3 ± 0.8	

Continued on p. 230

Table 8.2 (cont.)

1 Ball number	2 Date	3 Φ mm	4 q' $10^{-2}e$	5 $\Delta q'$ $10^{-2}e$	6 d_z^M $10^{-2}\|e\| \times$ m	7 d_z^E $10^{-2}\|e\| \times$ m
28	12/5/80	0.3	−6.9	10 5	−106 ±6 0	
29	13/5/80	0 3	+6.8	6 5	96.2 ± 5.3	96.8 ± 3.7
30	17/5/80	0.3	+8 2	6.6	−21.6 ± 1.9	−16.1 ± 4.1
31	18/5/80	0.3	−0 5	8.3	3 2 ± 1 9	5.9 ± 3 0
32	18/5/80	0 3	+1 4	4 7	27 2 ± 1.8	29.8 ± 1.2
33	19/5/80	0 3	0 0	6.2	−51.7 ± 3.5	
34	21/5/80	0 3	+5.2	8.0	8 9 ± 2.0	12 8 ± 2 4
35	24/5/80	0.3	+5.3	7.6	−9.0 ± 1.7	
36	24/5/80	0 3	+3 8	5 7	−53.7 ± 3.0	
37	26/5/80	0 3	+30.8	3.1	−9 3 ± 1.3	
38	28/5/80	0 3	+20 7	7 3	−7 8 ± 1.4	
39	29/5/80	0 3	+3 7	7 2	−8.0 ± 1 4	
40	2/6/80	0.2	+0.6	4.3	11 9 ± 1.1	
41	3/6/80	0.2	+8.5	2.7	1 1 ± 0.8	1.7 ± 1.1
42	4/6/80	0.2	−2.2	3.7	−28.5 ± 1.7	
43	5/6/80	0.2	+6.5	2 1	−3.7 ± 0.8	−2.5 ± 0.7
44	10/6/80	0 2	+4 7	4 1	−5 9 ± 0 9	
45	10/6/80	0 2	+5.1	4 8	8.6 ± 1.2	
46	11/6/80	0.2	+4.4	1.7	−0 7 ± 0.5	−0 1 ± 0.5
47	13/6/80	0 2	+6.4	2.8	−11 0 ± 0 8	
48	14/6/80	0.2	+7.9	3 5	13 2 ± 1.0	14.2 ± 1.1
49	23/11/80	0.2	+6.6	1.8	−3.0 ± 0.7	−2.9 ± 0.7
50	26/11/80	0.2	+9 5	3.1	9.0 ± 0.8	8 5 ± 0 6
51	27/11/80	0 2	+11.0	6.9	42 0 ± 2 5	42 2 ± 2.0
52	29/11/80	0.2	+14.3	2.4	14 7 ± 1.0	14 3 ± 0.9
53	2/12/80	0.2	+11 1	2.5	−9 6 ± 1.0	−10.1 ± 0.9
54	10/12/80	0.2	+7 6	3 4	−5.3 ± 0.8	−4.8 ± 0 6
55	14/12/80	0.2	+9.1	2 2	5.0 ± 0.6	4.2 ± 0.7
56	15/12/80	0.2	+10.8	1.7	3.2 ± 0.9	2.9 ± 0.5
					2.0 ± 0.7	2 7 ± 0.6
					1 1 ± 0 6	1 8 ± 0 6
57	30/12/80	0.2	+6.6	3 9	−14 5 ± 1.3	
58	13/1/81	0 2	+7 4	1 9	−2 4 ± 0.6	−3 1 ± 0 6
59	16/1/81	0 3	+31 5	4 7	−15 3 ± 1.3	−16 1 ± 1 5
60	20/1/81	0.2	+7.5	1.5	−3 5 ± 0.6	−2.9 ± 0.7
					-2.0 ± 0.7	-1.4 ± 0.4

Continued on p 231

Table 8.2 (cont.)

1 Ball number	2 Date	3 Φ mm	4 q' $10^{-2}e$	5 $\Delta q'$ $10^{-2}e$	6 d_z^M $10^{-2}\|e\| \times$ m	7 d_z^E $10^{-2}\|e\| \times$ m
61	26/1/81	0.3	+32.9	6.0	33.4 ± 2.5	
62	2/2/81	0.3	+7.7	3.7	10.1 ± 1.0	8.3 ± 1.0
63	4/2/81	0.2	+3.9	2.2	3.1 ± 0.6	
64	6/2/81	0.3	+6.3	4.0	14.9 ± 1.1	
65	6/2/81	0.3	+0.1	5.6	26.1 ± 2.0	
66	13/2/81	0.2	+1.6	1.9	−13.5 ± 0.9	−12.4 ± 0.7
67	15/2/81	0.3	+2.6	5.6	−47.5 ± 3.0	
68	17/2/81	0.2	+1.7	2.1	10.6 ± 0.8	9.5 ± 0.7
69	19/2/81	0.3	+0.7	4.5	−13.4 ± 1.7	
70	6/3/81	0.2	+1.6	2.2	15.4 ± 1.0	14.7 ± 1.6

Table 8.2 gives for each ball the value of q' with its total error $\Delta q'$. The balls are listed in temporal order. Balls belonging to the same run appear in the table between two horizontal lines. Thus the balls nrs. 2 and 3 or the balls 6, 7 or 11, 12, 13 belong to a run whereas ball 1 or ball 10 or ball 40 are separate measurements.

Note that we have performed some "mixed runs" measuring balls with $\Phi = 0.2$ and 0.3 mm in succession without opening the levitation chamber: thus the balls 58 and 59 belong to a mixed run; the same is true for the balls 63, 64, 65 and for the balls 66, 67, 68, 69.

The figures 8.8 and 8.9 reproduce in different ways the contents of table 8.2. Figure 8.8 is a time ordered plot of the q' values of all 70 balls; in this figure the values of q' of the large ($\Phi = 0.3$ mm) balls (indicated by a triangle) have been *divided* by $(1.5)^3$ to make a comparison easy (see the eq. (3.3)) with the q' values of the small balls (0.2 mm) indicated by a dot. Figure 8.9 is a time ordered plot of the q' values of the 0.3 mm balls where, instead, the q' values of the 0.2 mm balls measured immediately before or immediately after a large (0.3) ball have been multiplied by $(1.5)^3$ for the same purpose of easy comparison.

The maximum $|q'|$ found for the 0.2 mm balls has been $0.14|e|$ (ball nr. 52); the maximum $|q'|$ of the 0.3 mm balls has been $0.33|e|$ (ball nr. 61). The average $|q'|$ (0.2) is $5.25 \times 10^{-2}e$, and the average $|q'|$ (0.3) is $11.04 \times 10^{-2}e$. The above values are incidentally in good agreement with the expectation from the discussion of section 4.1. (Note, incidentally, that in the period of 3.6.80 to 22.1.81 in which the patches were large we did measure 20 balls with $\Phi = 0.2$ mm but none with $\Phi = 0.3$ mm; this accounts for the fact that the average $|q'|$ s of the 0.2 and 0.3 balls are not in the ratio $(1.5)^3$.)

8.9. The extraction of the true residual charge

From the data on q' discussed above we must now extract the true charge q of each ball. We discuss separately the balls of diameter 0.2 mm, the mixed runs, and the 0.3 mm balls.

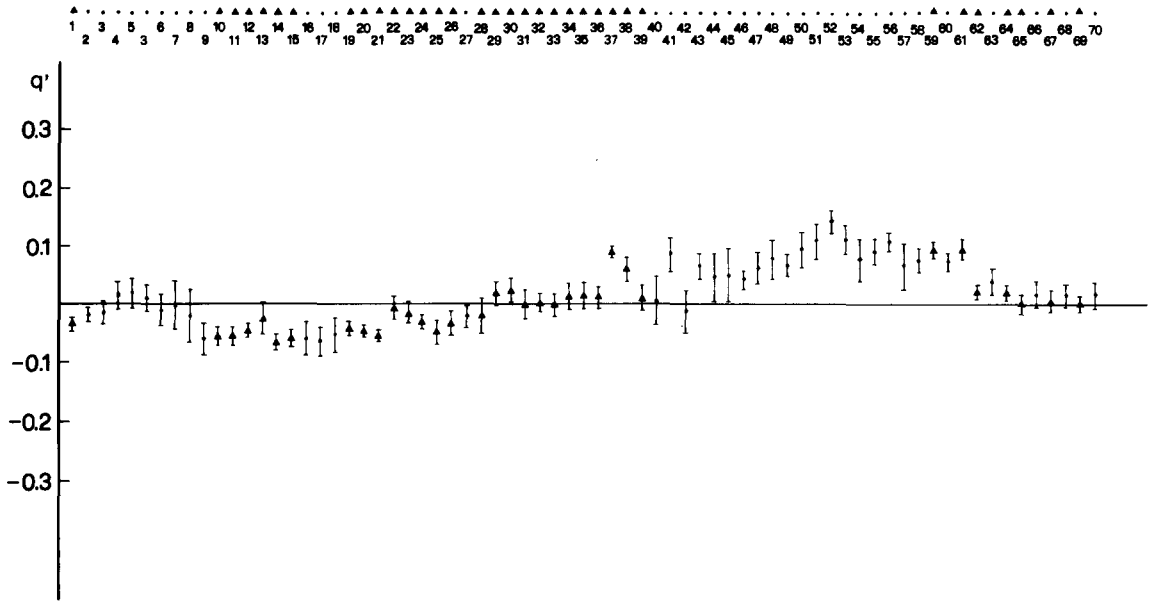

Fig. 8.8. The values of q' (in electron charges) for all balls. The balls indicated by a triangle have diameter 0.3 mm and their q' values appear in the figure after division by the scale factor $(1.5)^3$ (see text). The balls indicated by a full circle have diameter 0.2 mm and their values of q' given in the figure are directly the results of the measurement.

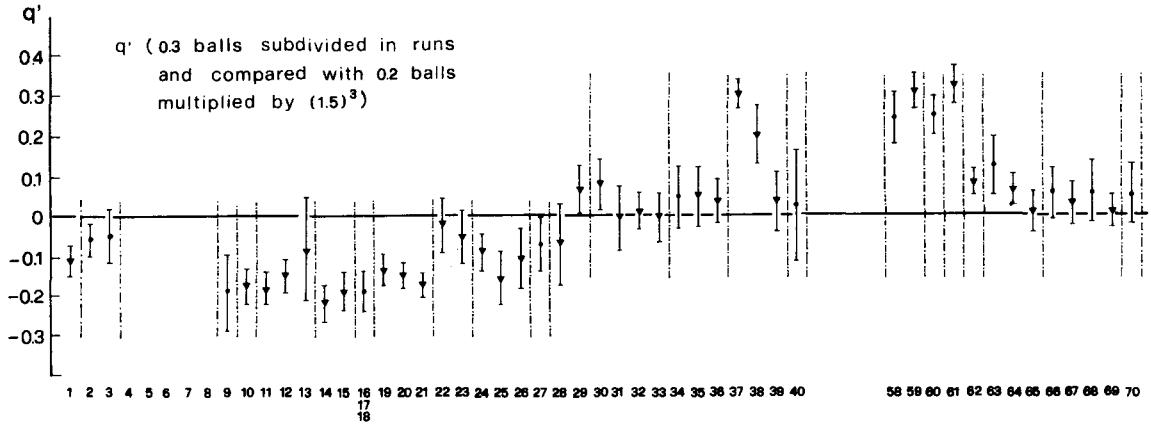

Fig. 8.9. The measured value of q' for the 0.3 balls. We have also plotted the values of q' for the 0.2 balls measured immediately before or after a 0.3 ball; these q' values of the 0.2 balls have been multiplied by $(1.5)^3$. Vertical dotted bars specify runs (see text).

8.9.1. The 0.2 mm balls

For the 0.2 mm balls q' is found to be in no case larger than $0.14|e|$; this is, by itself, an *indication* for the absence of quarks in any one of the balls. In other words a natural interpretation of the data on all the 0.2 mm balls is to assign true charge zero to each of them and a patch charge up to $0.14|e|$. To be more quantitative and to determine the true residual charge for each of the 36 balls with $\Phi = 0.2$ mm we proceed as follows: consider all differences between subsequent balls:

$$q'_i - q'_{i+1} = q_i - q_{i+1} + (Q_i^{(V)} - Q_{i+1}^{(V)}) . \tag{8.29}$$

If the balls i and $i+1$ belong to the same run we can safely assume that the patch is constant ($Q_i^{(V)} = Q_{i+1}^{(V)}$) and thus the differences $q'_i - q'_{i+1}$ are equal to the differences between the true charges:

$$q'_i - q'_{i+1} = q_i - q_{i+1} . \tag{8.30}$$

But for *all* balls of 0.2 mm (we underline all) the values of $q'_i - q'_{i+1}$, where i and $i+1$ belong to the same run do not differ significantly, as to their order of magnitude, from the values of $q'_i - q'_{i+1}$ when an opening of the levitation chamber took place between the measurements of i and of $i+1$; both the above values $q'_i - q'_{i+1}$ are near to zero. Thus eq. (8.30) can be applied – inside the errors – to all 36 measured balls with $\Phi = 0.2$ mm. If we plot all values of $q'_i - q'_{i+1}$, fig. 8.10 is obtained. On the basis of eq. (8.30) the fig. 8.10 shows that all the differences between q_i and q_{i+1} are consistent with zero (to a confidence level that will be considered later). Thus, either: (a) *all* 0.2 mm balls contain a free quark, or

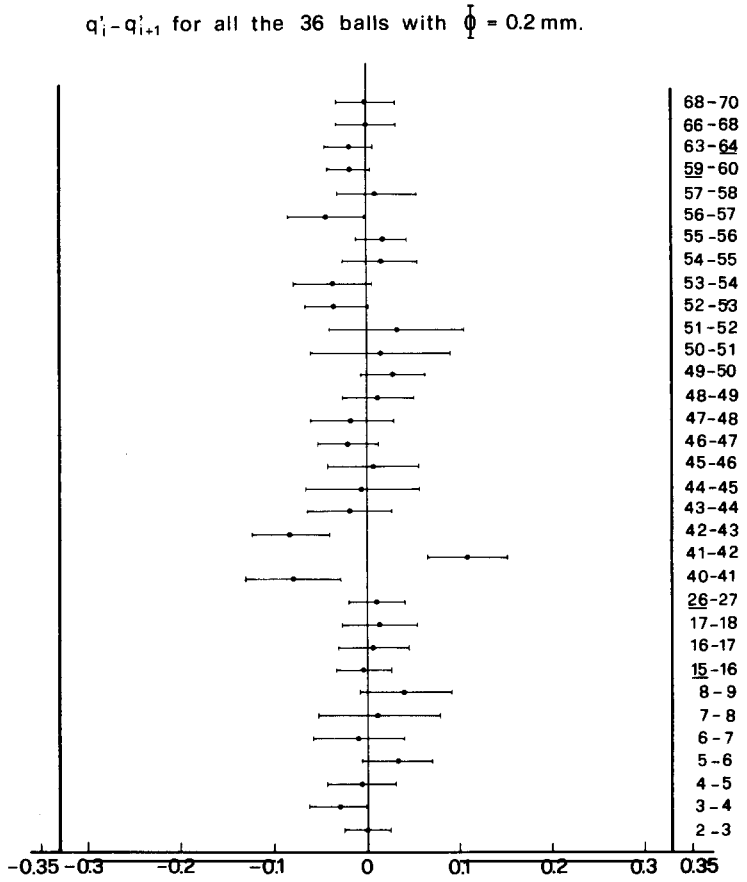

Fig. 8.10. The values of the differences between the q' values of successively measured balls for all 36 balls with diameter 0.2 mm. Balls with a bar below the ball number are 0.3 balls with their q' divided by $(1.5)^3$. Note that the errors on the differences are of course larger than the errors on the individual q' due to the (quadratic) composition of the errors. Also, as stated in the text, a systematic error of $\pm 0.01e$ was added to the error of all the 0.2 mm balls.

(b) none does. Because the probability that in a world where quarks are abundant 36 different balls all contain one – and precisely one – or two – and precisely two – free quarks is $2[\frac{1}{3}]^{36} \approx 10^{-17}$ the first alternative (a) can be dismissed. As to the confidence levels that, on the basis of the respective errors, can be assigned to the individual 0.2 mm balls the values for these confidence levels range from 10^4 (in a few cases) to 10^{50} or more; the large majority of the balls has a confidence level larger than 10^{15}, that is a ratio between the probabilities of one quark and no quark smaller than 10^{-15}.

8.9.2. The mixed runs

The mixed runs (those runs where – without opening the levitation chamber – we measure in succession balls with $\Phi = 0.2$ mm and 0.3 mm) confirm the conclusion of the previous paragraph and show at the same time that five 0.3 mm balls measured in these runs do not contain quarks.

Indeed, once it is established that the q' of the 0.2 mm balls is due only to the patch effect, the q' of the 0.3 balls belonging to the mixed runs are expected to be $(1.5)^3$ times larger than the q's of the 0.2 mm balls of each mixed run. This is in fact so, as shown in the figs. 8.11 and 8.12.

Note that we cannot use our three mixed runs to determine – only with their help, that is ignoring all the rest of the data – the q and $Q^{(v)}$ values of the balls involved. In principle this use of the mixed runs is possible, but in our case (due to the error bars) more than one solution exists for each of the three mixed runs. To extract information from the mixed runs we have used, and we need to use, the important fact stated already: that is that the patch charge of the 0.2 mm balls is in practice affected only very slightly by the opening of the levitation chamber.

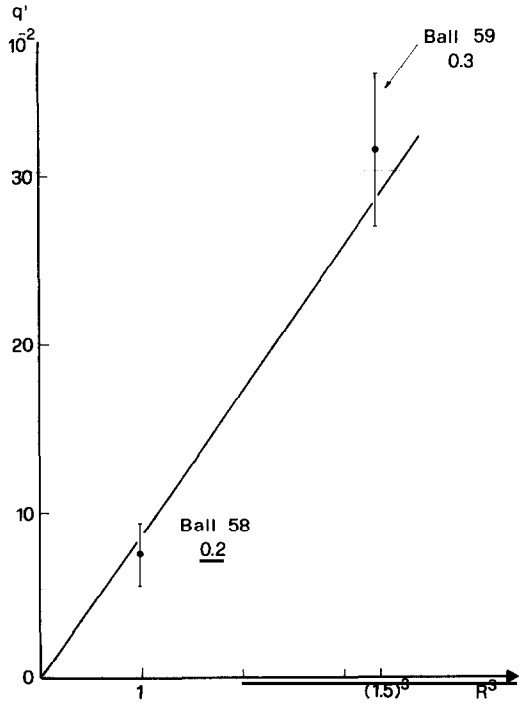

Fig. 8.11. Comparison of the q' values of two balls in a mixed run.

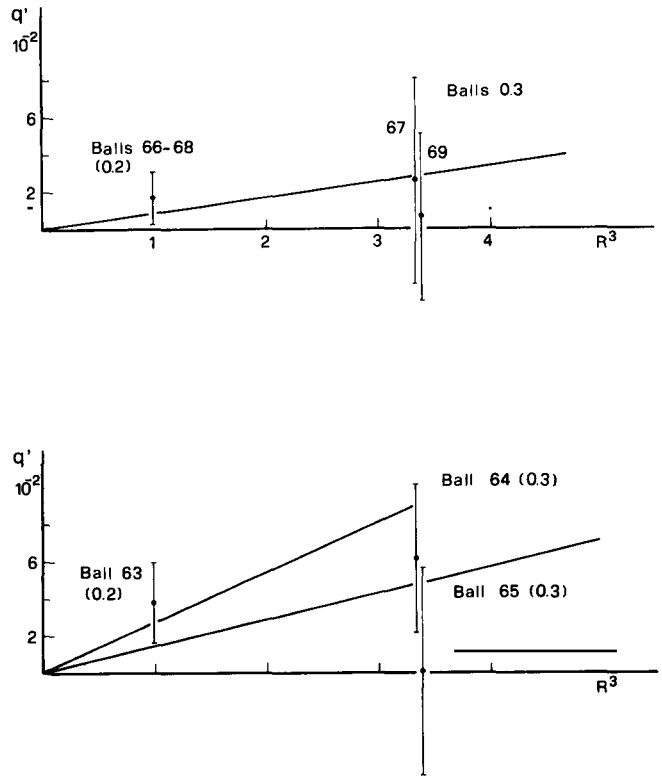

Fig. 8.12. The results of two additional mixed runs; the one in the upper figure contains two balls 0.2 and two balls 0.3. The one in the lower figure contains one ball 0.2 and two balls 0.3.

8.9.3. The 0.3 mm balls

Differently from the case of the 0.2 mm balls the modification of the patches produced by the opening of the levitation chamber and the occasional "cleaning" of the plates are felt by the 0.3 mm balls (these effects are almost 3.4 times larger for the 0.3 mm balls than for the 0.2 mm balls). In extracting information on the true charges of the 0.3 mm balls we must therefore limit to compare those balls that are measured inside runs. Figure 8.13 gives all the values of $q'_i - q'_{i+1}$ measured for the 0.3 mm balls (inside runs). Except for some cases in which the errors are so large that no conclusion can be reached we again find that (inside runs) the $q'_i - q'_{i+1}$ values and therefore the $q_i - q_{i+1}$ values are all consistent with zero. This means that either (a) all the balls of a given run contain one quark or (b) none does.

In paragraphs 8.9.1 and 8.9.2 we found that inside 36 balls of diameter 0.2 mm and inside 5 balls of diameter 0.3 mm no free quarks are present; this corresponds to no quark in 1.75 mg of material. On this basis the probability that both balls of a run of two balls contain a quark is $\sim 4 \times 10^{-3}$ and the probability that all three balls of a run of three balls contain a quark is $\sim 2.5 \times 10^{-4}$. We conclude that in each case the solution "no quark on all balls" is preferred with respect to the solution "one quark on all balls of a run" in the ratios stated above. At this stage one can estimate for each individual ball on the basis of the error bars of the particular measurements the ratio of the probabilities that it contains or does not contain a quark. The values obtained are given in the left column of fig. 8.13.

The balls with $\Phi = 0.3$ mm (not belonging to the mixed runs – these have already been considered)

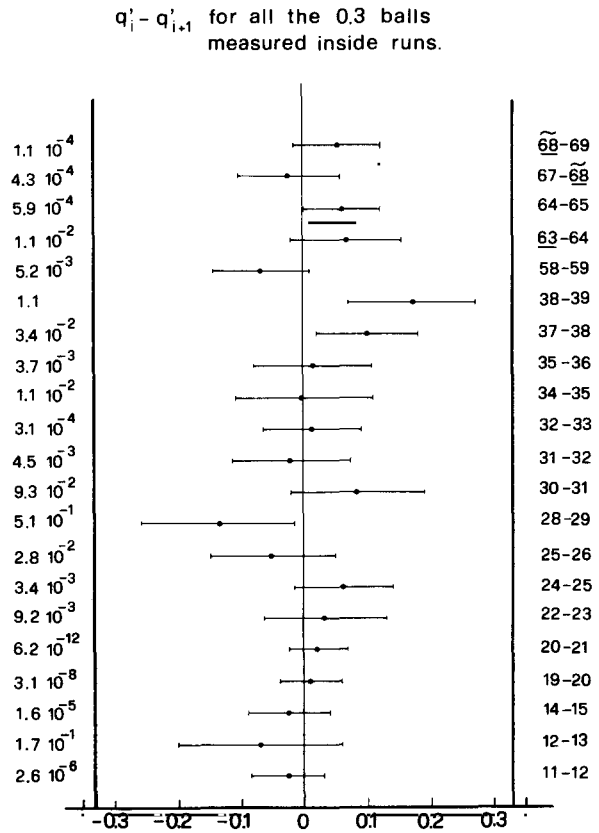

Fig. 8.13. The values of the differences between the q' of successively measured balls for all the 0.3 balls measured inside runs. Balls with a bar below their ball number are 0.2 balls (belonging to the mixed runs) with their q' multiplied by $(1.5)^3$. The numbers on the left of the figure give (on the basis of the error) for each pair of balls the ratio between the probabilities that the point in question corresponds to a difference in charge of $\pm 1/3$ or zero.

for which a confidence level of 99% or larger can be established are seen, from fig. 8.13, to be 17, corresponding to a total mass of ~1.9 mg.

We therefore conclude that on a total mass of ~3.7 mg no quarks have been seen (at the confidence levels discussed in this and the previous paragraphs).

As to the remaining 12 balls with $\Phi = 0.3$ mm (not included in the 3.7 mg stated above) four are individual measurements (they do not belong to runs: balls 1, 10, 61, 62 fig. 8.12). The remaining 8 balls (nrs. 13, 26, 28, 29, 30, 37, 38, 39) have errors corresponding to confidence levels less than the one accepted above (compare fig. 8.13). We nevertheless reported also the data for these balls because we adopted the rule of reporting all balls measured.

8.10. The equality of d_z^{M} and d_z^{E}

As discussed in section 4.4 the quantity β in (8.1) is equal to d_z/H_z where H_z is the vertical magnetic field at the position of the ball and d_z is the z component of the electric dipole moment of the ball. A measurement of β thus entails (knowing H_z) a measurement of d_z. We call the value of d_z obtained in this way d_z^{M} where the suffix M stays for "measured magnetically".

We can also determine d_z creating a known z gradient of the electric field at the position of the ball and measuring the additional force that the ball experiences:

$$F_x^{(d)} = d_z^E(\partial E_z/\partial x)\,. \tag{8.31}$$

In (8.31) $\partial E_z/\partial x$ is the gradient of the electric field produced by a prescribed inclination of the plate P_1. We call d_z^E the electric dipole moment measured electrically. As already stated in section 4.4 one should find $d_z^M = d_z^E$. Because the two procedures to measure d_z are completely different and independent, the equality $d_z^M = d_z^E$, if satisfied, is a very gratifying check of the internal consistency of the measurements.

8.10.1. The measurement of d_z^M

We now give the equations that are used to extract d_z^M from the data. From the equations (8.8) and (8.9) it is easy to derive (compare ref. [41]):

$$d_z^M = \beta H_z^\circ = -X\,\frac{H_z^\circ(1-\varepsilon^2)}{2\,\Delta H_{xx}\,(1-\varepsilon H_{xx}^\circ/\Delta H_{xx})} \tag{8.32}$$

where $X = Q^- - Q^+$ (see eq. (8.10)); H_z° is the vertical magnetic field at the position of levitation of the ball in the absence of current in the C coils (-525 ± 20 gauss); $H_{xx}^\circ = 22.8 \pm 0.6$ gauss/cm is the x derivative of the x component of $\boldsymbol{H}$ at the position of the ball in the absence of current in the C coils; $\Delta H_{xx} = (H_{xx}^+ - H_{xx}^-)/2 = -6.05 \pm 0.25$ gauss/cm is the difference between the x derivatives of H_x at the position of the ball when the current in the C coils is +2A and when it is −2A; $\varepsilon = (H_z^+ - H_z^-)/2H_z^\circ = 3.7 \times 10^{-2}$ is the relative variation of H_z at the position of the ball when the current in the C coils is changed from +2A to −2A.

Inserting into eq. (8.32) the numerical values indicated above (obtained from magnetic measurements in agreement with those mentioned in ref. [41], but somewhat improved in precision) we get:

$$d_z^M = -(0.381 \pm 0.02)X \qquad (|\text{electron charge}| \times \text{meter}) \tag{8.33}$$

where X is the measured value of $Q^- - Q^+$ (expressed in electron charges) with its error.

8.10.2. The measurement of d_z^E

To determine electrically the electric dipole moment we produce – using the micrometer I (fig. 7.10a) – an inclination of the plate P_1 with respect to the plate P_0. This inclination can be performed at a stage of the measurement when the current in the C coils is −2A or is +2A or zero; this is irrelevant provided that, to calculate the force, we use in each case the value of the step appropriate to the situation. Inclining the plate P_1 has two effects: (1) it increases the horizontal electric field E_x by some amount because the distance between the two plates is effectively decreased. The increase in E_x corresponding to the inclination that we usually produce – we advance the micrometer by 2 mm – is measured to be a factor 1.085. (2) It produces a gradient of E_x with respect to z that, acting on d_z, introduces an additional force on the ball. If we write the force when the two plates are parallel as:

$$F_x = QE_x \tag{8.34}$$

where Q is the total effective charge (true plus patch plus magneto-electric), the force F_x with P_1

inclined is:

$$F_x = Q\bar{E}_x + d_z(\overline{\partial E_x/\partial z}) \tag{8.35}$$

where barred quantities refer to P_1 inclined. Defining for convenience:

$$\bar{Q} = \bar{F}_x/\bar{E}_x = Q + d_z\left(\overline{\frac{1}{E_x}\frac{\partial E_x}{\partial z}}\right) \tag{8.36}$$

we note that the quantities directly extracted from the data are $\bar{Q}$ and Q, the latter quantity given by (8.34).

We obtain from eq. (8.36):

$$\bar{Q} - Q = d_z\left(\overline{\frac{1}{E_x}\frac{\partial E_x}{\partial z}}\right). \tag{8.37}$$

The value of $(\overline{(1/E_x)\partial E_x/\partial z})$ corresponding to the inclination that we produce on P_1 is:

$$\left(\overline{\frac{1}{E_x}\frac{\partial E_x}{\partial z}}\right) = -3.0 \text{ meters}^{-1}.$$

Putting numbers into eq. (8.37) we thus get:

$$d_z^{\mathrm{E}} = (\bar{Q} - Q)\left(\overline{\frac{1}{E_x}\frac{\partial E_x}{\partial z}}\right)^{-1} = (-0.333 \pm 0.01)(\bar{Q} - Q)\,(|\text{electron}| \times \text{meter}) \tag{8.38}$$

where, of course, the error of ±0.01 in (8.38) has to be compounded with the error in the measurement of $\bar{Q} - Q$.

8.11. *The measurements of* d_z^{M} and d_z^{E}

We have measured d_z^{M} and d_z^{E} by the procedure described in section 8.9 on 25 different balls. The results are given in table 8.2 and shown in fig. 8.14. The equality is satisfied in all cases.

Here a comment is in order with respect to the paper [28] of Buckingham and Herring. Besides establishing the very important equation $\beta = d_z/H_z$, Buckingham and Herring made in [28] a comment stating that some of our data did not satisfy the equality $d_z^{\mathrm{M}} = d_z^{\mathrm{E}}$. This comment is incorrect, as we noted in [42], because B. and H. used an incorrect equation to extract d_z^{M} from the experimental measurements; indeed they used (8.32) with $\varepsilon = 0$ and, therefore, their determination of d_z^{M} was always 13% larger than the correct value (with our revised values of the magnetic data this is now 14%). Taking this factor into account the equality $d_z^{\mathrm{M}} = d_z^{\mathrm{E}}$ is always satisfied.

To conclude this subsection we add one remark: in some cases where "drifts" are present (compare section 8.4) we have measured at various times both d_z^{M} and d_z^{E}. If the drift is due – as we mentioned (section 8.4) – to a slow variation with time of the dipole moment of the ball, we must find that d_z^{M} and d_z^{E} change with time in the same way. This has indeed found to be the case: compare fig. 8.15 referring to ball 3; or the similar check on ball 60 reported in table 8.2.

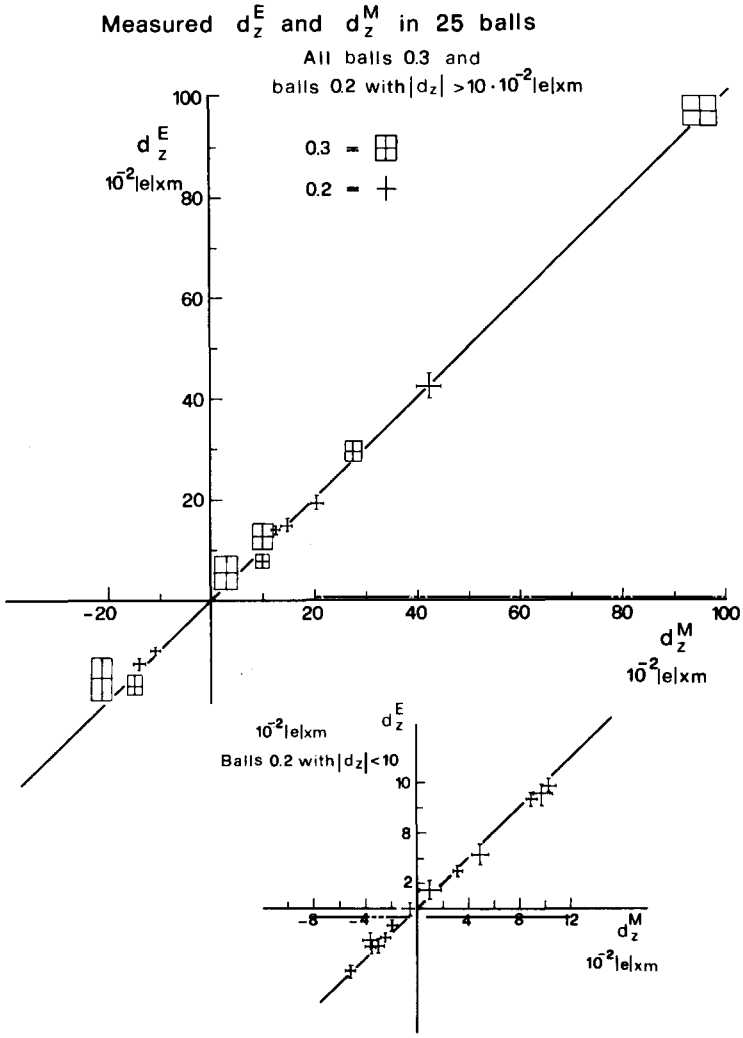

Fig. 8.14. The electric dipole moments d_z^M and d_z^E (in units: 10^{-2} |electron charge| × meter) plotted for those 25 balls for which both have been measured. We have divided the figure in two parts to avoid overcrowding the central region.

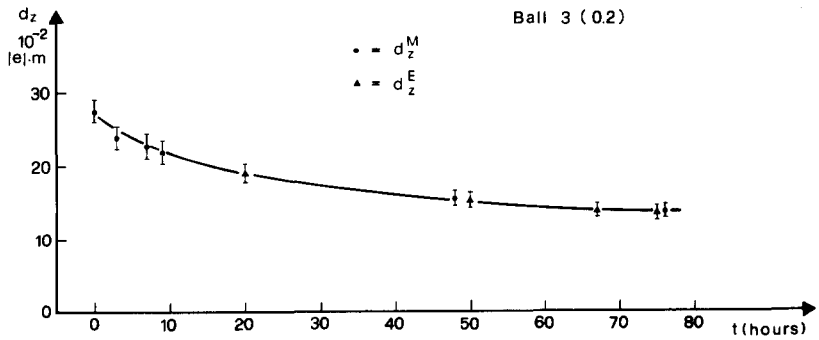

Fig. 8.15. A case of drift with time of the "permanent" electric dipole moment showing that the measurements of d_z performed electrically and magnetically produce at any time the same result; that is d_z^E and d_z^M drift in the same way.

8.12. Some remarks on the question of further increasing the sensitivity

Before concluding this section we touch the following question: suppose that we decided to reundertake this experiment so as to achieve a further increase in sensitivity (to be definite, assume that the goal were to exclude or confirm the presence of charges $\frac{1}{10}e$ (not $\frac{1}{3}e$) in balls of 0.3 mm); which improvements should we introduce on the basis of the experience gained so far? We list below some points of importance:

1. Work in a less noisy environment: by comparing our measurements during the quiet and noisy periods we feel that a reduction by a factor four or more in the time needed for a measurement could be easily achieved.
2. Reduce the magnitude of the spurious force and/or reduce the errors on their measurement. Clearly because the true charge is obtained after subtraction of the magneto-electric and patch forces these spurious forces must be either measured with a small error or minimized to reduce the errors in the subtraction process. An easy possibility to improve the measurement of the magneto-electric force is to amplify the variation of $\partial H_x/\partial x$ with respect to that used here.

As to the patch force the only way to reduce it is to have the plates more spaced: this implies scaling up the size of the whole apparatus (in particular of the coils A and B and of their cores). Operating with the plates at a distance of 3 cm rather than 2 cm the largest patch effect would have been smaller by 4/9 than the one we had; as a consequence the differences between the q' values for subsequent balls would have been reduced by the same amount. Of course increasing the spacing between the plates introduces, as discussed in section 4.2, edge effects, unless at the same time the diameter of the plates is increased; this implies scaling up the whole apparatus as stated before. (An alternative possibility to increase the spacing and size of the plates, without scaling up the whole size of the instrument, can be to work with horizontal plates; and instead of using a resonance method, measure the force needed to keep the ball at rest under the action of the square wave electric field; we have started a project in this direction.)

These remarks have been inserted only to orient the discussion; clearly any modification with respect to our design has implications that are interconnected and should be carefully evaluated.

9. The Stanford experiment

9.1. Scope of this section

Having surveyed our results in detail, we now consider the Stanford experiment. As already stated (section 1) its principle is the same as ours: the Stanford set-up exploits (as we did originally with graphite [5a]) the phenomenon of diamagnetic levitation instead of the ferromagnetic levitation with feedback; niobium balls are levitated at low temperature. Below the transition temperature niobium is superconducting and, therefore, diamagnetic.

Due to the use of superconducting levitation and the need of liquid He temperatures, the technical aspects of the Stanford experiment are considerably different from ours. We will not enter into many details because an extensive report has been announced by the authors [45]; but it is necessary, for the completeness of this survey, to give, on the basis of the papers published so far [23, 43, 44, 45, 46, 47] at least a short description of the Stanford apparatus and of its operation.

In particular it is appropriate: (a) to list the main differences between our instrument and the Stanford one, (b) describe their observations, (c) comment on the compatibility of their results with ours.

9.2. A list of the main differences between the Genoa and Stanford instruments and procedures

We first list these differences and comment later separately on the implications of most of them (section 9.3).

(a) Our geometry, with vertical plates, is indicated schematically in fig. 9.1a; the Stanford geometry – with horizontal plates – appears in fig. 9.1b. The electric and main magnetic fields are orthogonal in our case, parallel in the Stanford set-up.

(b) Signal detection. We used an optical detection method (differential photodiodes – section 7.4); Stanford uses a SQUID (positioned just above the upper plate) measuring the variation of the magnetic field due to the oscillation of the levitating ball.

(c) Damping and signal analysis. In our case the oscillation of the ball due to the square wave electric field is damped electronically with a stable and prescribed Q value (section 7.3). This damping corresponds (in the conditions of operation adopted) to a value of $N_{1/2}$ from 15 to 20, corresponding to a Q value of the oscillator of about 70 to 90. Thus the resonance is, in our case, comparatively broad; the noise rejection is accomplished by a lock-in having its reference channel piloted by the square wave electric signal and a long integration time. In the Stanford experiment the damping is due to the residual gas – and possibly to other effects – and corresponds usually to very large Q values (of the order 8000 or 10000 for balls prepared on a heated Nb substrate – compare section 9.4.1); this damping is not stable: during a night it can change by 20%; due to this a procedure (to be described in section 9.3.2) measuring the derivative of the envelope of the amplitude of oscillation of the ball must be used, instead of our procedure of simply measuring the amplitude and phase of oscillation of the ball under the action of the square wave applied field.

(d) Absence in the force of terms out of phase with the applied electric field. The absence in the force of terms not in phase with the applied electric field is established on each spinning ball in our case; in the Stanford instrument the analogous check is not performed and would not be easy.

(e) The rate of spontaneous change in charge is several hours in our case, about 15 minutes in the Stanford instrument.

(f) Spinning. The ball is kept spinning around the z axis in our experiment; it does not spin in the Stanford apparatus.

(g) Measurement of the electric dipole moment of the ball. Due to spinning only the z component of the permanent electric dipole moment of the ball has to be measured in our case. The two other components vanish. In the Stanford experiment all the three components have to be determined.

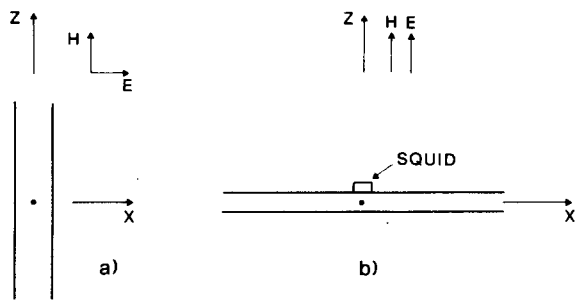

Fig. 9.1. This figure illustrates the difference in geometry between our set-up (a) and the Stanford one (b). The plates, the levitating object, and the directions of the magnetic and electric fields are shown. In the Stanford set-up the position of the SQUID detector is schematically indicated; the magnetic field sustaining the object is produced by a coil configuration sketched in fig. 2.2a.

(h) Distance between the plates: it is 2 cm in our case and 1 cm in the Stanford set-up; the relative position between the ball and the plates is moved in the Stanford instrument; the ball is kept midway between the plates in our case.

(i) Replacement of a ball with another. The vacuum – normally 0.8 μ Hg – must be worsened during this operation in the Stanford set-up. Also to extract the surplus charge from a newly levitated ball takes many hours in the Stanford apparatus and ~20 minutes in our case.

(l) Visual observation of the levitating ball. In the Stanford set-up it is not possible to observe the *details of the surface* of a ball after its levitation.

9.3. A short discussion of the differences between the two experiments

The values of the charges in the Stanford experiment are reported to be only ~0 and ~ $\pm\frac{1}{3}e$. For this reason in the presentation that follows we will, deliberately, forget about effects – peculiar to the Stanford set-up – that might produce spurious charges. Indeed any such effects should conceivably give rise to a continuous distribution in charge and not only to the discrete values reported by the Stanford group. On the other hand it must be stated clearly that several facts to be described in sections 9.4.2 and 9.4.3 are hard to understand if the Stanford interpretation of their signals – as representing $\pm\frac{1}{3}$ fractional charges – is accepted.

In the rest of this subsection we confine to clarify some of the consequences that the differences listed in section 9.2 between the two experiments imply.

9.3.1. Geometry and spinning (points a and f of section 9.2)

In the Stanford geometry and in an ideal situation the magneto-electric spurious charge (given in our case by the term $\beta\partial H_x/\partial x$) is absent, as remarked by Buckingham and Herring. Here by ideal situation we mean: (a) that the magnetic field at the position of levitation is perfectly vertical; (b) that the niobium ball is homogeneous. Only if the conditions (a) and (b) are not satisfied tiltings can be present. In refs. [45, 46] the maximum expected tilting due to inhomogeneities of the ball is calculated and shown to be unimportant. Although details on the verticality of H and on the upper limits to $\partial H_z/\partial x$ or $\partial H_z/\partial y$ at the position of levitation are not mentioned explicitly in [45], it is reasonable to assume that careful consideration has been given to these points.

Thus, in conclusion, in the ideal situation the magneto-electric spurious charge is absent in the Stanford set-up (aside from unexpectedly large magneto-electric *effects*, not due to tilting, in some of the superconducting Nb balls) whereas it is present and has to be measured and subtracted in ours.

Another spurious force has, however, to be considered in the Stanford case. It is the force $\boldsymbol{d}\cdot\partial\boldsymbol{E}^{(\mathrm{image})}/\partial z$ produced on the permanent electric dipole moment $\boldsymbol{d}$ of a ball by the image electric field $\boldsymbol{E}^{(\mathrm{image})}$ due to the electric moment induced in the ball by the square wave applied electric field. Here by image field we mean, of course, the electrostatic image(s) from the plates. The image field depends on the distance of the plates from the object; $\partial\boldsymbol{E}^{(\mathrm{image})}/\partial z$ vanishes only at the mid-point between the plates for symmetry reasons. As a matter of fact in the Stanford set-up the measurement from which the residual charge is extracted is performed at this position. Stated more precisely the quantity $\partial E_z^{(\mathrm{image})}/\partial z$ is mapped as a function of z with the help of an auxiliary measurement (creating by a battery an artificial *induced large static* d_z^{I}) and the position z_0 at which $d_z^{\mathrm{I}}\partial E_z^{(\mathrm{image})}/\partial z$ vanishes is determined; the extraction of the residual charge is then performed using the data at z_0. For reasons that we have not clear z_0 deviates very appreciably from the mid-position in the early Stanford measurements; in the more recent runs the situation is considerably more symmetric.

Note that – aside from the larger distance between the plates – the force due to the image dipole field is cancelled by the spinning in our geometry.

9.3.2. The damping and the detection of the force on the ball (point c of section 9.2)

The instability of the damping in the Stanford experiment entails that, for a given force on the ball, there is not a constant ratio between the force and the resonance amplitude of the oscillation. Therefore to determine the force (and thus the residual charge) one cannot rely on a simple measurement of the amplitude of the oscillation; one has to make recourse to a more complex procedure that we are going to summarize below (for details, of course, ref. [46] should be consulted). The procedure must fulfill two requirements: (a) ensure that the square wave electric field is always applied at the proper resonance frequency of the vertical oscillation of the ball, (b) provide a measurement of the residual charge independent of the value of the damping. We mentioned the requirement (a) explicitly because since the Stanford resonance is very narrow – corresponding, as we have mentioned, to Q values of 8000 or larger – a specific procedure is needed to stay always at resonance. In its essence the method used in the Stanford set-up consists in exciting the vertical oscillation of the ball to a reasonably high amplitude (e.g. 25 μ) and to have then the square wave electric field directly piloted by the oscillating ball. To simplify things we shall only say here that an appropriate vertical "push" to the ball can provide the requested excitation of the vertical oscillation; and that, during the measurements such pushes have to be repeated from time to time; the smaller the damping is, the larger the interval between two pushes can be.

The measurement of the residual charge is then performed on this heavily oscillating ball operating as follows: the square wave electric field piloted in the way just described is applied for some short period (say 50 oscillations of the ball) with its phase at +90° with the oscillation; then it is reversed, that is it is applied for the subsequent 50 oscillations with its phase at −90°; and so on and so forth. Assume that the charge of the ball does not change spontaneously during, say, three of these "reversals" of the square wave field. (Three is, of course, just an example, it might be two, or four or five ....) Then one observes that (aside from the natural damping) the envelope of the (already large) amplitude of oscillation of the ball, increases, say, during the first 50 cycles at some rate depending on the charge of the ball; it then decreases during the subsequent 50 cycles at (minus) the same rate; and so on during the two subsequent field reversals, as shown schematically in fig. 9.2. If at time T there is a change in charge, this is reflected in a different rate of increase or decrease of the envelope of the amplitude, as again shown in fig. 9.2; note incidentally that fig. 9.2a shows an ideal situation in which the noise is absent; the noise implies much more fuzzy records of the increase or decrease of the signal above the large background amplitude (fig. 9.2b). Anyway it can be shown (compare ref. [46] eq. (38)) that the difference between the *rate of increase* of the envelope of the amplitude and the *rate of decrease* of the same during the subsequent 50 cycles gives (at constant charge) a measurement of the force produced by the electric field independent of the damping (thus eliminating, in this respect, the drawback of a varying damping).

We have repeatedly mentioned above the number of 50 cycles; again this number has nothing special; the choice of this number, that is of the duration of the interval during which one keeps the phase of the electric field at +90°, before reversing to −90°, depends on the frequency of spontaneous changes in charge. Before ending this description we add two remarks:

(1) One should realize that the measurement of the charge is made in the Stanford procedure exploiting comparatively small increases or decreases in amplitude; small as compared to the large background amplitude needed to keep the electric square wave locked at the resonance frequency.

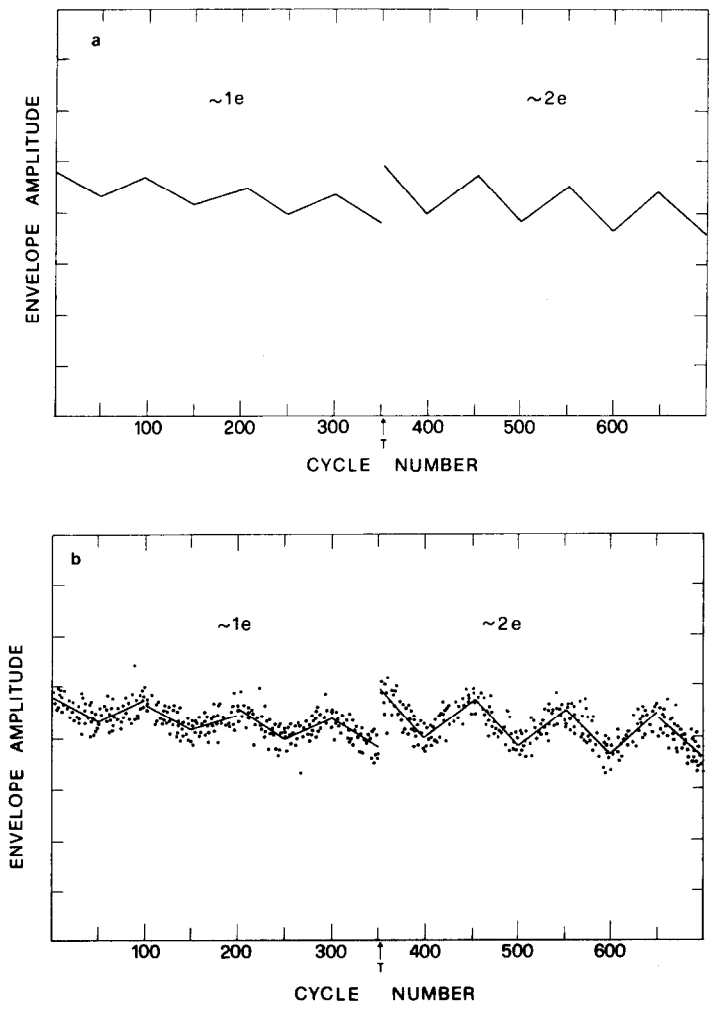

Fig. 9.2. (a) The (vertical) amplitude of oscillation of the ball versus the time in the Stanford experiment (instead of time the number of oscillations is given in the abscissa – the period of oscillation is approximately 1 sec). The ball oscillates with a large amplitude and each 50 cycles the square wave electric field is reversed (that is its phase is changed by 180°). Corresponding to these reversals the amplitude of oscillation increases or decreases at a rate depending on the value of the residual charge of the ball (including, of course, any spurious charge). In the figure – a schematic plot not including noise – a change of charge from $\sim 1e$ to $\sim 2e$ takes place at time T. The overall slow decrease of the amplitude of oscillation is due to the natural damping; when the amplitude of oscillation becomes too small a "push" must be given to the ball to increase it again, as explained in the text. (b) The same plot as shown in (a) but with the effect of noise indicated (from ref. [46]).

(2) We have not discussed above the whole question of the errors on the raw data (we call raw data a plot like that in fig. 9.2 or 9.3); nor of the composition of these errors when the residual charge is deduced from the raw data.

9.3.3. Measurement of the permanent electric dipole moment (point g of section 9.2)

The spinning of the ball implies in our case that only the z component of the permanent electric dipole moment of the ball – the component parallel to the spinning axis – is present; the x and y components of $\boldsymbol{d}$ are averaged out. We measure this one number d_z precisely simply creating a known

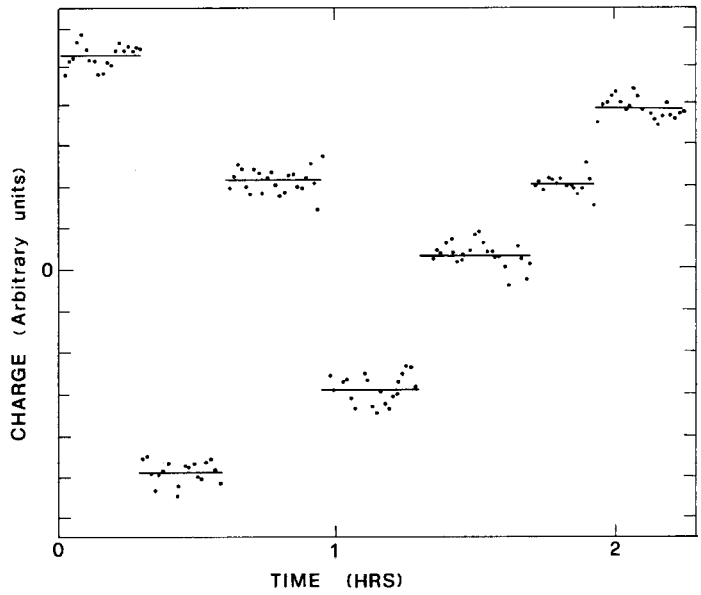

Fig. 9.3. The charge "levels" versus time deduced from a plot like that of fig. 9.2b. In this plot 6 changes in charge (taking place in two hours) appear (ref. [46]).

gradient $\partial E_z/\partial x$ of the electric field via a prescribed inclination of one plate (as described in section 7.5).

In the Stanford set-up, due to the absence of spinning, all three components of the permanent electric dipole moment are, in general, non-zero. Starting with ref. [44] they were measured creating prescribed electric gradients by the insertion of a grounded metallic sphere in between the plates, near to the levitating ball.

9.3.4. Distance between the plates and related effects (point h of section 9.2)

The last point that we consider in some detail is related to the different distance between the plates in the two instruments: 1 cm in the Stanford set-up, 2 cm in our instrument. This has some implications:

(a) At equal magnitude of the patches, the effects of the patches are four times larger in the Stanford instrument (compare eq. (4.8) of section 4.1) than in ours. As stated in section 8.8 the maximum value of the patch spurious charge that we did record in our case for a ball of 0.3 mm diameter has been $0.33e$; it has been $0.14e$ for the balls of 0.2 mm diameter (we underline that, as shown by the figures 8.8 and 8.9 the values just mentioned were the maximum values). If, for some reason, the patches should slowly change during a run, the differences in the spurious charges due to the patches of subsequent balls are expected to be a small fraction of the above values. If, instead of $0.33e$, we had a patch spurious charge four times as big, also the possible changes might be larger. Stated more generally we have to fight with spurious patch charges having an *average* magnitude of $|q'_{\text{patch}}| = 0.11e$ (for the 0.3 mm balls) and of $0.05e$ (for the 0.2 mm balls) whereas in the Stanford measurements the patch spurious charges often correspond to values larger than one for balls of 0.3 mm diameter (compare the values shown in figures 2, 3, 4, 5, 6 of ref. [45] for balls of diameter 0.28 mm all around one or larger; or the value of the patch spurious charge of $-0.45e$ shown in fig. 5 of ref. [45] for the ball of diameter 0.196 mm).

(b) Our larger distance between the plates implies some tiny gradient effects from the edges; these have been both measured and calculated and, in the usual conditions of operation, they are unimportant

as discussed in section 4.2. In the Stanford set-up the edge gradients are expected to be many orders of magnitude smaller than ours (compare eq. (4.3)) and therefore, a fortiori, totally irrelevant. On the other hand the Stanford set-up must take into account the mirror image electric fields, as already mentioned (section 9.3.1). Also these image fields are negligible effects in the vicinity of z_0 and for the usual values of the permanent electric dipole moments of the ball; in fact they should vanish midway between the plates for symmetry reasons. In this respect one should understand – as we have already mentioned – why, except for the runs described in ref. [45], there are large violations of the electrical symmetry with respect to the mid-plane. In one case (runs C and D of ref. [43]) z_0 is displaced 2 mm from the center (it stays at 7 mm from one plate and 3 from the other); in run A of ref. [43] z_0 is off-center by 1.2 mm; it is off by ~1 mm in the first cool-down of ref. [44] and 0.5 mm in the second cool-down.

(c) We finally consider the procedure of Stanford for extracting the residual charge. On each ball the measurement of the force is performed at many different positions between the plates (the plates are displaced, not the ball). A best fit – for the details of which we refer to [46, 47] – is made and the force is then evaluated at z_0. While it is clear that this procedure was in a sense compulsory before the introduction of the method of measuring directly the permanent electric dipole moment (mentioned in section 9.3.3) one can well ask why this procedure has been continued by the Stanford group once the electric dipole moment could be known via a separate measurement. Indeed good measurements all performed at z_0 should be enough; at equal noise and for equal total time spent – in other words, at equal statistical error – performing measurements at various distances from the plates does not in itself provide a better check of the constancy of the patch spurious charge than that obtained by a precision measurement or repeated precision measurements all performed at z_0.

The answer to this question is, we presume, that in comparing the residual charges of two different balls, one has to be sure that they levitate at the same position (z_0) within very strict limits because the difference in the patch spurious charge at different heights of levitation can otherwise produce a spurious charge difference. In the Stanford set-up the equality in the height of levitation is not guaranteed automatically because different balls can have different trapped flux etc. The way chosen by the Stanford group to be sure that a ball is at z_0 is to perform on each ball the auxiliary measurement described in section 9.3.1 (measuring the force $d_z^1 \partial E^{(\text{image})}/\partial z$). This implies performing a sequence of measurements at different distances from the plates. In our case all this can be avoided because different balls levitate at the same position within a few microns.

9.4. The Stanford observations

9.4.1. Introduction

The first Stanford report on the search for quarks by a magnetic levitation electrometer was published in 1971 [23]; only one ball was examined; the apparatus is, in its essentials similar to the present one, but with a reduced distance between the plates (0.6 cm). In these conditions the patch spurious charge is expected to be huge. The ball of ref. [23] was stated to have a residual charge compatible with a quark assignment, but it was added that any definite conclusion could be made only after an examination of the spurious effects. No further reference to these observations appears in the literature (see, however, [48] for more details).

In three papers published in 1977, 1979, 1981 under the titles "Evidence for the existence of fractional charges in matter" [43], "Further evidence for fractional charges in matter" [44] and "Observation of fractional charges $\frac{1}{3}e$ on matter" [45] the Stanford group describes evidence for the

existence of fractional charge $\pm\frac{1}{3}e$. In each of the above mentioned papers some improvement in the apparatus is introduced. The main improvement from ref. [43] to ref. [44] was the introduction of the method, already mentioned (section 9.3.3), to measure the three components of the permanent electric dipole moment of the ball; and in ref. [45] the method of replacing one ball with another was improved, minimizing the disturbance to the plate surfaces during this operation. As it is normal in this type of experiments some prejudices were corrected in the course of the work. We mention here two because the interested reader who wishes to study the three papers [43, 44, 45] is helped in his analysis knowing that some statements in ref. [43] were later corrected "de facto".

(1) Patch effects. It was explicitly stated in ref. [43] that copper, at low temperature – below the liquid He temperature – does not have patch static potentials (this assertion was based on previous work by J.M. Lockhart, F.C. Witteborn and W.M. Fairbank [49]). It was also stated that indeed the first runs with copper plates confirmed the absence of patches in copper. While this last point is not clear to us – because the runs with copper plates in ref. [43] included only balls with the same radius (namely the balls 6, 7, 8) and therefore the absence of patches could not be so easily established – the statement that copper is exempt from patches was later found not to be correct, and the subsequent analysis were performed taking the patches into account.

(2) The measurements in ref. [43] were performed on two kinds of Nb balls: (a) balls prepared on a heated W substrate, and (b) balls prepared on a Nb heated substrate. The reason of these two preparation procedures was an attempt to reduce the sticking of the balls to the holder [48] and, at the same time, their natural damping [47b]; indeed noise rejection and the procedure described in section 9.3.2 require a damping as small as possible. It was found that the balls prepared on a W substrate had a Q of 1000, whereas those prepared on a Nb substrate had a much higher Q value (from 8000 to 10000). Thus the latter preparation appears preferable. However in ref. [43] the three cases of balls as having fractional charge (namely ball nr. 3 and, twice, ball nr. 6) had been prepared on a W substrate. It was therefore hypothetized in ref. [43] that quarks might have passed from the W substrate into the Nb balls during the treatment. (It has been for this reason that a few attempts by other groups were made [50, 51] to search quarks in small quantities of W; indeed if the quarks were so abundant in W to be transferred easily into Nb, it should have been easy to find them in W. No evidence, however, emerged in [50, 51].) In the subsequent papers from the Stanford group [44, 45, 47], although some balls were still treated on W, the correlation between W treatment and quarks is not mentioned anymore.

To conclude these introductory remarks we add a few words on the question of the data rejection in the Stanford experiment; the same words used by the authors in ref. [44] will be transcribed here: "We have required that the data satisfy the criterion that the plate function remains constant during the measurements of at least two balls for the data to be considered valid. If the plate functions change with time because of the presence of a foreign substance in one of the plates, the run is discontinued". We only add in this respect that it might help to have some clarification on cases like that of ball 6 in fig. 5 of ref. [45] showing a small but, apparently, significant change in the plate functions but nevertheless included among the valid data; it would also be of interest to know something on the frequency of occurrence of situations with changing patches and on the rate of change.

9.4.2. The Stanford plot

We now describe the Stanford results published in refs. [43, 44, 45]*. A total of 13 different Nb balls

* At the San Francisco and Lisbon Conferences, respectively in June and July 1981, some additional measurements were illustrated but no published data on these is available to us at the moment.

have been measured, many of them several times; 9 of these balls had a diameter of 0.28 mm (to be called "large" in what follows), 2 of 0.232 mm ("medium"), 2 of 0.196 mm ("small"). Table 9.1 presents the results in chronological order. Figure 9.4 – a modification of fig. 1 of ref. [45] – gives for each ball from 1 to 13 the residual charge in its successive measurements.

Some remarks are in order: (a) all the values of the residual charges reported are in the vicinity of 0 and $\pm\frac{1}{3}e$; (b) the majority of the balls measured more than once loses or gains fractional charge $\frac{1}{3}e$ by the simple act of depositing on its holder, that is by the simple act of touching a plastic or metal surface (in some cases the balls were also washed in acetone between successive levitations); (c) the ball 6 (large) changes nine times its fractional charge in a total of 13 levitations, as follows: $+\frac{1}{3}$, $+\frac{1}{3}$, 0, $+\frac{1}{3}$, 0, 0, $-\frac{1}{3}$, $+\frac{1}{3}$, $-\frac{1}{3}$, 0, $+\frac{1}{3}$, $+\frac{1}{3}$, 0. Here $+\frac{1}{3}$, 0 and $-\frac{1}{3}$ are abbreviations for the measured values reported in table 9.1 or fig. 9.4; note that among the changes listed above two double changes (from $-\frac{1}{3}$ to $+\frac{1}{3}$ and vice versa) are present; (d) the ball 10 (small) has always charge 0 and never changes in 8 levitations; (e) the other balls have been levitated a smaller number of times; among the balls levitated more than twice, at least three over four changed charge once touching a surface.

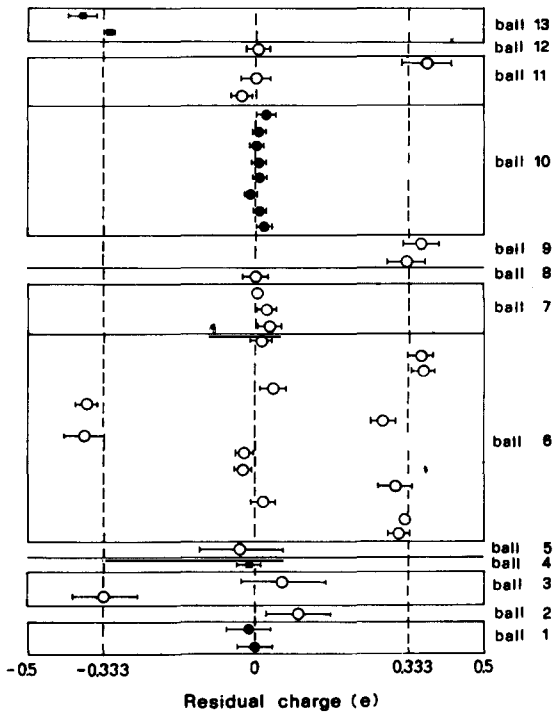

Fig. 9.4. The residual charge measurements in the Stanford experiment on the 13 balls studied from the first [43] to the last [45] report. Several balls were measured many times; between one measurement and the next one the ball was deposited in a holder (of plastics or metallic) and – in some cases – washed with acetone. For each ball – numbered from 1 to 13 – the residual charge in subsequent levitations is reported. Open circles refer to balls with radius $R = 0.14$ mm, solid squares to balls with $R = 0.116$ mm and solid circles with $R = 0.098$ mm. It is apparent – see text – that some balls (e.g. nr. 6) change extremely often their fractional charge, whereas others (e.g. nr. 10) have never departed from zero (the top point of ball nr. 7 was *assumed* to be zero and has not to be counted).

Table 9.1
The residual charges measured in refs. [43, 44, 45] (this table is taken from a slightly enlarged preprint version of ref. [47], presented at the 1980 Wisconsin Conference on high energy physics). The measurements are reported in chronological order. Different cool-downs imply that the apparatus has been opened in between; in a given cool-down a "set" of measurements stays for measurements showing no change of the plate functions.

Cooldown	Set	Ball	q_r / e
Data reported in refs. [43, 44]			
A		1	-0.007 ± 0.039
A		2	$+0.089 \pm 0.073$
A		3	-0.331 ± 0.070
A		4	-0.016 ± 0.030
B		1	-0.015 ± 0.054
B		3	$+0.060 \pm 0.092$
B		5	-0.034 ± 0.093
C		6	$+0.313 \pm 0.019$
C		7	$+0.030 \pm 0.023$
D		8	-0.001 ± 0.026
D		6	$+0.327 \pm 0.010$
E		6	$+0.016 \pm 0.024$
E		6	$+0.304 \pm 0.040$
E		6	-0.029 ± 0.017
E		6	-0.026 ± 0.016
E		7	$+0.023 \pm 0.015$
F		9	$+0.325 \pm 0.043$
F		7	$0e$ assumed
F		9	$+0.361 \pm 0.040$
Data first reported in refs. [45, 47]			
G	1	6	-0.376 ± 0.045
G	1	10	$+0.014 \pm 0.016$
G	2	6	$+0.277 \pm 0.026$
G	2	10	$+0.006 \pm 0.009$
G	2	6	-0.371 ± 0.025
G	2	10	-0.015 ± 0.009
G	2	6	$+0.038 \pm 0.026$
G	2	10	$+0.006 \pm 0.009$
G	2	6	$+0.364 \pm 0.023$
G	2	10	$+0.003 \pm 0.011$
G	2	6	$+0.357 \pm 0.026$
H	1	10	-0.001 ± 0.010
H	1	6	$+0.010 \pm 0.021$
H	1	11	-0.033 ± 0.024
H	1	12	$+0.003 \pm 0.024$
H	1	13	-0.324 ± 0.014
H	2	10	$+0.002 \pm 0.012$
H	2	11	-0.004 ± 0.030
H	3	13	-0.385 ± 0.032
H	3	11	$+0.370 \pm 0.056$
H	3	10	$+0.018 \pm 0.020$

9.5. Are the Genoa and Stanford results compatible?

Clearly the Stanford fractionary charges seem to be able to leave Nb or attach to it very easily. The double changes in charge mentioned above (for ball 6) would indicate that two quarks stick to the ball or leave it in the deposition between two levitations. The contrast between the behaviour of ball 6 and that of ball 10 is certainly mysterious if the Stanford signals are in fact due to fractional electric charge. If the quarks attach so often to ball 6 why don't they attach themselves to ball 10? Or, similarly, if the quarks leave ball 6 so easily, why is this typical of ball 6 and not shared by ball 10? Moreover if so many quarks are around, why are some of them not found in the steel balls used in our experiment?

Altogether the amount of Nb contained in the 13 balls listed above is 1.1 mg, to be compared with 3.7 mg explored in our experiment. Fractional charges are claimed by the Stanford group on five of these 13 balls. If we could forget the loss and gain of the fractionary charges just described the two experiments might, perhaps, be compatible: one might conclude simply that the Stanford sample of Nb is richer in quarks by a factor ~18 than our sample of steel. But, due to the gain and loss of fractional charges described above, the situation is not so simple: this frequent loss and gain indicates that if the interpretation of the Stanford results as fractional charges is correct, then there must be many around; and if they are capable of abandoning the Nb so easily, it is not clear why they should not be everywhere, not only in the plastic holder on which the niobium balls are deposited between successive levitations, or in the acetone with which they are washed. This being the situation it seems that in fact there are signs of contradiction between the results of our experiment and the results of Stanford. If we could be sure that the Stanford signals come from Nb* we might, possibly, test this using balls manufactured with a Fe–Nb alloy (with ~20% Nb) that we have found to be ferromagnetic† (assuming that balls of this alloy can be fabricated with the necessary precision characteristics). A clarification of this point appears essential to understand the nature of the signal that the Stanford group is reporting and to justify starting an attempt to explore the Fe–Nb alloy with our apparatus.

10. Other experiments and developments in the search of quarks in matter

10.1. Introduction

This report has been intentionally limited to the search of quarks in matter with the magnetic levitation electrometer; a limitation motivated both by size requirements and by the fact that most of the other searches of quarks in matter have been extensively surveyed [9, 10, 11, 12, 13]. Nevertheless, before concluding, it seems appropriate to say a few words on the different kinds of experiments in this field. It also seems convenient to expand a little on the Millikan type experiments that recently underwent some interesting development.

10.2. A short summary of the non-Millikan type techniques

The following types of non-Millikan techniques have been used or considered in the search of quarks in matter:

* At the San Francisco and Lisbon Conference Prof. Fairbank has mentioned the possibility that the source of their fractional charges is the polishing substance used by the firm producing the Nb balls during the preparation process.

† We thank Prof. G. Olcese, of the Dept. of Physical Chemistry, for the preparation of this alloy.

(1) Optical spectroscopy.
(2) Emission of negative ions from filaments.
(3) Energy spectroscopy.
(4) Cyclotron mass spectroscopy.
(5) Gas efflux.

Let us first note that the last mentioned method (gas efflux – a method invented a long time ago [52] to look for a possible tiny difference in charge between the electron and the proton) does not in fact – in its present form – produce information on the existence of quarks. We mention this because sometimes one finds in the literature the statement that the results obtained by this method [53] establish – as a by-product – a strong upper limit for the non-existence of fractionally charged quarks. This does not appear to be the case (compare the discussion in ref. [11b]).

As to the other methods listed above, all the experiments (except nr. 4) have one aspect in common: the material under consideration is first subjected to an *enrichment procedure* trying to concentrate all the quarks that it might contain into a very small filament or foil; this is then explored. In principle this is a sensible thing to do and this procedure can certainly increase the chance of finding a quark. The only – minor – objection is that if quarks are not found (as it has been the case in all these experiments) this procedure raises some question when one tries to express the negative results in terms of an upper limit to the quark concentration; indeed to know really the enrichment factor that has been used – often assumed to be very large (10^6 or more) – implies more knowledge of the quark chemistry than we do possibly have.

Let us now briefly describe a few among the above experiments. (More information is found in the survey articles quoted, especially in [9].) As far as the optical spectroscopy is concerned an experiment by Rank [16] exemplifies the situation. The experiment tries to find evidence for lines in the ultraviolet from atoms of the type $(q^{2/3}e^-)$. The spectrometer is sensitive up to 7000 Å, and this fact limits the search to the Lyman lines of the $(q^{2/3}e^-)$ (~2500 Å) excluding the Balmer lines or the lines from $(q^{+1/3}e^-)$. The samples examined were taken from sea water, lake water, oysters and plankton and the quarks contained in a few kilos of material were collected on foils of Au or Pt by vaporizing the sample in an electric field. Because the spectroscopic sensitivity is low (a signal can be seen only if there is more than a quarkic atom per 10^{10} normal atoms) a positive result would correspond – *assuming* an enrichment factor of 10^7 – to an abundance of more than one quark per 10^{17} atoms in the original material. The result of the search is negative and is expressed by the author as follows "At a wave-length corresponding to a possible Lyman line a signal from some sample was seen, but there was no evidence for other (expected) Lyman lines".

The negative ion emission by filaments enriched in quarks has been the basis of a long series of experiments conducted by the Argonne group [17, 54]. In one of the methods used a filament (of Pt) is "enriched" in quarks trying to transfer on it all the quarks contained in large amounts of several substances: sea water, dust from air conditioners, Lunar soil, manganese nodules from the ocean, etc. The idea of the method is that the behaviour of a quark emitted from a filament, on heating, should be similar to that of a negative ion. If this is so the enriched filaments, when heated, should – according to the authors – emit more negative ions than the non-enriched filaments. Because in a typical experiment less than 10^5 counts of excess are found, it is concluded that quarks, if present, have an abundance of less than 10^{-21} quarks/nucleon in the enriched filaments. Mass spectroscopy is also used to explore in some cases the masses of the emitted negative ions with inconclusive results.

Energy spectroscopy. Under this heading we refer to an experiment performed by Cook et al. [55]; its idea is very simple (although in practice it is of difficult realization and interpretation: "enrich" in

quarks a Ta foil and evaporate (by heating) the quarks it contains. If their charge is $e/3$ (e is the electron charge) they should acquire, when accelerated through a potential V, a kinetic energy precisely equal to one third of the kinetic energy of a charge e accelerated by the same potential difference. The question is how to measure this kinetic energy; this is not easy because the ions are presumably massive – either because the quark itself is massive, or because the atom to which it is attached is such. Due to this high mass the velocity of the ions arriving on a Si detector when accelerated by a potential difference, say 50 kV (the value used in the experiment [55]) is too low to be in the region where the detector gives a signal proportional to the kinetic energy. This difficulty appears clearly in fig. 10.1. The full curve gives the signal from an *electron* current accelerated by $V = 50$ kV. Due to the high velocity of the electrons a very clean peak appears at $T = 50$ kV as expected. If the electrons are then swept away by an appropriate magnetic field, the remaining negative ion signal is given – in the scale on the right – by the dashed line. One can see that this signal has a peak at 40 kV rather than 50 kV; the small bump around 15 kV might be, in principle, a quark peak masked by a bad resolution but is also perfectly compatible with other interpretations; on comparing the signal from foils enriched differently no clear conclusion can be reached and only an upper limit to the quark abundance in the enriched samples can be given: $<10^{-24}$ quarks per nucleon, with an assumed enrichment factor of $\sim 10^7$.

Finally we list the use of a *cyclotron as mass spectrometer.* It was in this way that, in 1939, Alvarez and Cornog [56] discovered the ^{3}He. So far this technique has been mainly employed to search for integrally positive charged quarks [57] ("anomalous hydrogen"); in the case of quarked tungsten (the reason for this choice is apparent from section 9.4.1) a related technique [51] was also used to search for fractionally charged quarks; no quark signal appeared.

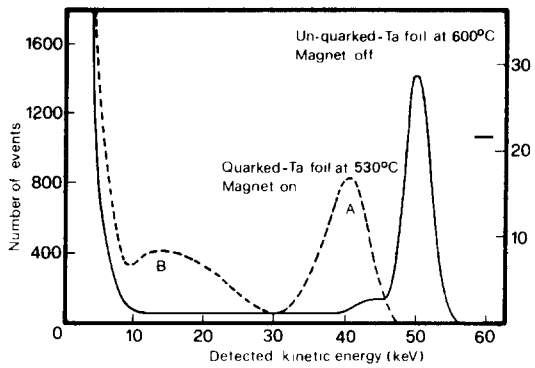

Fig. 10.1. Schematic plots (taken from ref. [9]) of the experiment of Cook et al. [55]. The full curve refers to the spectrum from an unquarked foil at 600°C. The counts are almost entirely electrons. The scale for this curve is on the left. The dashed curve refers to the measured spectrum of a quarked foil at 530°C. The electrons have been swept away by a magnetic field; the scale to this figure is given on the right. The bump at B is compatible with O^- or OH^- ions, that of A to objects as H_2^-.

10.3. Developments in the Millikan-type experiments

10.3.1. Searches of quarks in tungsten

The first Millikan experiment after the suggestion of quarks was – as far as we know – that by Chupka, Schiffer and Stevens [17] exploring 1000 polyethylene spheres, each of mass 6×10^{-11} g. No quark was found. After this experiment (and the attempt by Rank already mentioned [16]) the Millikan technique (with some variants) was again used in 1977 following the Stanford [43] claim that Nb balls

heated on a tungsten substrate produced quark signals. Two experiments were performed by Bland et al. [18] and by Putt and Yock [19] using tungsten microspheres of radius $\sim 1\ \mu$. In both cases – as well as in the study of ref. [51] – the total amount of W explored was $\sim 3 \times 10^{-10}$ g. (The quantity of W explored globally in the three experiments is comparable to that attached to one Nb ball if a monolayer of W were formed in the heating process described in [43].) Bland et al. conclude that no quark signal appears from 69 well measured tungsten microspheres with a confidence level corresponding to 9 standard deviations; Putt and Yock conclude that there is no evidence of fractional charge on 22 microparticles and plot a histogram showing residual charges centered at zero and extending between $-0.12e$ and $+0.12e$.

10.3.2. The San Francisco automated Millikan experiment

More recently an automated Millikan apparatus has been constructed by Bland and coworkers (San Francisco State University) in a search for quarks in Hg [20]. Here automated refers both to the measuring technique (data taking) and to the data analysis; the automation allows to explore rapidly droplets of mass around 8×10^{-10} g. The principle of the method is the following. The mercury drops are viewed by appropriately positioned photomultipliers and recorded while falling through air at regime velocity (fig. 10.2). If a is the drop radius, η the viscosity of the air, m the mass of the drop and v_1 and v_2 the regime velocities when the same electric field is applied first upwards (v_1) and next downwards (v_2) it is easy to show that:

$$mg = 6\pi\eta a \frac{v_1 + v_2}{2}$$

and

$$qE = 6\pi\eta a \frac{(v_2 - v_1)}{2}.$$

These two equations hold provided that the charge q of the drop does not change during the whole measurement; to determine if a change in charge Δq has occurred two additional measurements of the

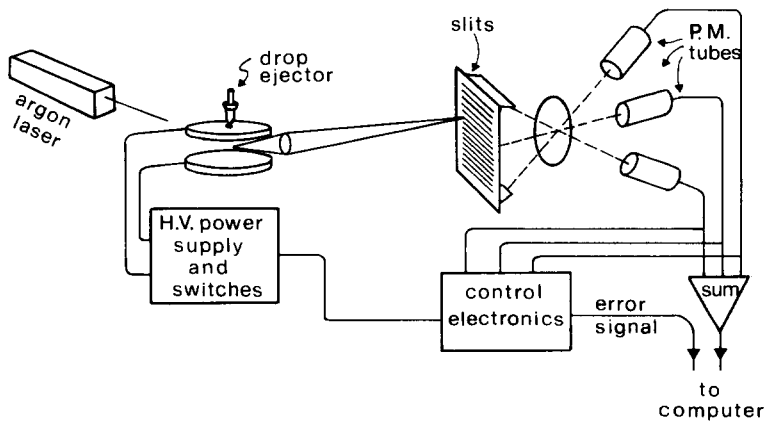

Fig. 10.2. A schematic diagram of the San Francisco automated Millikan apparatus (ref. [20]).

velocity v_3 and v_4 are made, with the electric field in the same direction; v_3 is recorded just at the beginning and v_4 at the end of a measurement (altogether a measurement takes a few seconds); it can be shown that $\Delta q = 6\pi\eta a(v_4 - v_3)$.

It would lead us too far to describe all the details of the experiment, which is an important progress over the original Millikan technique; the interested reader is referred to [20]; besides describing the basic features of the instrument, ref. [20] lists the criteria of the automated analysis and in particular the programmed rejection criteria; that is the automated criteria used to exclude events where a change of charge took place or events corresponding to a ball radius (determined via the previous equations from a measurement of v_1 and v_2) outside preselected limits; or events with excessive noise. This rejection procedure should be free from a possible subjective bias.

Altogether ~100 000 drops were analyzed in the period January 8–20, 1981; of these 53 973 survived the rejection criteria; their total mass was 42 micrograms: 29 micrograms were drops of native mercury and 13 micrograms of distilled mercury. Both kinds were explored in order to avoid the possibility that quarks might be eliminated at the start in the distillation process. No quark was found; the conclusion [20] is that quarks are not present in these samples of Hg at a concentration greater than one per 14 micrograms with 95% confidence. Figure 10.3 gives a typical plot referring to the 13 micrograms of distilled mercury (in the abscissa the charge ranges from 0 to 1e instead of the more customary range $-0.5e$, $+0.5e$, but this is equivalent).

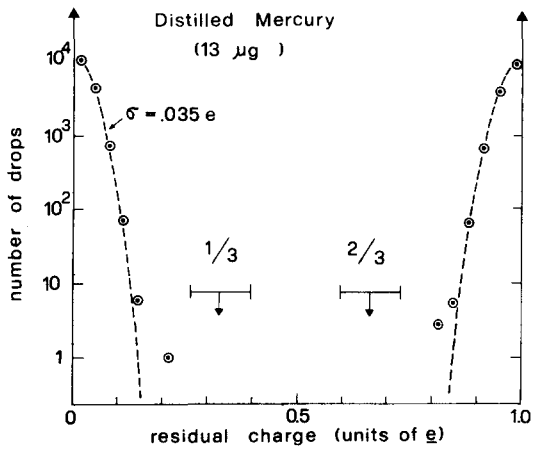

Fig. 10.3. The results of ref. [20] for a sample of balls of distilled mercury (13 micrograms). On the abscissa the measured charge, on the ordinates the number of drops; σ, the standard error in these measurement, is $3.5 \times 10^{-2}e$.

The above result – in spite of the comparatively small mass* – is a valuable one: it shows the potentiality of the automated Millikan technique and it also indicates that a heavy element like Hg is not a particularly rich deposit of quarks (the idea that – for reasons not too clear to us – quarks might prefer heavy elements has circulated widely after the Stanford experiments).

10.3.3. Future developments

In this paragraph we shall mention only a technique that is currently under active development at several laboratories [58]; for a list of other methods being currently considered for searching quarks in matter a summary of the San Francisco Conference (June 1981) can be consulted [59]. The technique

* A preprint by the same authors (San Francisco State University, to be published – August '81) received when this survey had already been completed, reports measurements on a significant mass of Hg: 185 micrograms, approximately $\frac{1}{6}$ of the Stanford mass and $\frac{1}{20}$ of ours. About $\frac{2}{3}$ of the Hg explored is native, $\frac{1}{3}$ is distilled. No quark has been observed.

mentioned above consists essentially in a vertical, fast, automated Millikan experiment (in vacuum); droplets of equal mass fall in a horizontal electric field created between two parallel vertical plates; the deflection from the no field (vertical) trajectory measured at the bottom of the plates is used to determine the charge of the droplets. The original aspect of the experiment is not the idea of the vertical geometry (used already a long time ago, first by Hopper and Laby [60]), but consists in: (a) the use of recent techniques to produce electrically conducting liquid spheres: according to the authors (compare [58] where references to the literature are given) such spheres may be formed at rates exceeding $10^5\,\mathrm{sec}^{-1}$, have a very small spread in mass ($\delta m/m \leq 10^{-3}$), in speed ($\delta v/v \leq 10^{-3}$), be highly parallel ($\partial v_{\mathrm{perp.}}/v \leq 10^{-6}$) and have – when formed – prescribed values of the electric charge; (b) in a complete automation of the measurements, that is of the determination of the end-points of the individual trajectories so as to establish the charge of each droplet.

According to the project the rate at which mass is examined by the apparatus should be larger than 5×10^{-5} g/sec (corresponding to 1 sphere each 1.3×10^{-4} sec; the spheres considered in the project [58] are Hg spheres of diameter 10 μ). In one day – if everything works as planned – one should explore 5 grams of material. We found it appropriate to conclude this report with this short section because – as mentioned – efforts in this direction are now going on in different laboratories (in the U.S.A.): at the Lawrence Berkeley Lab. (under G. Hirsch), at the Lawrence Livermore Lab. (under C. Hendricks) and at the Argonne Lab. (under R. Hagstrom). The size of the Argonne apparatus – essentially determined by the height of the plates between which the electric potential is applied – is planned to be considerably larger than that of the other two: it will be sited in a tower 24 meters high. The other two instruments are two or three meters high.

10.4. Concluding remarks

We end with a few trivial remarks: (1) except for the Stanford experiment, all the remaining searches of quarks in matter provide no evidence for the presence of free fractionally charged quarks in the samples of materials explored so far. (2) There does not seem to be any firm evidence from cosmic rays or accelerator searches [10] for the production of fractionally charged quarks. (3) The above conclusions do not imply (aside from the Stanford experiments) that quarks – or other fractionally charged particles – do not exist: clearly the existing accelerators cannot produce quarks heavier than some mass; and the terrestrial experiments have only explored some milligrams of matter. (4) How to proceed? Our point of view is that there is still interest in both kinds of searches provided that each new experiment presents a substantial increase in the mass explored or in the energy used (probably, as far as the energy is concerned, a big program of study of rare events in cosmic rays should be implemented). (5) What is the conclusion if, after these further efforts free fractional quarks should not appear?

Confinement? Quarks as collective degrees of freedom of some kind? Our inability to predict the future and our dislike to get involved in purely philosophical questions suggest to stop at this point.

Acknowledgments

This work could not have been done without the skillful and intelligent work of the technical staff of this department and in particular of Mr. E. Bozzo, G. Franzone and O. Rosati. The assistance of Mr. A. Pozzo has also been very useful. We are deeply indebted to Miss G. Giuliano for her secretarial work and we thank Mr. G. Massari and R. Barbieri for help with the drawings. Finally we owe much to Mr.

M. Silvi, whose exceptional sense of responsibility has allowed the day and night operation of the laboratory during so many troubled years.

References

[1] G. Morpurgo, Physics (N.Y.) 2 (1965) 95 (reprinted in: J. Kokkedee, The Quark Model (Benjamin, N.Y., 1969) p. 132).
[2] C. Becchi and G. Morpurgo, Phys. Rev. 140B (1965) 687; 149 (1966) 1284; Phys. Lett. 17 (1965) 352; G. Morpurgo, Phys. Lett. 20 (1966) 684; 22 (1966) 214 and references listed in [3].
[3] G. Morpurgo: a) Rapporteur talk, in: Proc. XIV Int. Conf. on high energy physics, Vienna 1968, eds. J. Prentky and J. Steinberger (CERN Sci. Inf. Services, Geneva, 1968) p. 225; b) Lectures on the quark model, in: Theory and phenomenology in particle physics – part A, ed. A. Zichichi (Academic, N.Y., 1969) p. 83; c) Ann. Rev. Nucl. Science 20 (1970) 105; d) Quarks and hadronic structure (Plenum, N.Y., 1977) p. 1.
[4] M. Gell-Mann, Phys. Lett. 8 (1964) 214; G. Zweig, CERN preprint TH 492 (1964) unpublished.
[5] a) C. Becchi, G. Gallinaro and G. Morpurgo, Nuovo Cimento 39 (1965) 409; b) G. Gallinaro and G. Morpurgo, Phys. Lett. 23 (1966) 609; see also refs. [22, 29, 30, 31, 37, 38, 39, 40, 42].
[6] Refs. [32, 33, 34, 35].
[7] Refs. [23, 43, 44, 45, 46, 47, 48].
[8] O.W. Greenberg, Phys. Rev. Lett. 13 (1964) 598; Ann. Rev. Nucl. Sci. 28 (1978) 327.
[9] J. Kim, Contemp. Physics 14 (1973) 289.
[10] L. Jones, Rev. Mod. Phys. 49 (1977) 717.
[11] a) G. Morpurgo, in; Subnuclear Phenomena, part B, ed. A. Zichichi (Academic, N.Y., 1970) p. 640; b) G. Morpurgo, Acta Physica Austriaca, Suppl. XXI (1979) pp. 5–80 (Lectures given at the XVIII Schladming School, February 1979).
[12] L. Lyons, Current status of quark search experiments, Oxford preprint, October 1980 (nr. 77/80).
[13] A.S. Goldhaber and J. Smith, Rep. on progress in physics 38 (1975) 731.
[14] R. Millikan, The Electron (The University of Chicago Press, 1963).
[15] G. Holton, in: Historical Studies in the Physical Sciences, Vol. 9, eds. R. McCormach and L. Pyenson (The John Hopkins Univ. Press, Baltimore, 1978) p. 161.
[16] D.M. Rank, Phys. Rev. 176 (1968) 1635.
[17] W.A. Chupka, J.P. Schiffer and C.M. Stevens, Phys. Rev. Lett. 17 (1966) 60.
[18] R. Bland, D. Bocobo, M. Eubank and J. Royer, Phys. Rev. Lett. 39 (1977) 369.
[19] G.D. Putt and P.C. Yock, Phys. Rev. D17 (1978) 1466.
[20] R. Bland et al. (Quark search group – San Francisco State University), preprint of a paper presented at the New York Meeting of the Am. Phys. Soc. January 26, 1981; Phys. Rev. Lett. 47 (1981) 1651.
[21] A. Ashkin and J. Dziedic, Phys. Rev. Lett. 36 (1976) 276.
[22] G. Morpurgo, G. Gallinaro and G. Palmieri, Nucl. Instr. and Methods 79 (1970) 95.
[23] A.F. Hebard and W. Fairbank, Proc. 12th Int. Conf. on Low Temperature Physics, Kyoto 1970 (Keigaku Publ. Co., Tokyo, 1971) p. 885.
[24] S. Earnshaw, Trans. Camb. Phil. Soc. 7 (1842) 97; compare also ref. [36].
[25] E.T. Whittaker and G.N. Watson, Modern analysis (Cambridge Univ. Press, 4th ed., 1952).
[26] G.N. Watson, A treatise on the theory of Bessel functions (2nd ed., Cambridge Univ. Press, 1952).
[27] W. Magnus and F. Oberhettinger, Formeln und Sätze für spezielle Funktionen der mathematisches Physik (II Auflage, Springer, Berlin, 1948).
[28] M.J. Buckingham and C. Herring, Phys. Lett. 98B (1981) 461.
[29] M. Marinelli and G. Morpurgo, Phys. Lett. 94B (1980) 427.
[30] M. Marinelli and G. Morpurgo, Phys. Lett. 94B (1980) 433.
[31] M. Marinelli and G. Morpurgo, Proc. XX Int. Conf. (1980) on high energy physics (Madison, Wisconsin), eds. L. Durand and L.G. Pondrom, AIP publ. conf. series nr. 68 (1981) p. 308.
[32] V.B. Braginskii, Ya.B. Zeldovic, V.K. Martinov and V.V. Migulin, JETP 27 (1968) 51.
[33] R.W. Stover, T. Moran and J. Trischka, Phys. Rev. 164 (1967) 1599.
[34] E.D. Garris and K.O.H. Ziock, Nucl. Instr. and Methods 117 (1974) 467.
[35] V.B. Braginskii, L.S. Kornienko and S. Poloskov, Phys. Lett. 33B (1970) 613.
[36] W. Braunbeck. Zs. für Phys. 112 (1939) 751, 764.
[37] G. Gallinaro, M. Marinelli and G. Morpurgo, in: Proc. 4th General Conf. of the EPS, York (U.K.) Sept. 1978 (Adam-Hilger, London, 1979) p. 562.
[38] G. Gallinaro, M. Marinelli and G. Morpurgo, Report INFN AE/76/1 (1976) (unpublished).
[39] G. Gallinaro, M. Marinelli and G. Morpurgo, Phys. Rev. Lett. 38 (1977) 1255.

[40] M. Marinelli, G. Gallinaro and G. Morpurgo, Nucl. Instr. and Methods 185 (1981) 129.
[41] J.K. Fremerey, Rev. Sci. Instr. 42 (1971) 753.
[42] M. Marinelli and G. Morpurgo, Phys. Lett. 98B (1981) 465.
[43] G. La Rue, W.M. Fairbank and A.F. Hebard, Phys. Rev. Lett 38 (1977) 1011.
[44] G. La Rue, W.M. Fairbank and J.D. Phillips, Phys. Rev. Lett. 42 (1979) 142.
[45] G. La Rue, J.D. Phillips and W.M. Fairbank, Phys. Rev. Lett. 46 (1981) 967.
[46] G. La Rue, Measurement of the residual charge of superconducting niobium spheres, Stanford dissertation, February 1978 (unpublished); also A.F. Hebard, Rev. Sci. Instr. 44 (1973) 425.
[47] G. La Rue, J.D. Phillips and W.M. Fairbank, Proc. XX Int. Conf. (1980) on high energy physics (Madison, Wisconsin), eds. L. Durand and L.G. Pondrom, AIP publ. conf. series nr. 68 (1981) p. 302.
[48] G. Lubkin, Physics Today, 30 (1977) 17.
[49] J.M. Lockhart, F.C. Witteborn and W.M. Fairbank, Phys. Rev Lett. 38 (1977) 1220.
[50] Refs. [18, 19].
[51] R.N. Boyd, D. Elmore, A.L. Mellissinos and E. Sugarbaker, Phys. Rev. Lett. 40 (1978) 216.
[52] A. Piccard and E. Kessler, Arch. Sci. Phys. et Nat. 7 (1925) 340.
[53] A. Hillas and T. Cranshaw, Nature 184 (1959) 892;
J. King, Phys. Rev. Lett. 5 (1960) 562.
[54] C.M. Stevens, J.P. Schiffer and W. Chupka, Phys. Rev. D 14 (1976) 716; and references quoted there.
[55] D. Cook, G. De Pasquali, H. Fraunfelder, R.N. Peacock, F. Steinrisser and A. Wattenberg, Phys. Rev. 188 (1969) 202.
[56] L. Alvarez and R. Cornog, Phys. Rev. 56 (1939) 379.
[57] R. Muller, L. Alvarez, W. Molley and E. Stephenson, Science 196 (1977) 521.
[58] G. Hirsch, R. Hagstrom and C. Hendricks, Lawrence Berkeley Lab. preprint (unpublished) LBL 9350, June 1979; also LBL 13636 (to be published).
[59] CERN Courier 21 (1981) 301.
[60] V.D. Hopper and T.H. Laby, Proc. Roy. Soc. A178 (1941) 243.

Notes added in proof (February 20, 1982)

a) Although the problem of the charge equality between positron and proton is outside the scope of this paper, this equality is so fundamental that it seems appropriate to mention it briefly. First when refs. [39] and [33] were written the existence of the magneto-electric force in this kind of experiments had not been established. Now (unlikely as it may be) one cannot strictly exclude the possibility that a magneto-electric force was present in each of the (few) objects measured in ref. [39] of an amount precisely such as to produce in all cases, via a compensation, an apparent zero residual charge to a precision $0.1e$; the upper limit given in eq. (2) of ref. [39] is then deteriorated by an order of magnitude. However we can now exploit some among the more precise data in table 8.2 (and the knowledge we have of the patches) to restore the result of eq. (2) of ref. [39]. We hope to improve this result further with the use of the instrument (under construction) mentioned in section 8.12.

b) The work by the S. Francisco group described in section 10.3.2 has now been published in Phys. Rev. Letters. It is the second reference listed under [20].

c) In a short note (Phys. Rev. Lett. 48 (1982) 213) J. Schiffer suggests that a possible way of reconciling the findings of the Stanford group with the non observations of the other quark searches is to assume that quarks have charge + 1/3 and that at room temperature the desorption of quarks from the various materials is very fast, whereas at cryogenic temperatures the desorption stops. It seems to us that the niobium spheres, before being brought to cryogenic temperatures in the Stanford experiments, have been produced and kept at high or normal temperatures; in order that the proposed explanation holds the spheres must therefore have captured the quark from the air *just* before being frozen. This would imply a great abundance of quarks in the air and only in the air. For this reason, and also because the Stanford balls are seen to change their charge by a fractionary amount when deposited on a holder at low temperature, we consider this explanation as unconvincing.

d) In a series of papers K. Lackner and G. Zweig discuss the chemistry of quarks. The first of these papers (Introduction to the chemistry of fractionally charged atoms: electronegativity) has appeared as Caltech preprint 68–865; others are announced. We have not discussed here the quark chemistry (a subject on which already a significant literature exists – compare [9] for several references –) because this was outside the scope of this paper. We only remark: 1) as stated in section 6.1 one of the motivations for developing the ferromagnetic levitation technique was precisely that to make it possible to explore a variety of alloys; with the details given in this paper it should be possible to construct the instrument and use it with a variety of substances. 2) Chemistry is however not everything in determining the fate of a quark once in the earth, and must be complemented by substantial additional information. Obviously by pure chemistry it would be difficult for instance to understand why gold mines are dominantly in South Africa (in fact it is also not easy to understand how mines were formed at all).

e) An article by A. Pickering: "The hunting of the quark" published in Isis 72 (1981) 262 contains an account of our and Stanford experiments from the point of view of an historian and philosopher of science. We certainly appreciate the intention of the study of dr. Pickering; however we disagree with many of his statements; and also we feel that it would have been advantageous for such a historical study to wait the conclusion of the experiments in question.